

OECD/NRC Benchmark Based on NUPEC PWR Sub-channel and Bundle Test (PSBT)

Volume I: Experimental Database
and Final Problem Specifications



NEA Nuclear Science Committee
NEA Committee on Safety of Nuclear Installations

**OECD/NRC Benchmark Based on NUPEC PWR
Sub-channel and Bundle Tests (PSBT)**

***Volume I: Experimental Database and Final
Problem Specifications***

A. Rubin, A. Schoedel, M. Avramova
Nuclear Engineering Programme
United States of America

H. Utsuno
Japan Nuclear Energy Safety Organisation

S. Bajorek, A. Velazquez-Lozada
US NRC

© OECD 2012

NUCLEAR ENERGY AGENCY
Organisation for Economic Co-operation and Development

ORGANISATION FOR ECONOMIC CO-OPERATION AND DEVELOPMENT

The OECD is a unique forum where the governments of 34 democracies work together to address the economic, social and environmental challenges of globalisation. The OECD is also at the forefront of efforts to understand and to help governments respond to new developments and concerns, such as corporate governance, the information economy and the challenges of an ageing population. The Organisation provides a setting where governments can compare policy experiences, seek answers to common problems, identify good practice and work to co-ordinate domestic and international policies.

The OECD member countries are: Australia, Austria, Belgium, Canada, Chile, the Czech Republic, Denmark, Estonia, Finland, France, Germany, Greece, Hungary, Iceland, Ireland, Israel, Italy, Japan, Luxembourg, Mexico, the Netherlands, New Zealand, Norway, Poland, Portugal, the Republic of Korea, the Slovak Republic, Slovenia, Spain, Sweden, Switzerland, Turkey, the United Kingdom and the United States. The European Commission takes part in the work of the OECD. OECD Publishing disseminates widely the results of the Organisation's statistics gathering and research on economic, social and environmental issues, as well as the conventions, guidelines and standards agreed by its members.

*This work is published on the responsibility of the OECD Secretary-General.
The opinions expressed and arguments employed herein do not necessarily reflect the official
views of the Organisation or of the governments of its member countries.*

NUCLEAR ENERGY AGENCY

The OECD Nuclear Energy Agency (NEA) was established on 1 February 1958. Current NEA membership consists of 30 OECD member countries: Australia, Austria, Belgium, Canada, the Czech Republic, Denmark, Finland, France, Germany, Greece, Hungary, Iceland, Ireland, Italy, Japan, Luxembourg, Mexico, the Netherlands, Norway, Poland, Portugal, the Republic of Korea, the Slovak Republic, Slovenia, Spain, Sweden, Switzerland, Turkey, the United Kingdom and the United States. The European Commission also takes part in the work of the Agency.

The mission of the NEA is:

- to assist its member countries in maintaining and further developing, through international co-operation, the scientific, technological and legal bases required for a safe, environmentally friendly and economical use of nuclear energy for peaceful purposes, as well as
- to provide authoritative assessments and to forge common understandings on key issues, as input to government decisions on nuclear energy policy and to broader OECD policy analyses in areas such as energy and sustainable development.

Specific areas of competence of the NEA include the safety and regulation of nuclear activities, radioactive waste management, radiological protection, nuclear science, economic and technical analyses of the nuclear fuel cycle, nuclear law and liability, and public information.

The NEA Data Bank provides nuclear data and computer program services for participating countries. In these and related tasks, the NEA works in close collaboration with the International Atomic Energy Agency in Vienna, with which it has a Co-operation Agreement, as well as with other international organisations in the nuclear field.

This document and any map included herein are without prejudice to the status of or sovereignty over any territory, to the delimitation of international frontiers and boundaries and to the name of any territory, city or area.

Corrigenda to OECD publications may be found online at: www.oecd.org/publishing/corrigenda.

© OECD 2012

You can copy, download or print OECD content for your own use, and you can include excerpts from OECD publications, databases and multimedia products in your own documents, presentations, blogs, websites and teaching materials, provided that suitable acknowledgment of the OECD as source and copyright owner is given. All requests for public or commercial use and translation rights should be submitted to rights@oecd.org. Requests for permission to photocopy portions of this material for public or commercial use shall be addressed directly to the Copyright Clearance Center (CCC) at info@copyright.com or the Centre français d'exploitation du droit de copie (CFC) contact@cfcopies.com.

Foreword

The need to refine models for best-estimate calculations, based on good-quality experimental data, has been expressed in many recent meetings in the field of nuclear applications. The needs arising in this respect should not be limited to the currently available macroscopic methods but should be extended to next-generation analysis techniques that focus on more microscopic processes. One of the most valuable databases identified for the thermal-hydraulics modelling was developed by the Nuclear Power Engineering Corporation (NUPEC), Japan, which includes sub-channel void fraction and departure from nucleate boiling (DNB) measurements in a representative Pressurised Water Reactor (PWR) fuel assembly. Part of this database has been made available for this international benchmark activity entitled “NUPEC PWR Sub-channel and Bundle Tests (PSBT) benchmark”. This international project has been officially approved by the Japanese Ministry of Economy, Trade, and Industry (METI), the US Nuclear Regulatory Commission (NRC) and endorsed by the OECD/NEA. The benchmark team has been organised based on the collaboration between Japan and the USA. A large number of international experts have agreed to participate in this programme.

The fine-mesh high-quality sub-channel void fraction and departure from nucleate boiling data encourages advancement in understanding and modelling complex flow behaviour in real bundles. Considering that the present theoretical approach is relatively immature, the benchmark specification is designed so that it will systematically assess and compare the participants’ analytical models on the prediction of detailed void distributions and DNB. The development of truly mechanistic models for DNB prediction is currently underway. The benchmark problem includes both macroscopic and microscopic measurement data. In this context, the sub-channel grade void fraction data are regarded as the macroscopic data and the digitised computer graphic images are the microscopic data, which provide void distribution within a sub-channel.

The NUPEC PSBT benchmark consists of two phases. Each phase consists of different exercises:

- Phase I – Void Distribution Benchmark
 - Exercise 1 – Steady-state single sub-channel benchmark
 - Exercise 2 – Steady-state bundle benchmark
 - Exercise 3 – Transient bundle benchmark
 - Exercise 4 – Pressure drop benchmark
- Phase II – DNB Benchmark
 - Exercise 1 – Steady-state fluid temperature benchmark
 - Exercise 2 – Steady-state DNB benchmark
 - Exercise 3 – Transient DNB benchmark

This report provides the specifications for the international OECD/NRC NUPEC PSBT benchmark problem. The specification report has been prepared jointly by the Pennsylvania State University (PSU), USA and the Japan Nuclear Energy Safety (JNES) Organisation, in co-operation with the US NRC and the NEA/OECD. The work is sponsored by the US NRC, METI-Japan, the NEA/OECD, and the Nuclear Engineering Programme (NEP) of Pennsylvania State University. The specifications cover the four exercises of Phase I, and the three exercises of Phase II. In addition, a CD-ROM has also been prepared with the complete NUPEC PWR database and is distributed along with the specifications to the participants, who have signed the NEA/OECD confidentiality agreement. The agreement as well as the other related information about the OECD/NRC PSBT benchmark can be found at: <http://www.nea.fr/html/science/egrsltb/PSBT/>.

Acknowledgements

The authors would like to thank Professor Hideki Nariai, President of the JNES, Japan, whose support and encouragement in establishing and carrying out this benchmark are invaluable.

This report is the sum of many efforts: those of the participants, the funding agencies and their staff - the METI, Japan, US NRC and the Organisation of Economic Co-operation and Development (OECD). Special appreciation goes to the report reviewer, Professor Kostadin Ivanov from the Pennsylvania State University (PSU). His comments, corrections, and suggestions were very valuable and significantly improved the quality of this report.

The authors wish to express their sincere appreciation for the outstanding support offered by the JNES personnel in providing the test data and discussing the test characteristics.

The authors would also like to thank Westinghouse Electric Company, Pittsburgh, PA, USA and Mr. Robert Salko, a PhD candidate at PSU, for their outstanding technical assistance and work in the preparation of the spacer grid data for this benchmark.

Particularly noteworthy are the efforts of Dr. Chris Hoxie and Dr. Jenifer Uhle from US NRC. With their help funding was secured, enabling this project to proceed. We also thank them for their excellent technical advice and assistance.

The authors would like to thank Dr. A. Hotta from TEPSYS, Japan, Professor J. Aragonés from Universidad Politécnica Madrid (UPM), Spain – member of NSC /NEA, and Professor F. D’Auria of University of Pisa (UP), Italy, member of CSNI/NEA, whose support and encouragement in establishing and carrying out this benchmark are invaluable.

Finally, we are grateful to Cristina Lebonetelle from NEA/OECD for having devoted her competence and skills to the final editing of this report.

Table of contents

Chapter 1: Introduction.....	10
1.1 Background.....	10
1.2 Objective.....	10
1.3 Outline of the PSBT Specification	11
1.4 Definition of Benchmark Phases	11
1.4.1 Phase I - Void Distribution Benchmark.....	11
1.4.2 Phase II - Departure from Nucleate Boiling (DNB) Benchmark.....	12
1.5 Benchmark Team and Sponsorship	12
Chapter 2: Test facilities	14
2.1 General.....	14
2.2 Test Loop	14
2.3 Test Section	16
2.3.1 Single Sub-channel Void Distribution Measurements.....	16
2.3.2 Bundle Void Distribution Measurements	17
2.3.3 Bundle DNB Measurements	18
2.4 Void Distribution Measurement Methods	19
2.5 DNB Measurement Methods	23
2.6 Studies on the Accuracy of the Void Fraction.....	23
Chapter 3: Test assembly data	28
3.1 General.....	28
3.2 Void Distribution Data	28
3.2.1 Single Sub-channel Specification	28
3.2.1.1 Heater Rod Structure for Sub-channel Test Assembly.....	30
3.2.1.2 Bundle Specification.....	30
3.2.2 Bundle Specification.....	30
3.2.2.1 Heater Rod Structure for Bundle Test Assembly.....	34
3.2.2.2 Spacer Grid Data	35
3.3 DNB Measurement	45
3.4 Thermo-Mechanical Properties	51
3.4.1 Properties of Inconel 600	51
3.4.2 Properties of Alumina	51
3.4.3 Properties of Titanium	51
Chapter 4: Benchmark phases and exercises.....	52
4.1 Introduction.....	52
4.2 Phase I - Void Distribution Benchmark.....	54
4.2.1 Exercise I-1 – Steady-State Single Sub-channel Benchmark	54
4.2.2 Exercise I-2 – Steady-State Bundle Benchmark.....	59
4.2.3 Exercise I-3 – Transient Bundle Benchmark	67
4.2.4 Exercise I-4 – Pressure Drop Benchmark	86
4.3 Phase II: DNB Benchmark	86
4.3.1 Exercise II-1 – Steady-State Fluid Temperature Benchmark	86
4.3.2 Exercise II-2 – Steady-State DNB Benchmark.....	89
4.3.3 Exercise II-3 – Transient DNB Benchmark.....	101
Chapter 5: Output requested	114
5.1 Introduction.....	114

5.2 Void Distribution Benchmark.....	114
5.3 DNB Benchmark	117
Chapter 6: Conclusions.....	119
6.1 Phase I - Void Distribution Benchmark.....	119
6.2 Phase II - DNB Benchmark	119
References.....	120

List of figures

Figure 1: PSBT Benchmark Team.....	13
Figure 2: System Diagram of NUPEC PWR Test Facility	15
Figure 3: Test Section for Central Sub-channel Void Distribution Measurement.....	16
Figure 4: Test Section for Rod Bundle Void Distribution Measurement	17
Figure 5: Cross-Section of Test Vessel.....	18
Figure 6: Void Fraction Measurement Procedure.....	20
Figure 7: Relation between Chordal and CT Averaged Densities in bundle S1	22
Figure 8: Deviation of Measured Void Fraction from Calculated Void Fraction.....	24
Figure 9: Deviation of Experimental Quality from Calculated Quality (Method 1; S1 and S2).....	25
Figure 10: Deviation of Experimental Quality from Calculated Quality (Method 2; S1 and S2).....	25
Figure 11: Deviation of Experimental Quality from Calculated Quality (Method 2; B5).....	26
Figure 12: Deviation of Experimental Quality from Calculated Quality (Method 2; B6).....	26
Figure 13: Deviation of Experimental Quality from Calculated Quality (Method 2; B7).....	27
Figure 14: Deviation of Experimental Quality from Calculated Quality (Method 2; B8).....	27
Figure 15: Cross-Sectional View of Sub-channel Test Assembly	29
Figure 16: Location of Pressure Taps	32
Figure 17: Radial Power Distribution Type A	33
Figure 18: Radial Power Distribution Type B	33
Figure 19: Cross-Section of Bundle Heater Rod	34
Figure 20: Three-Dimensional View of the Simple Spacer	36
Figure 21: Three-Dimensional View of the Non-Mixing Vane Spacer	37
Figure 22: Three-Dimensional View of the Mixing Vane Spacer	38
Figure 23: Dimensions of the Simple Spacer.....	39
Figure 24: Dimensions of the Non-Mixing Vane Spacer.....	40
Figure 25: Dimensions of the Mixing Vane Spacer.....	43
Figure 26: Radial Power Distribution Type C	48
Figure 27: Radial Power Distribution Type D.....	48
Figure 28: Location of Thermocouples for Test Assemblies.....	49
Figure 29: Fluid Temperature Measurements.....	50
Figure 30: Variation of Properties during Transient for Data Series 5T (Power Increase).....	70
Figure 31: Variation of Properties during Transient for Data Series 5T (Flow Reduction).....	70
Figure 32: Variation of Properties during Transient for Data Series 5T (Depressurisation).....	73
Figure 33: Variation of Properties during Transient for Data Series 5T (Temperature Increase).....	73
Figure 34: Variation of Properties during Transient for Data Series 6T (Power Increase).....	76

Figure 35: Variation of Properties during Transient for Data Series 6T (Flow Reduction).....	76
Figure 36: Variation of Properties during Transient for Data Series 6T (Depressurisation).....	79
Figure 37: Variation of Properties during Transient for Data Series 6T (Temperature Increase).....	79
Figure 38: Variation of Properties during Transient for Data Series 7T (Power Increase).....	82
Figure 39: Variation of Properties during Transient for Data Series 7T (Flow Reduction).....	82
Figure 40: Variation of Properties during Transient for Data Series 7T (Depressurisation).....	85
Figure 41: Variation of Properties during Transient for Data Series 7T (Temperature Increase).....	85
Figure 42: Variation of Properties during Transient for Data Series 11T (Power Increase).....	104
Figure 43: Variation of Properties during Transient for Data Series 11T (Flow Reduction).....	104
Figure 44: Variation of Properties during Transient for Data Series 11T (Depressurisation).....	107
Figure 45: Variation of Properties during Transient for Data Series 11T (Temperature Increase).....	107
Figure 46: Variation of Properties during Transient for Data Series 12T (Power Increase).....	110
Figure 47: Variation of Properties during Transient for Data Series 12T (Flow Reduction).....	110
Figure 48: Variation of Properties during Transient for Data Series 12T (Depressurisation).....	113
Figure 49: Variation of Properties during Transient for Data Series 12T (Temperature Increase).....	113

List of tables

Table 1: Range of NUPEC PWR Test Facility Operating Conditions.....	14
Table 2: Transient Parameters of NUPEC PWR Test Facility	14
Table 3: Reference Rated Operating Conditions of PWR	15
Table 4: Test Vessel and Flow Channel Structure Data	18
Table 5: Manufacturing Tolerances for Test Assembly.....	18
Table 6: Estimated Accuracy for Void Fraction Measurements.....	21
Table 7: Error Sources for Void Measurements	21
Table 8: Number of Gamma Ray Beams	22
Table 9: Time Required to Perform Void Fraction Measurements.....	22
Table 10: Estimated Accuracy for DNB Measurements.....	23
Table 11: Test Assemblies for Void Fraction Measurements.....	28
Table 12: Geometry and Power Shape for Test Assembly S1, S2, S3, and S4.....	29
Table 13: Geometric Characteristics of Sub-channel Assemblies	30
Table 14: Heater Rod Structure for Sub-channel Test Assembly.....	30
Table 15: Geometry and Power Shape for Test Assembly B5, B6, and B7.....	31
Table 16: Axial Power Distribution (Cosine)	33
Table 17: Heater Rod Structure for Bundle Test Assembly	34
Table 18: Bundle Average Spacer Pressure Loss Coefficients.....	35

Table 19: Test Assemblies for DNB Measurements.....	45
Table 20: Geometry and Power Shape for Test Assembly A0	46
Table 21: Geometry and Power Shape for Test Assembly A1, A2, and A3	47
Table 22: Geometry and Power Shape for Test Assembly A4, A8, A11, and A12	48
Table 23: NUPEC PSBT Benchmark Database.....	53
Table 24: Benchmark Conditions	53
Table 25: Test Series for Void Fraction Measurement	54
Table 26: Test Conditions for Steady-State Void Measurement Test Series 1	55
Table 27: Test Conditions for Steady-State Void Measurement Test Series 2	56
Table 28: Test Conditions for Steady-State Void Measurement Test Series 3	57
Table 29: Test Conditions for Steady-State Void Measurement Test Series 4	58
Table 30: Test Conditions for Steady-State Void Measurement Test Series 5	59
Table 31: Test Conditions for Steady-State Void Measurement Test Series 6.....	61
Table 32: Test Conditions for Steady-State Void Measurement Test Series 7	63
Table 33: Test Conditions for Steady-State Void Measurement Test Series 8	65
Table 34: Duplicated Cases in Test Series B5 and B8.....	66
Table 35: Test Conditions for Transient Void Measurement Test Series 5T, 6T, 7T	67
Table 36: Transient Void Fraction in Rod Bundle Test Series 5T (Power Increase).....	68
Table 37: Transient Void Fraction in Rod Bundle Test Series 5T (Flow Reduction)	69
Table 38: Transient Void Fraction in Rod Bundle in Test Series 5T (Depressurisation)	71
Table 39: Transient Void Fraction in Rod Bundle in Test Series 5T (Temperature Increase).....	72
Table 40: Transient Void Fraction in Rod Bundle in Test Series 6T (Power Increase)	74
Table 41: Transient Void Fraction in Rod Bundle in Test Series 6T (Flow Reduction)	75
Table 42: Transient Void Fraction in Rod Bundle in Test Series 6T (Depressurisation)	77
Table 43: Transient Void Fraction in Rod Bundle in Test Series 6T (Temperature Increase).....	78
Table 44: Transient Void Fraction in Rod Bundle in Test Series 7T (Power Increase)	80
Table 45: Transient Void Fraction in Rod Bundle in Test Series 7T (Flow Reduction)	81
Table 46: Transient Void Fraction in Rod Bundle in Test Series 7T (Depressurisation)	83
Table 47: Transient Void Fraction in Rod Bundle in Test Series 7T (Temperature Increase).....	84
Table 48: Test Series for DNB Measurement	86
Table 49: Test Conditions for Steady-State Fluid Temperature Benchmark	87
Table 50: Test Conditions for Steady-State DNB Test Series 0	89
Table 51: Test Conditions for Steady-State DNB Test Series 2	91
Table 52: Test Conditions for Steady-State DNB Test Series 3	93
Table 53: Test Conditions for Steady-State DNB Test Series 4	95
Table 54: Test Conditions for Steady-State DNB Test Series 8	97
Table 55: Test Conditions for Steady-State DNB Test Series 13	99
Table 56: Test Conditions for Transient DNB Test Series 11T and 12T.....	101
Table 57: Transient DNB Data in Rod Bundle in Test Series 11T (Power Increase).....	102
Table 58: Transient DNB Data in Rod Bundle in Test Series 11T (Flow Reduction).....	103
Table 59: Transient DNB Data in Rod Bundle in Test Series 11T (Depressurisation)	105
Table 60: Transient DNB Data in Rod Bundle in Test Series 11T (Temperature Increase).....	106
Table 61: Transient DNB Data in Rod Bundle in Test Series 12T (Power Increase).....	108
Table 62: Transient DNB Data in Rod Bundle in Test Series 12T (Flow Reduction).....	109
Table 63: Transient DNB Data in Rod Bundle in Test Series 12T (Depressurisation)	111
Table 64: Transient DNB Data in Rod Bundle in Test Series 12T (Temperature Increase).....	112

Table 65: Output Format of Steady-State Single Sub-channel Benchmark.....	114
Table 66: Output Format of Steady-State Bundle Benchmark	115
Table 67: Output Format of Transient Bundle Benchmark	115
Table 68: Output Format of Single Sub-channel Pressure Drop Benchmark	116
Table 69: Output Format of Bundle Pressure Drop Benchmark.....	116
Table 70: Output Format of Steady-State Fluid Temperature Benchmark	117
Table 71: Output Format of Steady-State DNB Benchmark	117
Table 72: Output Format of Transient DNB Benchmark.....	118

Chapter 1: Introduction

1.1 Background

Over the last four years the Pennsylvania State University (PSU) under the sponsorship of the US Nuclear Regulatory Commission (NRC) has prepared, organised, conducted and summarised the OECD/NRC Benchmark based on NUPEC BWR Full-size Fine-mesh Bundle Tests (BFBT). The international benchmark activities have been conducted in co-operation with the Nuclear Energy Agency (NEA), OECD and the Japan Nuclear Energy Safety (JNES) organisation, Japan. From 1987 to 1995, the Nuclear Power Engineering Corporation (NUPEC) in Japan performed a series of void measurement tests using full-size mock-up tests for both BWRs and PWRs. For BWRs, based on the state-of-the-art computer tomography (CT) technology, the void distribution was visualised at the mesh size smaller than the sub-channel under actual plant conditions. NUPEC also performed steady-state and transient critical power test series based on the equivalent full-size mock-ups. Considering the reliability not only of the measured data, but also other relevant parameters such as the system pressure, inlet sub-cooling and rod surface temperature, these test series supplied the first substantial database for the development of truly mechanistic and consistent models for void distribution and boiling transition.

Consequently, the JNES has made available the BWR NUPEC database for the purpose of the OECD/NRC BFBT international benchmark. This international benchmark has encouraged advancement in the uninvestigated fields of two-phase flow theory with very important relevance to the nuclear reactors safety margins evaluation. The BFBT benchmark is made up of two phases, each phase consisting of four different exercises and has been used for validation of CFD, sub-channel and system thermal-hydraulic codes. The BFBT benchmark activity has been very successful with about thirty (30) organisations from fifteen (15) countries participating in different benchmark exercises. The BFBT activity is being completed with final comparative reports to be published as US NRC NUREG and NEA/OECD reports. A special Nuclear Engineering and Design journal issue is being prepared devoted to the BFBT benchmark, which will document the models and results of the participants.

Based on the success of the OECD/NRC BFBT benchmark the JNES, Japan has decided to release also the data based on the NUPEC PWR Sub-channel and Bundle Tests (PSBT) for an international benchmark and has asked PSU to organise and conduct this benchmark activity. Void fraction measurements and departure from nucleate boiling (DNB) tests were performed at NUPEC under the conditions simulating PWR thermal-hydraulic conditions, including the steady-states and the transients such as the power increase, the flow reduction, the depressurisation and the temperature increase.

1.2 Objective

The established international OECD/NRC PWR Sub-channel and Bundle Tests (PSBT) benchmark, based on the NUPEC database, encourages advancement in sub-channel analysis of fluid flow in rod bundles, which has very important relevance to the nuclear reactor safety margin evaluation. This benchmark specification is being designed so that it can systematically assess and compare the participants' numerical models for the prediction of detailed sub-channel void distributions and departure from nucleate boiling (DNB) to full scale experimental data on a prototypical PWR rod bundle. Currently the numerical modelling of sub-channel void distribution has limited theoretical approach that can be applied to a wide range of geometrical and operating

conditions. In the past decade, experimental and computational technologies have tremendously improved the study of the flow structure. Over the next decade, it can be expected that mechanistic approaches will be more widely applied to the complicated fluid phenomena inside fuel bundles. The development of truly mechanistic models for DNB prediction is currently underway. These models must include processes such as void distribution, droplet deposition, liquid film entrainment and spacer grid behaviour. The benchmark specification requires participants to explain their modelling correlations between the measured DNB and the flow dominant processes.

It should be recognised that the purpose of this benchmark is not only the comparison of currently available computational approaches but above all, the encouragement to develop novel next-generation approaches that focus on more microscopic processes. In this context, the sub-channel grade void fraction data are regarded as the macroscopic data and the digitised computer graphic images are the microscopic data, which provide the detailed void distribution within the sub-channel. This benchmark specification is supplemented by a CD-ROM with complete NUPEC PWR Benchmark Database, which is distributed to all participants who have signed the confidentiality agreement.

1.3 Outline of the PSBT Specification

Chapter 1 of this specification discusses the main objectives of the international OECD/NRC PSBT benchmark. A definition of the benchmark phases and exercises is provided.

Chapter 2 discusses the NUPEC PWR PSBT facility and the specific methods used in the void distribution and DNB measurements.

Chapter 3 provides specifications of fuel assembly types and heater rods as well as spacer data and thermo-mechanical properties of structural materials.

Chapter 4 defines the NUPEC PSBT data to be used for the benchmark exercises. In total seven exercises of two phases will be performed in the framework of this benchmark.

Chapter 5 describes the requested output and the output format that the benchmark team will collect from the participants.

Chapter 6 summarises the conclusions of the specification.

1.4 Definition of Benchmark Phases

The test facility design and data from NUPEC include both macroscopic and microscopic measurements. There are two separate phases, each consisting of different exercises. These phases and exercises are discussed below.

1.4.1 Phase I - Void Distribution Benchmark

The purpose of this benchmark phase is three-fold:

- to provide data for validation of numerical models of void distribution;
- to provide data over a wide range of geometrical and operating conditions for validation of void distribution models;
- to provide data for development of mechanistic approaches widely applicable to the fluid phenomena inside fuel bundles.

Phase I includes four exercises:

- *Exercise 1* – Steady-state single sub-channel benchmark, which can be used to improve the current models of void generation and void distribution within a sub-channel.

- **Exercise 2** – Steady-state bundle benchmark, which can be applied to sub-channel and system thermal-hydraulic codes.
- **Exercise 3** – Transient bundle benchmark, which can be used to determine the capabilities of sub-channel and system thermal-hydraulic codes of predicting void generation during transients.
- **Exercise 4** – Pressure drop benchmark. Code-to-code comparisons will also be performed.

1.4.2 Phase II - Departure from Nucleate Boiling (DNB) Benchmark

The purpose of this benchmark is to develop truly mechanistic models for DNB prediction.

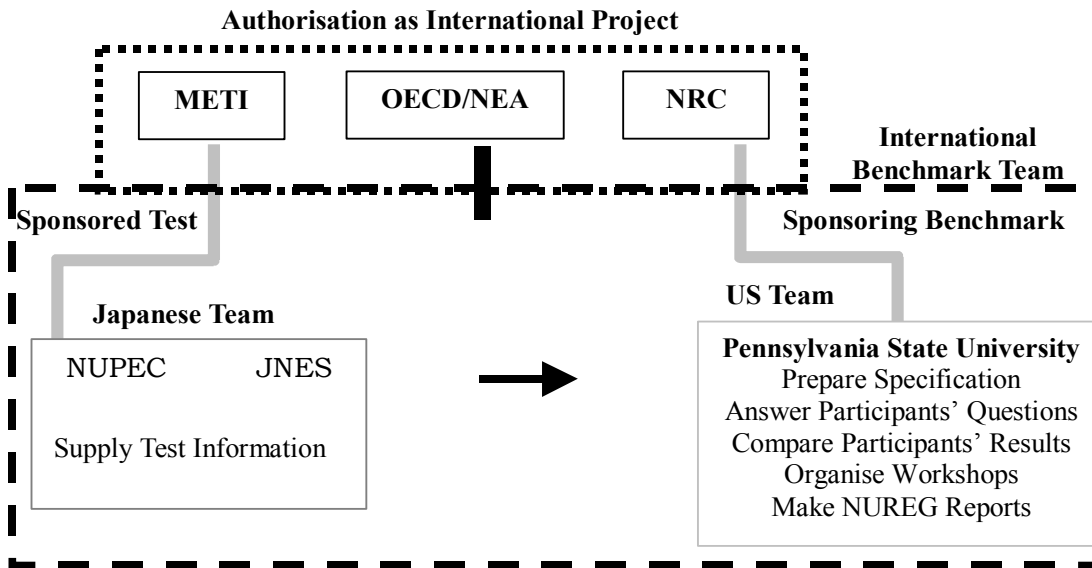
Phase II includes three exercises:

- **Exercise 1** – Steady-state fluid temperature benchmark, which can be applied to sub-channel and system thermal-hydraulic codes as well as CFD codes.
- **Exercise 2** – Steady-state DNB benchmark, which can be used to improve the current models of DNB prediction in PWR bundles at steady-state.
- **Exercise 3** – Transient DNB benchmark, which can be used to improve the current models of DNB prediction in PWR bundles during transients.

1.5 Benchmark Team and Sponsorship

The benchmark activities have been performed as an international project supported by the US NRC and METI (Japan) and endorsed by the OECD/NEA. The benchmark team has been organised based on the collaboration between the USA and Japan as shown in Figure 1. This approach has been very successful in the OECD/NRC BFBT benchmark, which has been completed. It has been recognised that METI had sponsored the NUPEC PWR sub-channel and bundle test project. The JNES on behalf of METI provides the test information and measured data. The OECD/NEA provides supporting activities for this international PSBT benchmark project. The US team, headed by Professor Avramova and Professor Ivanov from PSU, co-ordinates the benchmark project in co-operation with the US NRC. The PSU team prepares the benchmark specification, organises the technical content of the workshops (the logistics of the workshops is managed by the NEA/OECD), answers the questions issued by participants, compares and analyses participants' results and prepares comparison reports as NEA/OECD and NUREG reports. The basic activity of the US benchmark team (PSU team) is sponsored by the US NRC. In addition to the above described activities, the PSU team performs PSBT calculations using the PSU version of COBRA-TF and works in co-operation with the US NRC on the development and validation of a sub-channel model in TRACE using the PSBT data.

Figure 1: PSBT Benchmark Team



Chapter 2: Test facilities

2.1 General

The void distribution and DNB measurements took place at the facility described in Section 2.2. The facility is able to simulate the high-pressure, high-temperature fluid conditions found in PWR's. Although the same test loop was used for both phases, different test sections were constructed to represent a single sub-channel and a complete rod bundle.

2.2 Test Loop

The NUPEC test facility shown in Figure 2 consists of a high-pressure and high-temperature recirculation loop, a cooling loop, instrumentation and data recording systems. The recirculation loop consists of a test section, circulation pump, preheater, steam drum (acting as a pressuriser) and a water mixer. The design pressure is 19.2 MPa and the design temperature is 362°C. The operating conditions of the test facility are shown in Tables 1 and 2. Reference rated operating conditions of a PWR are listed in Table 3. Note that the units given for pressure in Table 3 may require conversion to more conventional units. The following conversions are to be used:

$$1 \frac{\text{kg}}{\text{cm}^2\text{a}} = \begin{cases} 0.980665 \text{ bar} \\ 14.223 \text{ psia} \end{cases}$$

Table 1: Range of NUPEC PWR Test Facility Operating Conditions

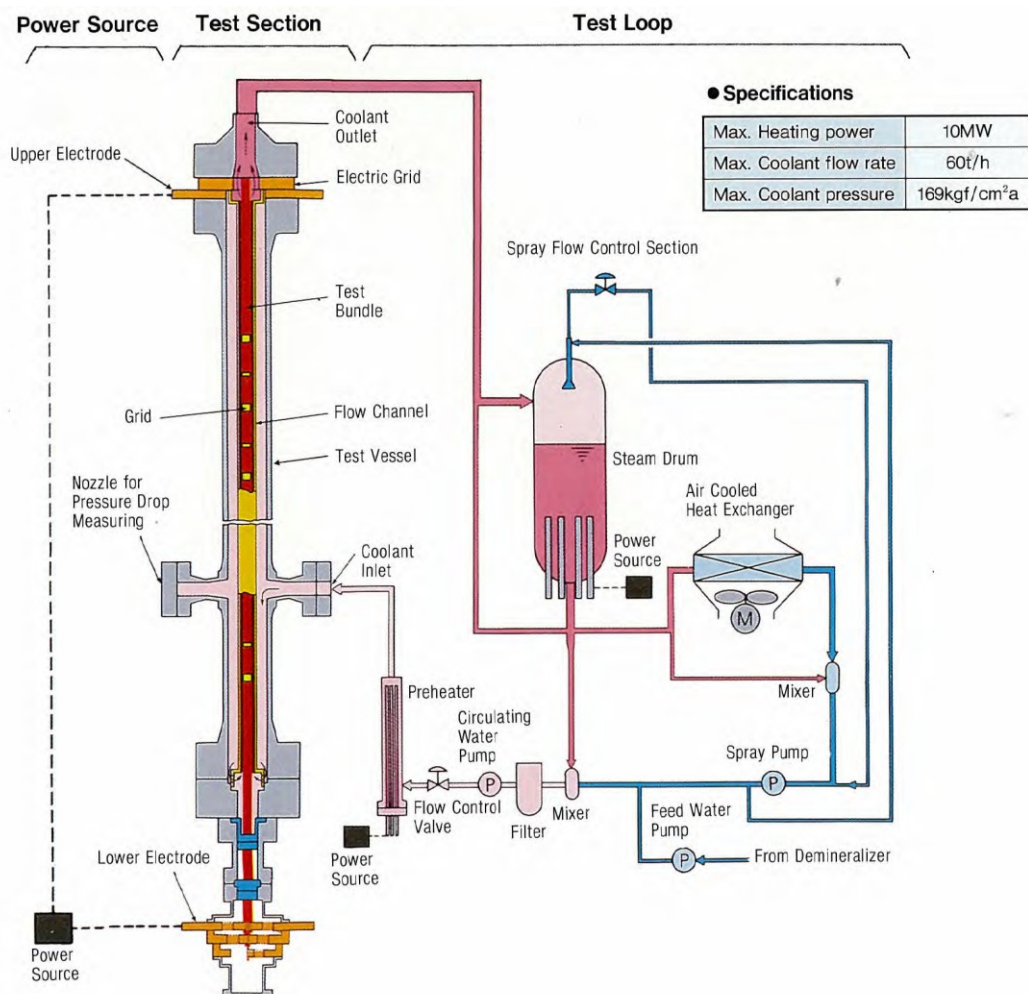
Quantity	Range
Pressure	4.9 – 16.6 MPa
Mass velocity	550 – 4150 kg/m ² s
Inlet coolant temperature	140 – 345°C

Table 2: Transient Parameters of NUPEC PWR Test Facility

Transient Scenario	Transient Change
Depressurisation	-0.03 MPa/s
Temperature increase	1 °C/s
Flow reduction	-25%/s
Power increase	15%/s

Table 3: Reference Rated Operating Conditions of PWR

Test section	Pressure (kg/cm ² a)	Mass flux (10 ⁶ kg/m ² h)	Heat flux (10 ⁶ kcal/m ² h)	Power (MW)	Inlet temperature (°C)
5×5 Rod bundle	158	12	0.5	2.7	290
6×6 Rod bundle	158	12	0.5	3.9	290

Figure 2: System Diagram of NUPEC PWR Test Facility

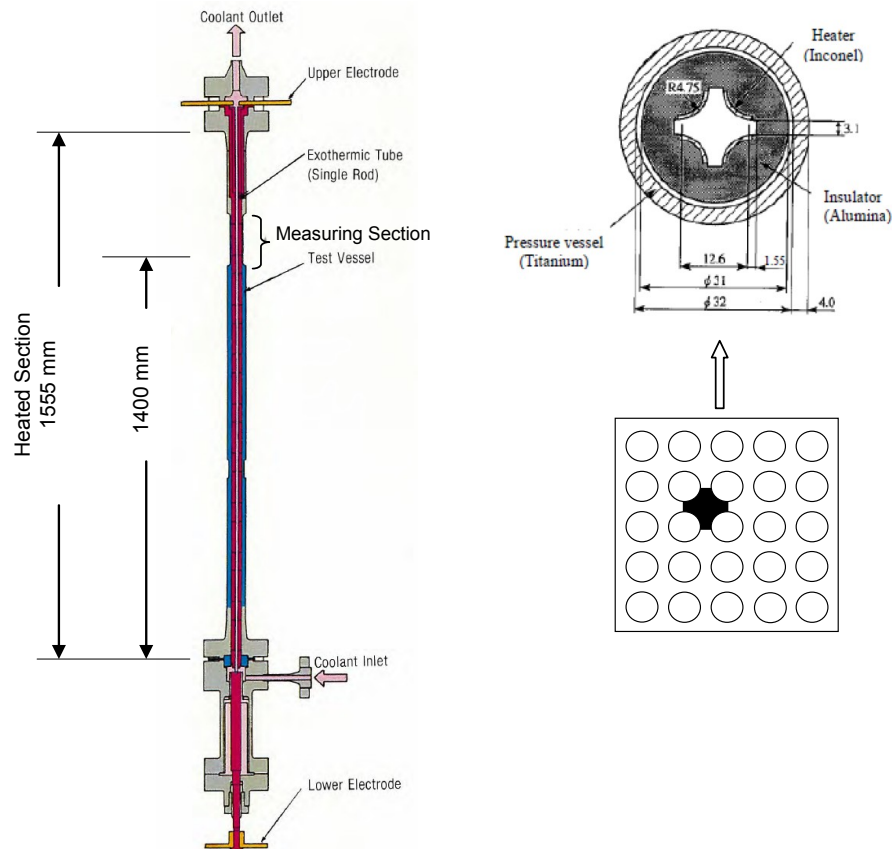
2.3 Test Section

Three different test sections were used to perform the void distribution measurement tests; one for the sub-channel void distribution test, one for the rod bundle void distribution test, and one for the bundle DNB measurements.

2.3.1 Single Sub-channel Void Distribution Measurements

Figure 3 shows the test section used for the central sub-channel void measurement. It simulates one of the sub-channel types found in a PWR assembly. Coolant flows in the pressure vessel horizontally through the coolant inlet nozzle located just below the heated section. Similar test sections were used for the central with thimble, side, and corner sub-channel types. The effective heated length is 1 555 mm, and the void measurement section begins at 1 400 mm from the bottom of the heated section [1].

Figure 3: Test Section for Central Sub-channel Void Distribution Measurement



2.3.2 Bundle Void Distribution Measurements

An electrically heated rod bundle was used to simulate a partial section and full length of a PWR fuel assembly. Figure 4 shows the test section used for the rod bundle void measurements. The effective heated length is 3 658 mm, which is broken into three sections (upper, middle, lower), measuring at 3 177 mm, 2 669 mm, and 2 216 mm, respectively. Coolant flows into the pressure vessel horizontally through the coolant inlet nozzle and down through the section between the flow channel and the pressure vessel. The coolant continues into the flow channel, flowing from the bottom of the pressure vessel up through the test assembly, where the bottom of the heated section is located 630 mm above the bottom of the pressure vessel. Table 4 provides data regarding the structure of the test vessel and flow channel. Table 5 shows the tolerances for the manufacture of the test assemblies.

Figure 4: Test Section for Rod Bundle Void Distribution Measurement

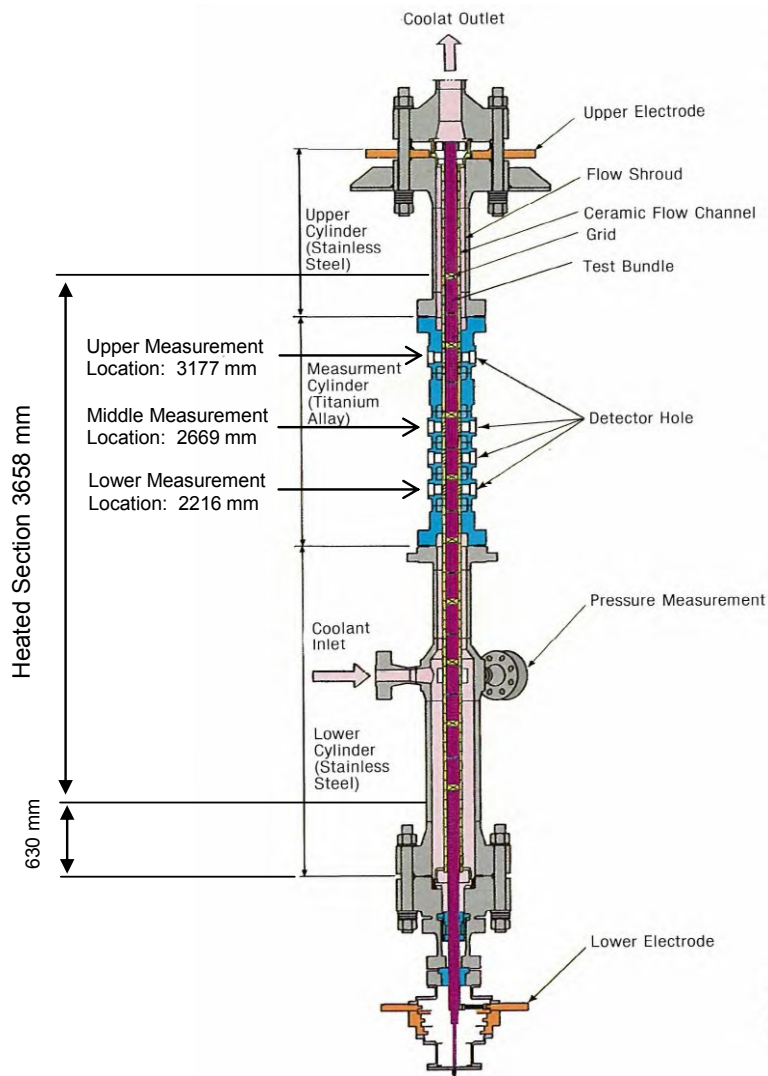
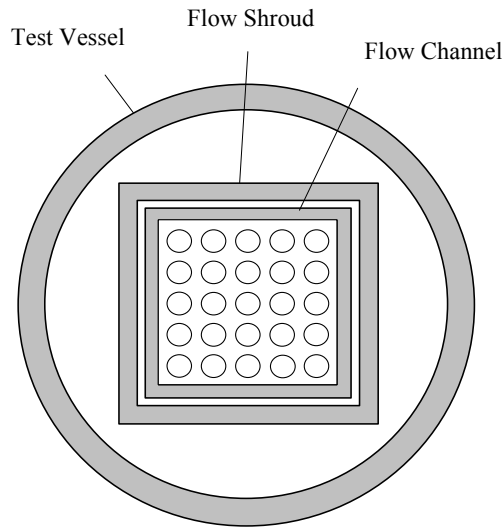


Figure 5: Cross-Section of Test Vessel**Table 4: Test Vessel and Flow Channel Structure Data**

	Item	Data
Flow channel	Inner length (mm)	64.9
	Thickness (mm)	5.0
	Material	Alumina
Flow shroud	Inner length (mm)	75.1
	Thickness (mm)	10
	Material	SUS304
Test vessel (upper cylinder)	Outer diameter(mm)	216.3
	Thickness (mm)	23.0
	Material	SUS304
Test vessel (lower cylinder)	Outer diameter(mm)	318.5
	Thickness (mm)	33.3
	Material	SUS304

Table 5: Manufacturing Tolerances for Test Assembly

Item	Tolerance
Rod bundle	
Heater rod diameter	0.02 mm
Heater rod displacement	0.45 mm
Flow channel inner width	0.05 mm
Flow channel displacement	0.20 mm
Power distribution	3 %

2.3.3 Bundle DNB Measurements

The DNB measurements were performed for full-length partial 5×5 and 6×6 array rod bundles, which simulate 17×17 PWR fuel assemblies. Measurements were performed both for steady-state and transients. The measurements were performed at the facility shown in Figure 2 using the assemblies described in Table 19.

2.4 Void Distribution Measurement Methods

The detailed explanation for the void fraction measurement procedure is provided in [2] and [3].

A gamma-ray transmission method was used to measure the density of the flow, which was converted to the void fraction of the gas-liquid two-phase flow. Figure 6 shows the procedure used to perform the void fraction measurements for the entire rod bundle. The top half of the figure shows the procedure used to perform the void fraction measurements for a single sub-channel. In the sub-channel experiments [3] a narrow gamma-ray beam CT scanner was used to measure the sub-channel averaged void fraction and a wide gamma-ray beam was used to measure the chordal averaged void fraction. For each sub-channel type - corner, side, or center – a relationship between the sub-channel averaged and the chordal averaged void fractions was individually derived. These relationships were then used to correct the sub-channel averaged void fraction measured with the wide beam in the bundle tests.

The void measurement systems shown in Figure 6 consist of gamma-ray sources (^{137}Cs); detectors; collimators, and signal processing units. The attenuation of the gamma-rays, which depends on the void fraction, was detected. The intensity of the gamma-ray source was determined to obtain the count-rate of the signal processing (30×10^4 cps).

The CT scanner system was used to determine the distribution of density/void fraction over the sub-channel at steady-state flow and to define the sub-channel averaged void fraction. The system was operated by translate/rotate method. At each translation/rotation location, the intensity of gamma-ray attenuated by the object, the so-called “projection data”, was detected. An image reconstruction was then performed by a filtered back-projection algorithm to obtain the distribution of the linear attenuation coefficient. A sufficient measuring time was given in order to avoid the effect of the flow motion.

Two densitometer systems – in x- and y-directions - were used in the chordal averaged void fraction measurements in the single sub-channel tests. Each of them consisted of a gamma source and a detector. They were located at the same tables (the same elevation) as CT, which was fixed during the measurements.

A multi-beam system was used to measure each sub-channel void fraction of the rod bundle. Six transmission data of x-direction and six transmission data of y-direction between the rod and rod/channel wall were used to reconstruct the void fraction of the 36 sub-channels by an iterative method. These sub-channel void fractions corresponded to the chordal measurements of the single sub-channel tests. The relationships between the sub-channel averaged void fraction and the chordal averaged void fraction obtained in the single sub-channel tests were used to determine the sub-channel averaged void fractions in the rod bundle tests. Such measurements were performed simultaneously at three axial elevations.

Table 6 shows the estimated accuracy of the void fraction measurements. Table 7 describes the sources of error in the void measurement process (these values correspond to one standard deviation, 1σ).

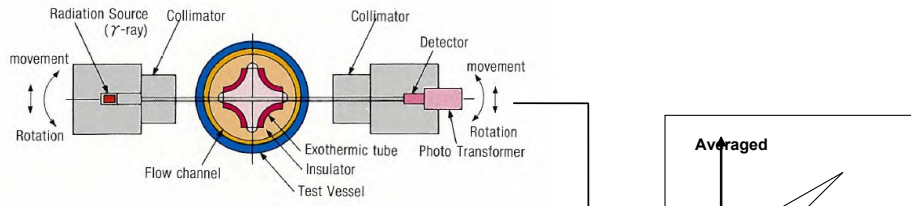
Figure 7 was used to determine the uncertainties inherent in the void measurements and to correct the measured values based on the pressure of the test case. The correlation between the chordal and CT averaged values is given by the best-fit curves and was introduced for the high and low-pressure conditions, respectively. The reference averaged density was 500 kg/m^3 . The uncertainty of the correlation was determined to be less than 18 kg/m^3 , which was regarded as three standard deviations (3σ). Therefore, one standard deviation (1σ) is 6 kg/m^3 . Table 8 provides information on the gamma beams used for these measurements.

Table 9 shows the time required to perform the void fraction measurements.

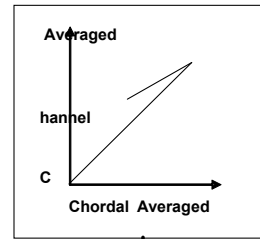
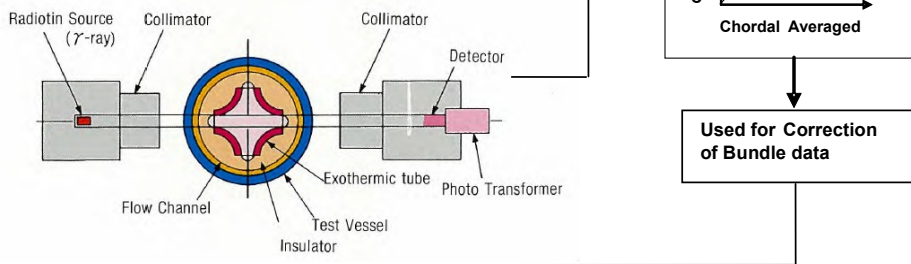
Figure 6: Void Fraction Measurement Procedure

Sub-channel Test

CT Measurement

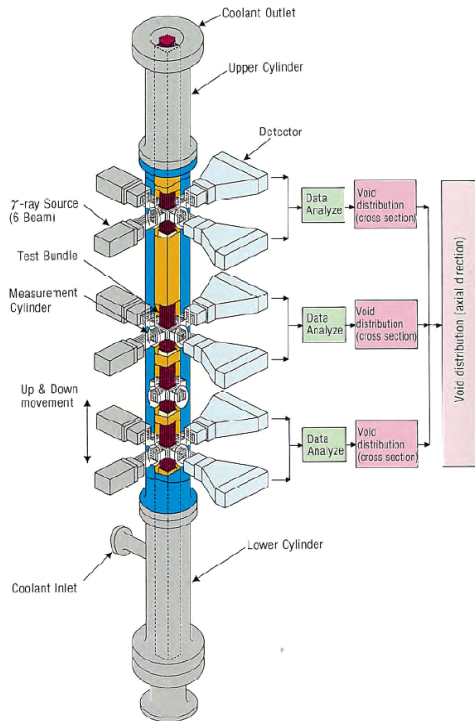


Chordal Measurement



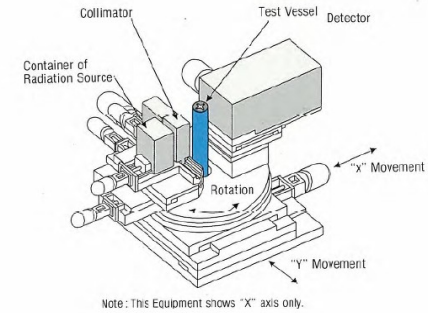
Used for Correction of Bundle data

Bundle Test



Void Measurement Equipment

Sub-channel Test



Bundle Test

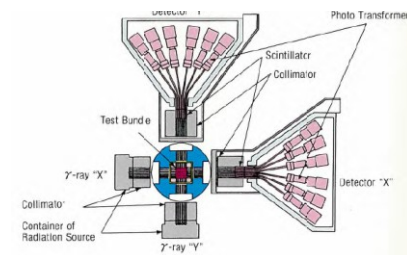


Table 6: Estimated Accuracy for Void Fraction Measurements

Quantity	Accuracy
Process parameters	
Pressure	1 %
Flow	1.5%
Power	1 %
Fluid temperature	1 Celsius
Void fraction measurement	
CT measurement	
Gamma-ray beam width	1 mm
Subchannel averaged (steady-state)	3% void
Spatial resolution of one pixel	0.5 mm
Chordal measurement	
Gamma-ray beam width (center)	3 mm
Gamma-ray beam width (side)	2 mm
Sub-channel averaged (steady-state)	4% void
Sub-channel averaged (transient)	5% void

Table 7: Error Sources for Void Measurements

Error source		Chordal Averaged		CT Averaged
		Steady-state	Transient	
γ-ray measurement	Effect of surrounding condition (magnetic-field and temperature) on measurement system	0.1%	0.1%	0.1%
	Randomness of γ-ray source decay	0.02%	0.2%	0.1%
	Correction error due to back ground	0.0%	0.0%	0.0%
	Correction error due to counting loss	<0.5%	<0.5%	<0.1%
	Calibration error	0.1%	0.1%	0.1%
	Correction error due to attenuation by surrounding water	0.0%	0.0%	-
	Correction error due to scattering from multi γ-rays	<0.2%	<0.2%	-
	Total	<0.55%	<0.6%	<0.2%
Sub-channel density	Transfer to density	<9 kg/m ³	<10 kg/m ³	<15 kg/m ³
	Distribution error to Sub-channel	<5 kg/m ³	<5 kg/m ³	-
Correlation error from Chordal averaged to CT averaged		<6 kg/m ³	<6 kg/m ³	-
Sub-channel density		<20 kg/m ³	<21 kg/m ³	<15 kg/m ³
Sub-channel void*		0.040	0.042	0.030
Uncertainty (1σ)		4 %	5 %	3 %

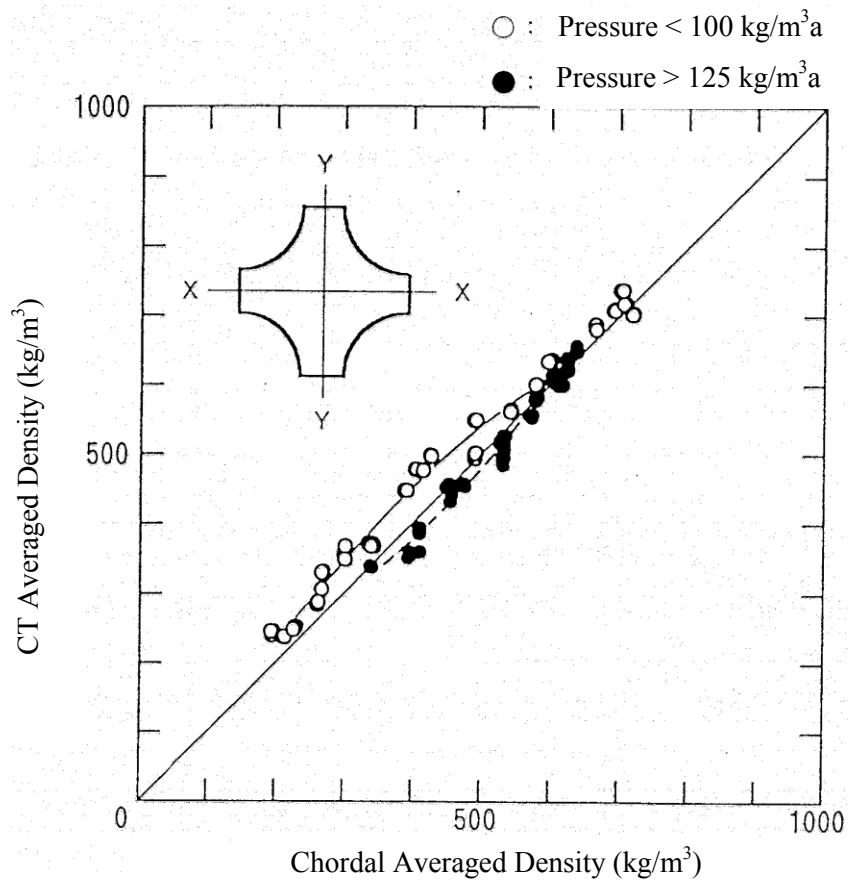
* Reference averaged density is 500 kg/m³ (see Figure 6).

Table 8: Number of Gamma Ray Beams

Test assembly	CT Measurement	Chordal Measurement
Sub-channel	2 (X and Y direction)	2 (X and Y direction)
Rod bundle	-	6 beam \times 2 \times 3 section (total 36 beams)

Table 9: Time Required to Perform Void Fraction Measurements

Item		CT Measurement	Chordal Measurement
Steady-state	Time needed	5 s/step ^T 33 ^R 17 step (it takes 2 h)	100 s sampling cycle 0.1 s
	Measurement	2 times	3 times
Transient	Time needed	-	200 s
	Measurement	-	1 time

Figure 7: Relation between Chordal and CT Averaged Densities in bundle S1

2.5 DNB Measurement Methods

The thermocouples described in Table 16 are used to determine the heat flux axially along the rod bundle. These thermocouples are attached to the inner surface of the heater rods and determine the boiling transition. The bundle power is increased gradually by fine steps to the vicinity of DNB power, which is based on preliminary analysis. The occurrence of DNB is confirmed by a rod temperature rise of more than 11°C (20°F) as measured by the thermocouples. The DNB power is defined as the power corresponding to the step just before the step where the temperature increased. Table 10 shows the estimated accuracies of different process parameters for the DNB measurements.

Table 10: Estimated Accuracy for DNB Measurements

Quantity	Accuracy
Process parameters	
Pressure	1 %
Flow	1.5%
Power	1 %
Fluid temperature	1 Celsius

2.6 Studies on the Accuracy of the Void Fraction

A deviation exists between the measured void fraction and the void fraction calculated using the measured fluid densities. Solving the standard equation for mixture density, $\bar{\rho} = \alpha\rho_g + (1 - \alpha)\rho_f$, for the void fraction gives $\alpha = (\bar{\rho} - \rho_f)/(\rho_g - \rho_f)$, where the liquid and vapour densities (ρ_f and ρ_g , respectively) are assumed to be at saturation. As it can be seen in Figure 8 the “measured” void fraction is consistently greater than the “calculated” void fraction.

Following the results of the study performed on the calculation of void fraction, the benchmark team evaluated the experimentally-determined quality for the selected cases in Test Series S1 and S2, the only sub-channel series for which quality was provided in the experimental database. Since temperature data at the measurement location was not available, the mixture enthalpy was determined using the measured density and pressure. These two parameters, along with steam table data, were used to determine the fluid temperature at the measurement location. The temperature and the given pressure were then used to determine the mixture enthalpy.

Once this mixture enthalpy was determined, and the fluid and vapour enthalpies (h_f and h_g , respectively) were found assuming saturation properties at the previously determined flow temperature, the equilibrium quality was evaluated using the equation $x = (h_{\text{mixture}} - h_f)/(h_g - h_f)$.

The differences between the experimental and “calculated” qualities (determined using the equation above, referred to as “Method 1”) for these two test series are shown in Figure 9. This procedure differs from that used for the original (NUPEC, referred to as “Method 2”) calculations of quality, which assumed conservation of energy in the test section. In this method, the mixture quality was expressed by:

$$h_{\text{mix}} [\text{kJ/kg}] = h_{\text{in}} [\text{kJ/kg}] + \frac{z_{\text{local}} [\text{mm}]}{z_{\text{total}} [\text{mm}]} Q [\text{kW}] \times \frac{3600 \left[\frac{\text{s}}{\text{h}} \right]}{A [\text{m}^2] G \left[\frac{\text{kg}}{\text{m}^2 \text{h}} \right]}$$

where h_{in} is taken at the inlet temperature and pressure. The above expression for quality can then be used, with the fluid and vapour enthalpies taken at saturation for the given pressure. The differences between the recalculated values and the experimental values are reflected in Figure 10 through Figure 14.

Figure 8: Deviation of Measured Void Fraction from Calculated Void Fraction

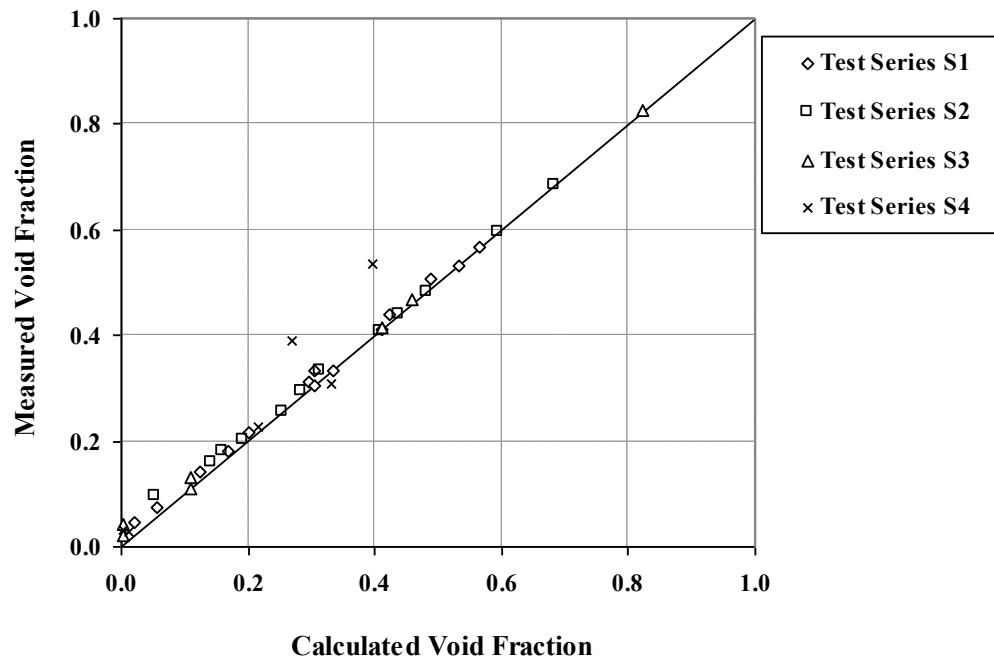


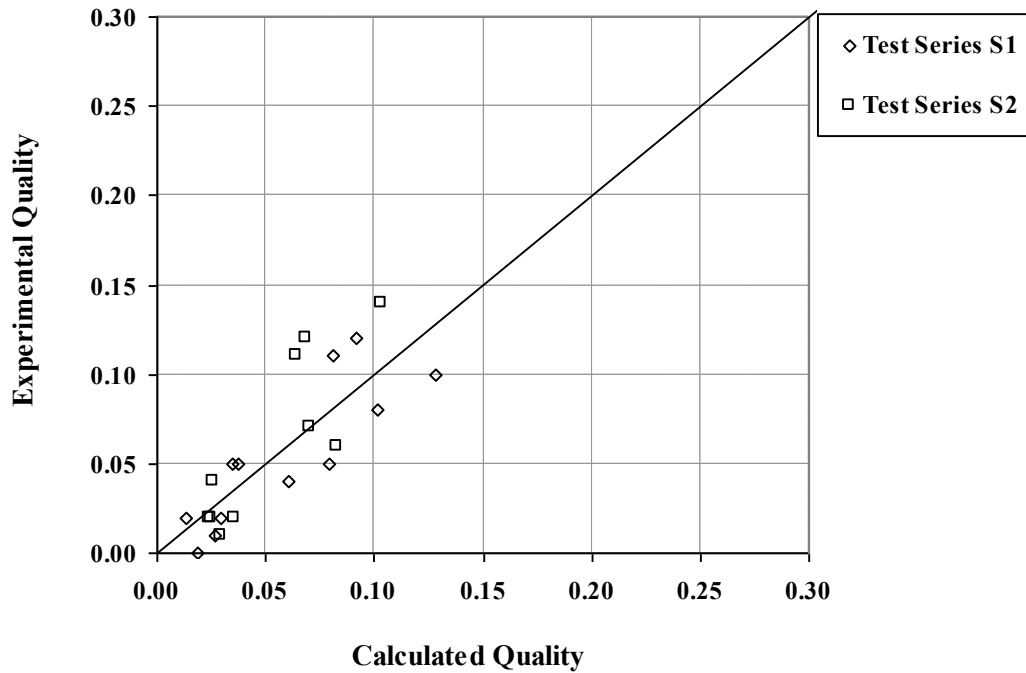
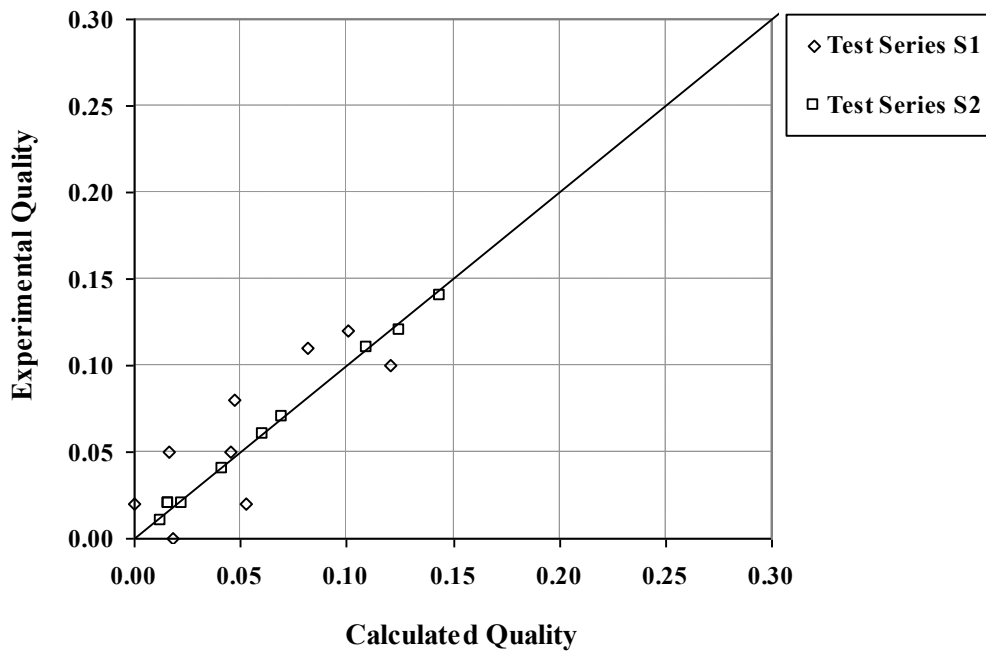
Figure 9: Deviation of Experimental Quality from Calculated Quality (Method 1; S1 and S2)**Figure 10: Deviation of Experimental Quality from Calculated Quality (Method 2; S1 and S2)**

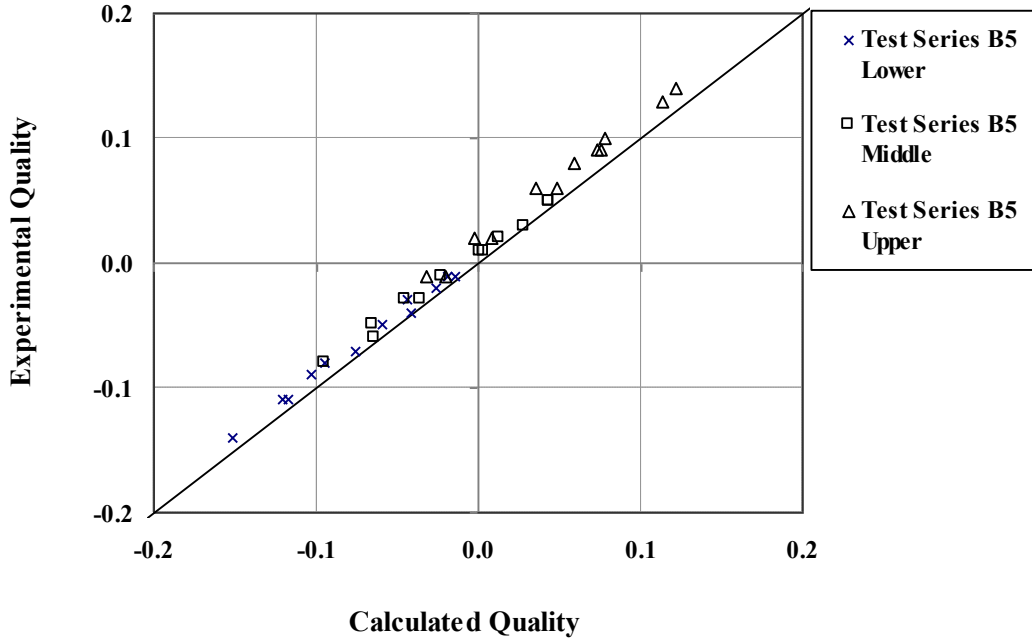
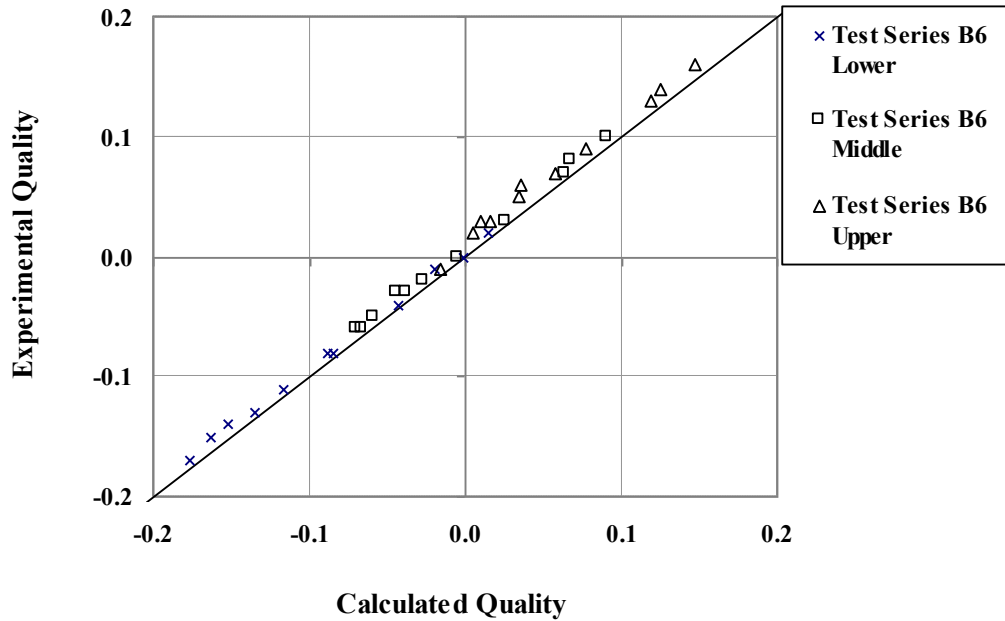
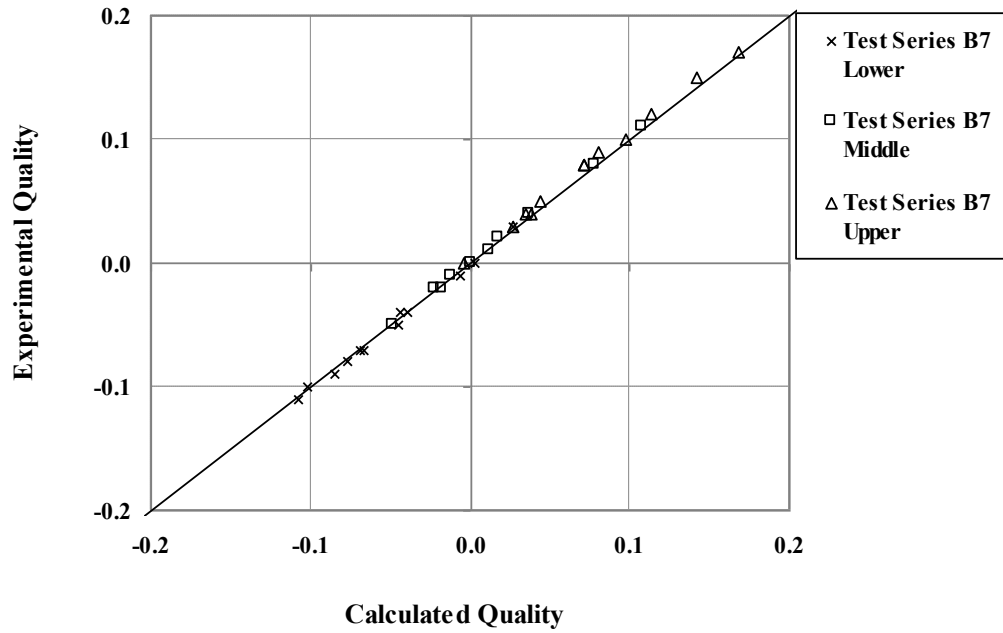
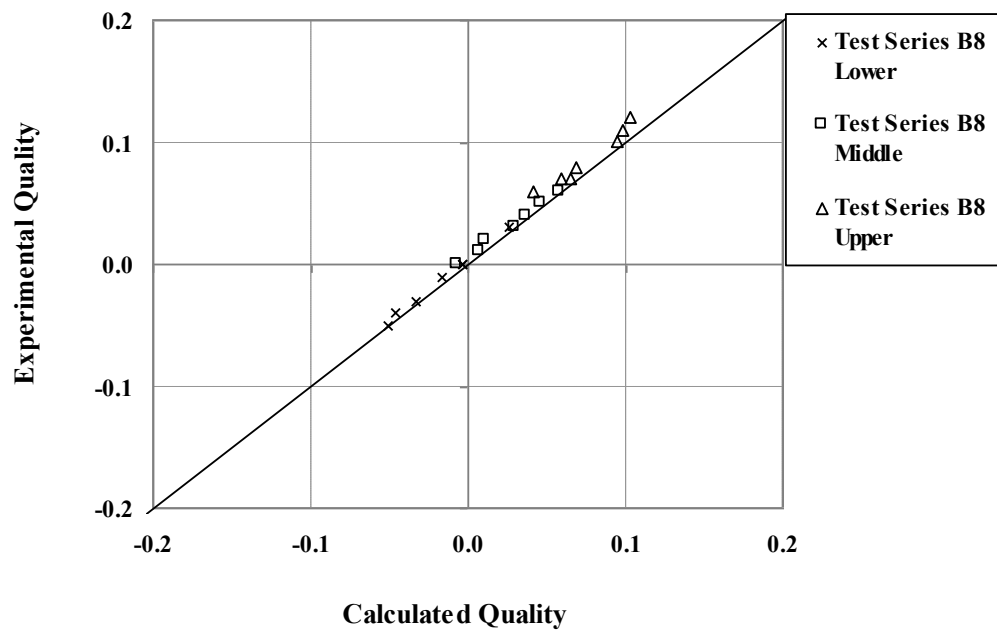
Figure 11: Deviation of Experimental Quality from Calculated Quality (Method 2; B5)**Figure 12: Deviation of Experimental Quality from Calculated Quality (Method 2; B6)**

Figure 13: Deviation of Experimental Quality from Calculated Quality (Method 2; B7)**Figure 14: Deviation of Experimental Quality from Calculated Quality (Method 2; B8)**

Chapter 3: Test assembly data

3.1 General

This chapter provides the participants with geometry and material data for the PWR rod bundles and the single sub-channel apparatus utilised in the void distribution and DNB measurements. The power distribution patterns, radial and axial, as well as the tests conditions are described. Data for the fuel assemblies and spacers' dimensions, heater rods specifications and material properties are also given.

3.2 Void Distribution Data

Two different test assemblies were used for the void distribution measurements: a single sub-channel and a full-size PWR fuel assembly. These assemblies and their characteristics are outlined in Table 11. The thimble rods in the bundle assemblies are filled with stratified water. In such rods, the bottom of the tube structure is open to the flow while a pin hole is located at the top of the structure.

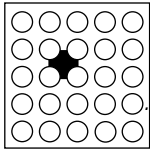
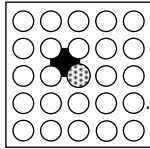
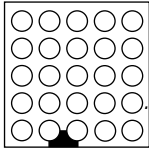
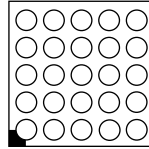
Table 11: Test Assemblies for Void Fraction Measurements

Assembly	Reference fuel type	Type of cell		Power distribution	
				Radial	Axial
S1	17×17 M	Subchannel	Center (Typical)	-	Uniform
S2			Center (Thimble)	-	Uniform
S3			Side	-	Uniform
S4			Corner	-	Uniform
B5	17×17 M	5×5 Rod bundle	Typical cell	A	Uniform
B6			Typical cell	A	Cosine
B7			Thimble cell	B	Cosine

3.2.1 Single Sub-channel Specification

Table 12 outlines the four different sub-channels used to perform the void distribution measurements. Figure 15 shows a cross-sectional view of the sub-channel test assembly.

Table 12: Geometry and Power Shape for Test Assembly S1, S2, S3, and S4

Item	Data			
Assembly (Subjected sub-channel)				
	S1	S2	S3	S4
Sub-channel type	Center (Typical)	Center (Thimble)	Side	Corner
Number of heaters	4×1/4	3×1/4	2×1/4	1×1/4
Axial heated length (mm)	1555	1555	1555	1555
Axial power shape	Uniform	Uniform	Uniform	Uniform

■ : Subjected sub-channel ○ Heated rod ⊙ Thimble rod

Figure 15: Cross-Sectional View of Sub-channel Test Assembly

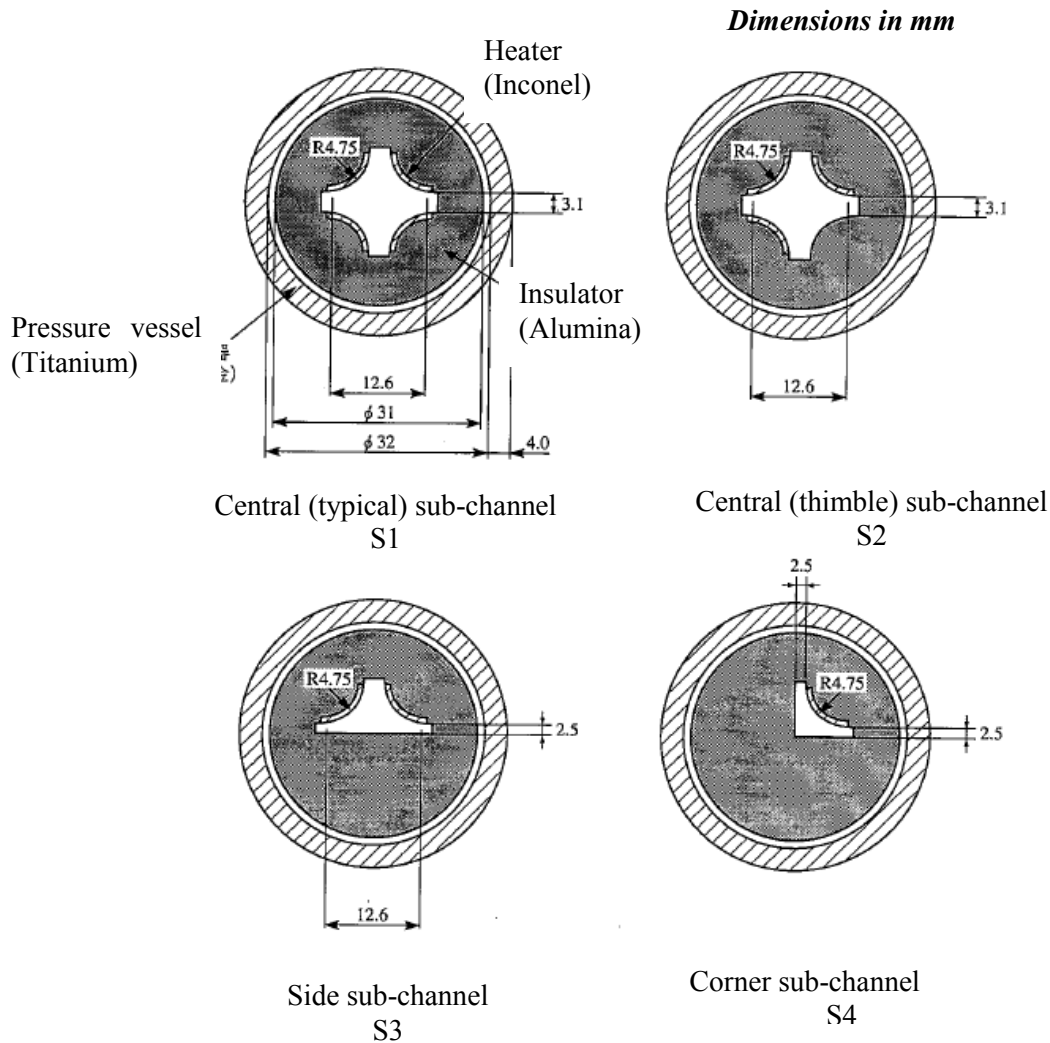


Table 13: Geometric Characteristics of Sub-channel Assemblies

	Sub-channel type			
	Typical (S1)	Thimble (S2)	Side (S3)	Corner (S4)
Flow area, mm ²	107.098	107.098	68.464	42.592
Heated perimeter, mm	29.845	22.384	14.923	7.461
Wetted perimeter, mm	54.645	54.645	44.923	33.161

3.2.1.1 Heater Rod Structure for Sub-channel Test Assembly

Table 14 describes the properties of the heater rod used in the sub-channel test assembly. Figure 15 provides a diagram of the cross-sectional structure of the heater rods in the sub-channel test assembly.

Table 14: Heater Rod Structure for Sub-channel Test Assembly

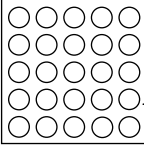
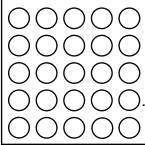
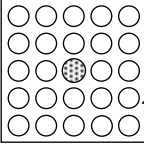
Item		Data
Heater	Outer radius (mm)	4.75
	Thickness (mm)	0.85
	Material	Inconel 600
	Heating method	Direct Heating
Insulator	Outer diameter (mm)	31
	Material	Alumina
Pressure vessel	Inner diameter (mm)	32
	Thickness (mm)	4
	Material	Titanium

3.2.2 Bundle Specification

Table 15 outlines the three different bundles used to perform the void distribution measurements. Figure 16 shows the locations of the ten pressure taps inserted into the rod bundle to measure pressure loss. Figures 17 and 18 show the two different radial power distributions, named A and B, respectively. All powers shown are relative powers.

Table 16 shows the axial power distribution (based on a cosine shape) that was used in the bundle tests.

Table 15: Geometry and Power Shape for Test Assembly B5, B6, and B7

Item	Data		
Assembly			
	B5	B6	B7
Rods array	5×5	5×5	5×5
Number of heated rods	25	25	24
Number of thimble rods	0	0	1
Heated rod outer diameter (mm)	9.50	9.50	9.50
Thimble rod outer diameter (mm)	-	-	12.24
Heated rods pitch (mm)	12.60	12.60	12.60
Axial heated length (mm)	3658	3658	3658
Flow channel inner width (mm)	64.9	64.9	64.9
Radial power shape	A	A	B
Axial power shape	Uniform	Cosine	Cosine
Number of MV spacers	7	7	7
Number of NMV spacers	2	2	2
Number of simple spacers	8	8	8
MV spacer location (mm)	471, 925, 1378, 1832, 2285, 2739, 3247		
NMV spacer location (mm)	2.5, 3755		
Simple spacer location (mm)	237, 698, 1151, 1605, 2059, 2512, 2993, 3501		

○: Heated rod ⊗: Thimble rod

MV: Mixing vane, NMV: No mixing vane

Spacer location is distance from bottom of heated length to spacer bottom face.

Figure 16: Location of Pressure Taps

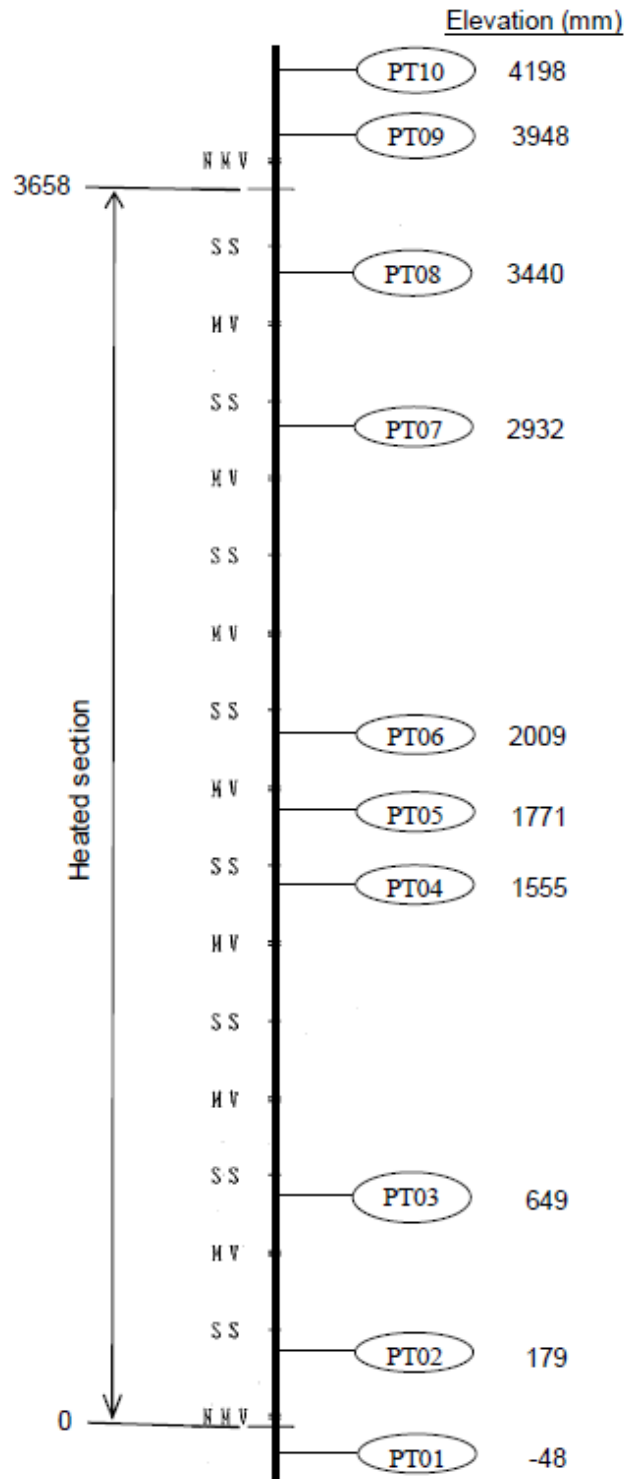


**Figure 17: Radial Power Distribution
Type A**

0.85	0.85	0.85	0.85	0.85
0.85	1.00	1.00	1.00	0.85
0.85	1.00	1.00	1.00	0.85
0.85	1.00	1.00	1.00	0.85
0.85	0.85	0.85	0.85	0.85

**Figure 18: Radial Power Distribution
Type B**

0.85	0.85	0.85	0.85	0.85
0.85	1.00	1.00	1.00	0.85
0.85	1.00	0.00	1.00	0.85
0.85	1.00	1.00	1.00	0.85
0.85	0.85	0.85	0.85	0.85

Table 16: Axial Power Distribution (Cosine)

Node	Relative Power
	<i>Cosine</i>
<i>(Bottom)</i>	
1	0.42
2	0.47
3	0.56
4	0.67
5	0.80
6	0.94
7	1.08
8	1.22
9	1.34
10	1.44
11	1.51
12	1.55
13	1.55
14	1.51
15	1.44
16	1.34
17	1.22
18	1.08
19	0.94
20	0.80
21	0.67
22	0.56
23	0.47
24	0.42
<i>(Top)</i>	

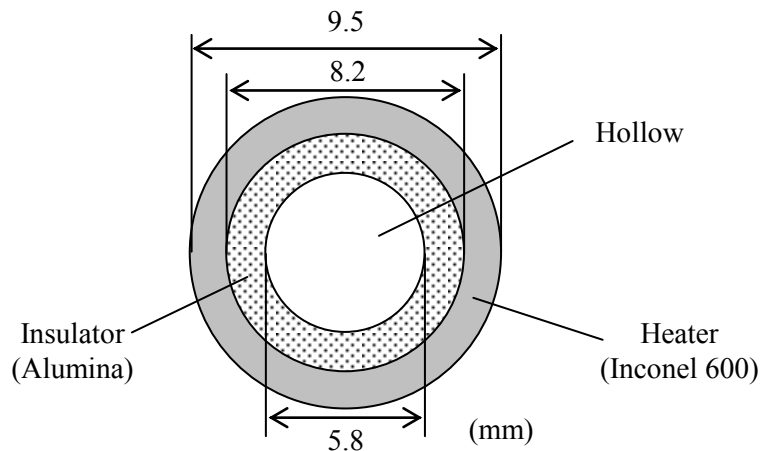
3.2.2.1 Heater Rod Structure for Bundle Test Assembly

Table 17 describes the properties of the heater rods used for the rod bundle test assembly. The insulator and the heater are made of inconel and alumina respectively, and the gap between the heater and insulator could be assumed zero contact. The rod is a single-ended, grounded electrical heater rod, which simulates the heat generation from a fuel rod. Figure 19 shows a cross-sectional view of the bundle heater rod.

Table 17: Heater Rod Structure for Bundle Test Assembly

Item		Data
Heater	Outer diameter (mm)	9.5
	Thickness (mm)	0.65
	Material	Inconel 600
	Heating Method	Direct Heating
Insulator	Outer diameter (mm)	8.2
	Inner diameter (mm)	5.8
	Material	Alumina

Figure 19: Cross-Section of Bundle Heater Rod



3.2.2.2 Spacer Grid Data

There were three types of spacers instrumented along the axial length: simple spacer (SS), spacer with no mixing vanes (NMV), and spacer with mixing vanes (MV). The simple spacer has only dimples while NMV and MV have dimples and springs. The grids straps are made out of Inconel 600 alloy.

Three-dimensional views of the different spacer types are given in Figure 20 through Figure 22.

Figures 23, 24 and 25 show the dimensions of the simple spacer, the non-mixing vanes spacer, and the mixing vanes spacer, respectively. Note that the dimensions in Figure 23 are in millimetres, while the dimensions in Figures 24 and 25 are in inches. The drawings of the spacers were developed using the SolidWorks® mechanical design software package.

Table 18 provides the bundle average spacer pressure loss coefficients for the three types of grids. Depending on the participants' computer code, and using the provided spacer data, each participant may choose the sub-channel grids loss coefficients or other required input values.

Table 18: Bundle Average Spacer Pressure Loss Coefficients

Spacer type	Loss coefficient
Simple spacer (SS)	0.4
Non-mixing vanes spacer (NMV)	0.7
Mixing vanes spacer (MV)	1.0

Figure 20: Three-Dimensional View of the Simple Spacer

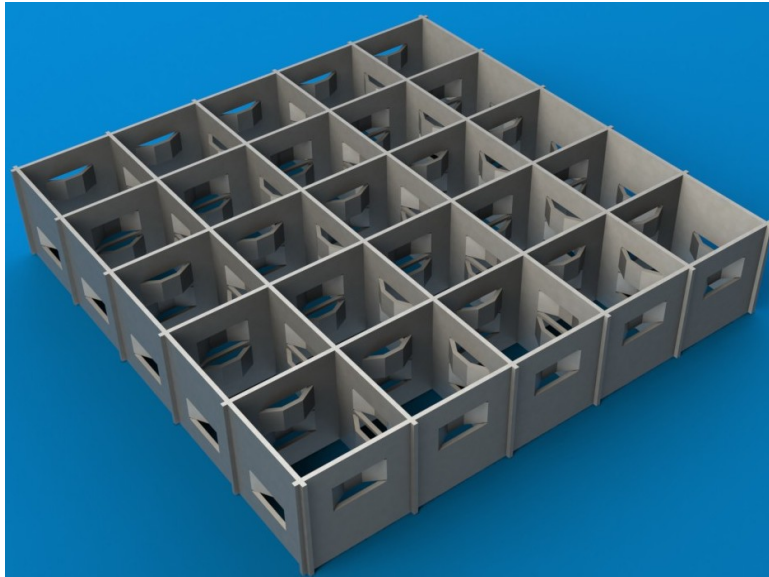


Figure 21: Three-Dimensional View of the Non-Mixing Vane Spacer

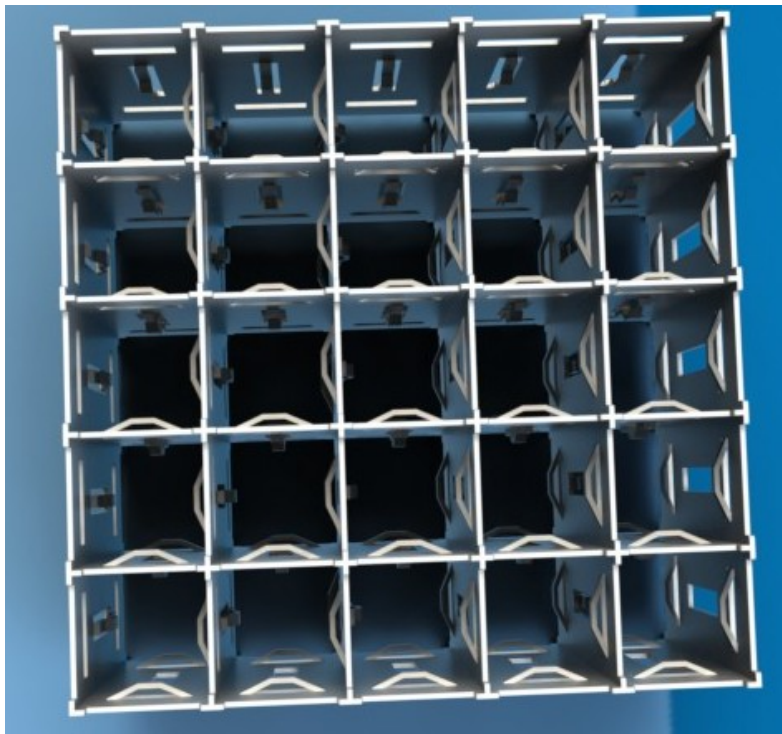
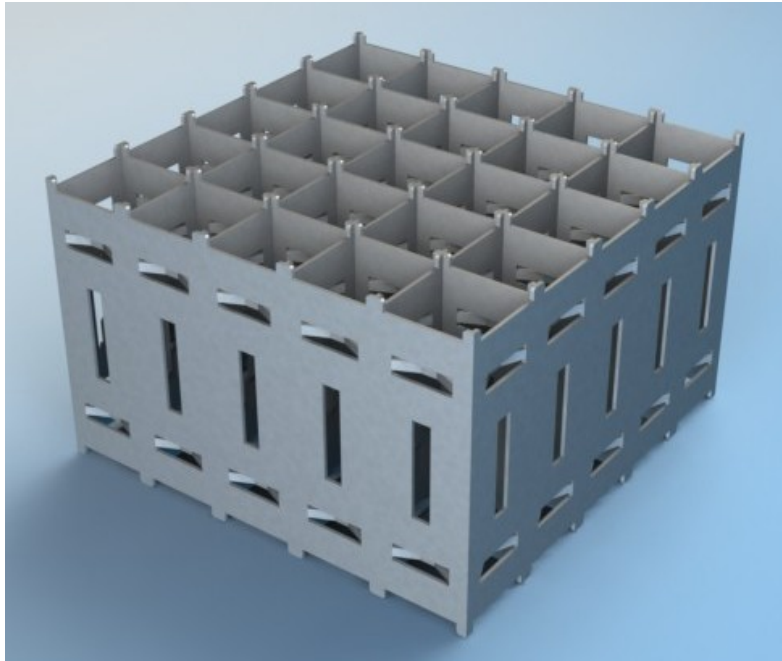


Figure 22: Three-Dimensional View of the Mixing Vane Spacer

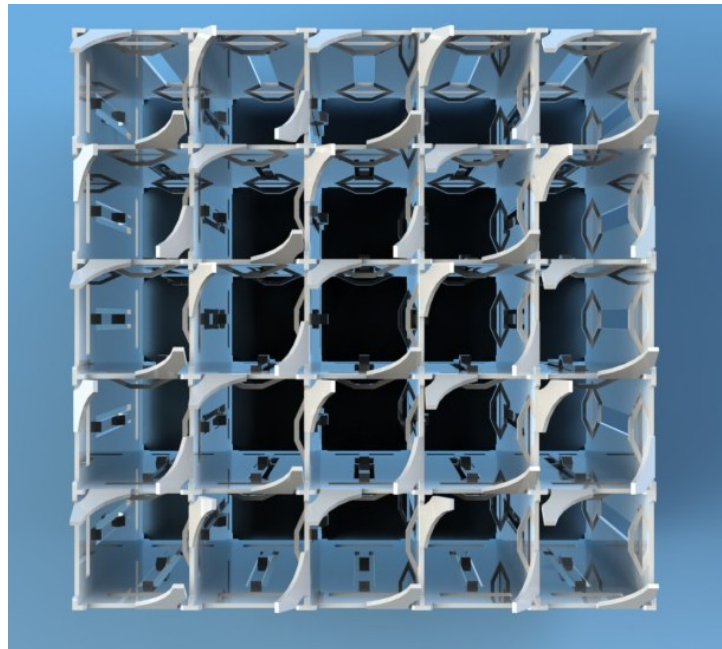
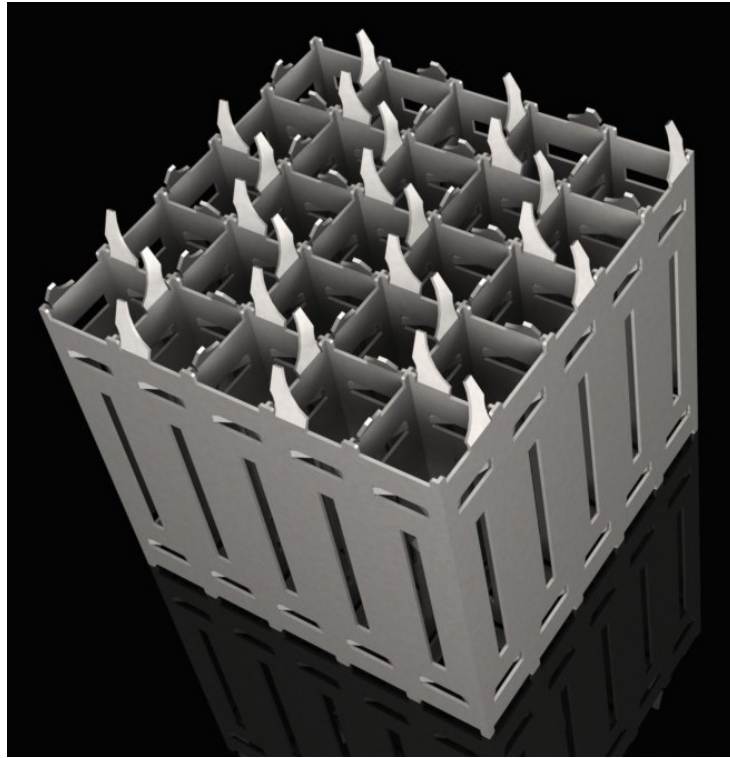
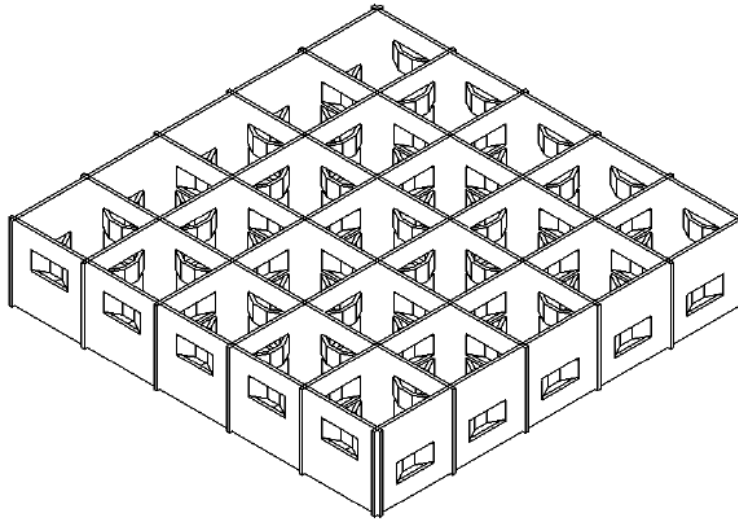
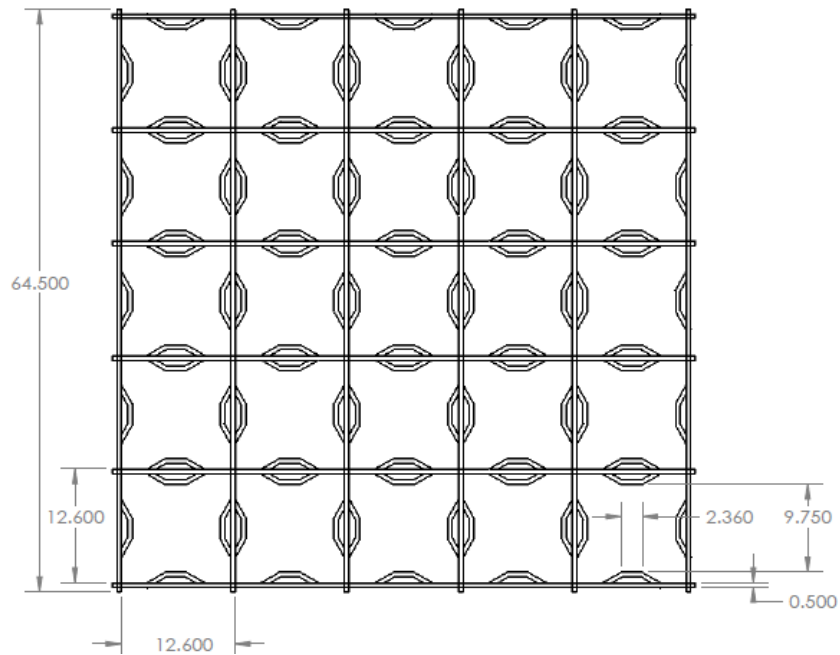
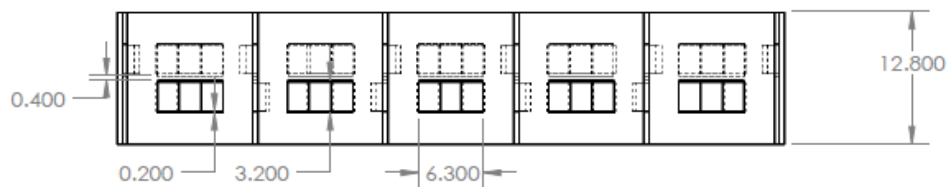


Figure 23: Dimensions of the Simple Spacer

a) Overall Schematic

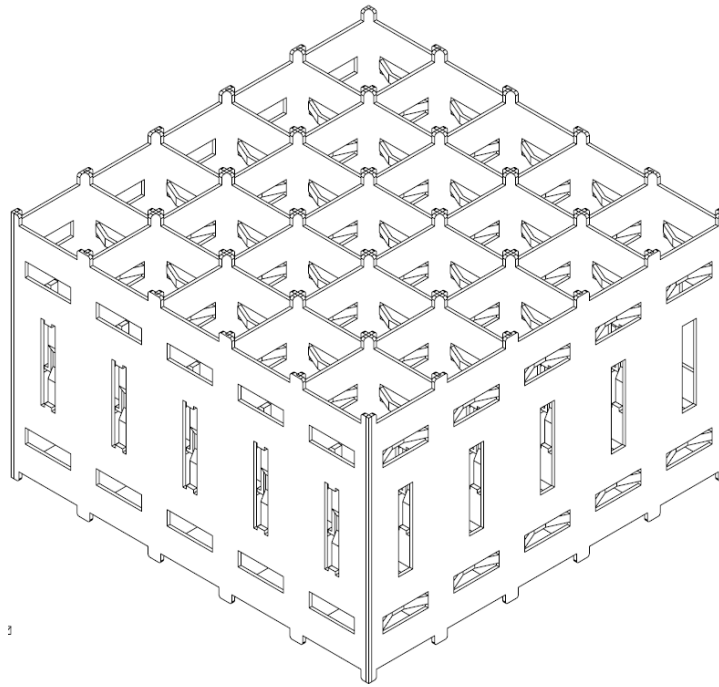


b) Top View

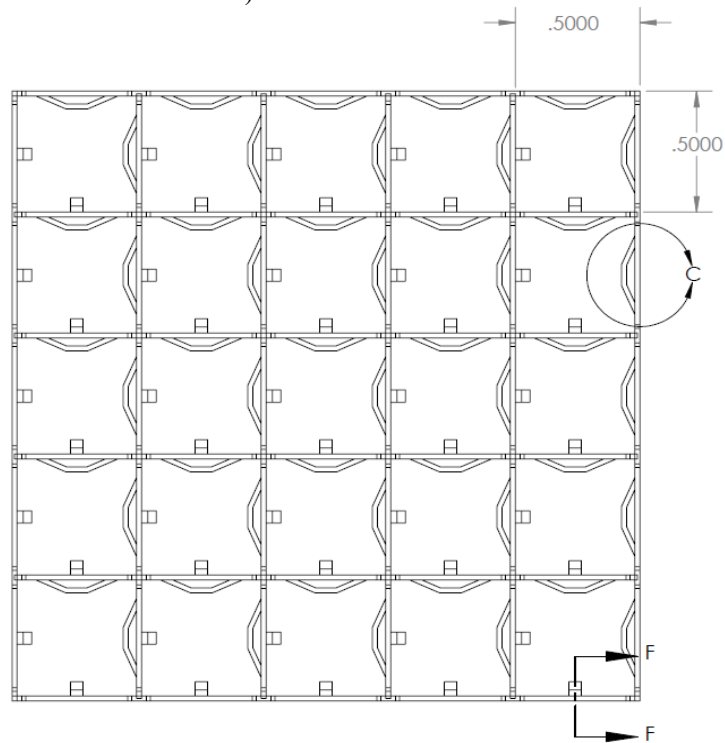


c) Side View

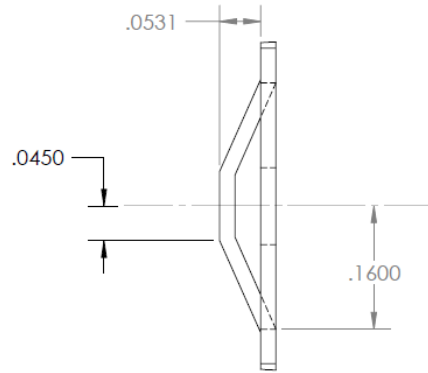
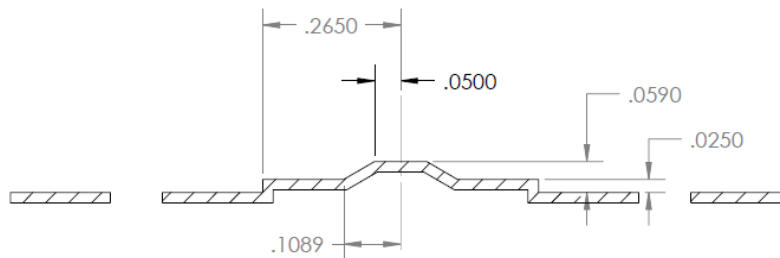
Figure 24: Dimensions of the Non-Mixing Vane Spacer



a) Overall Schematic

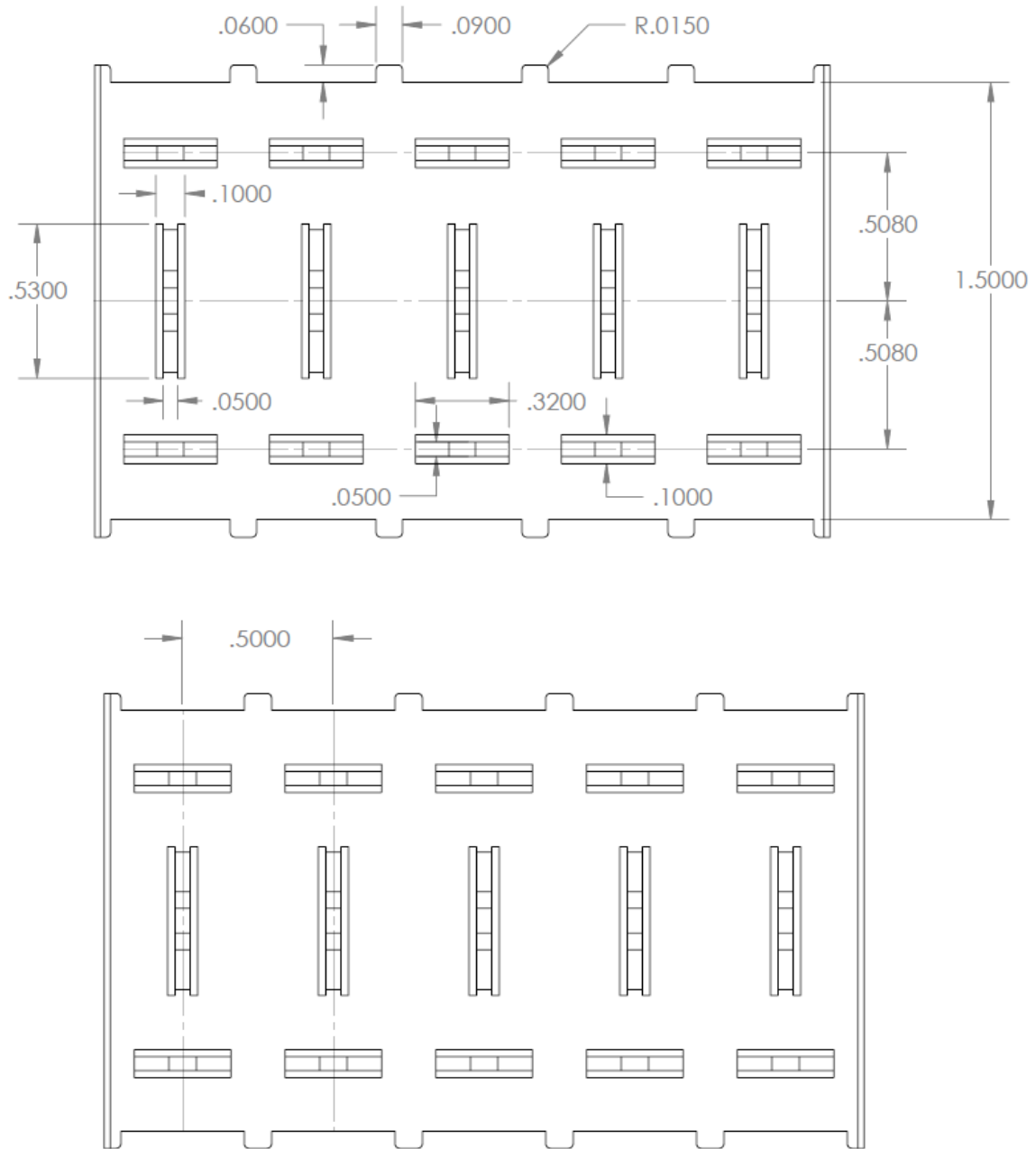


b) Top View

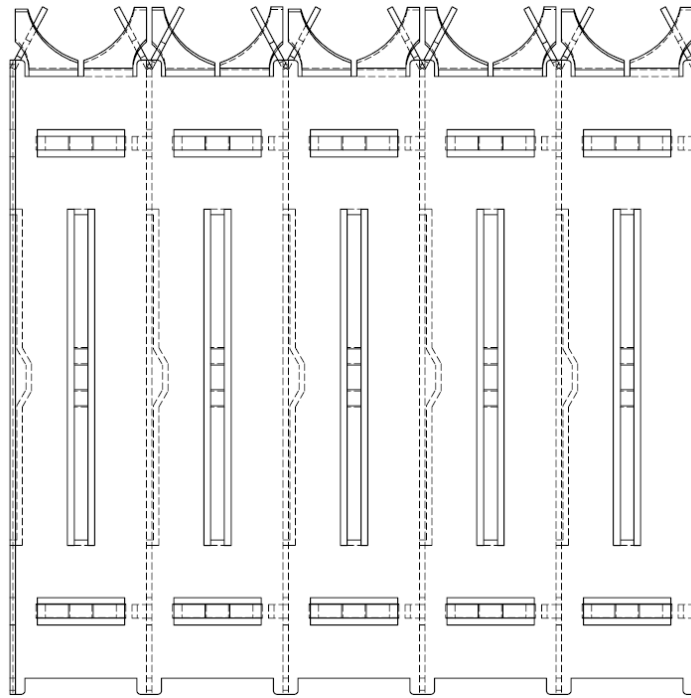
Figure 24: Dimensions of the Non-Mixing Vane Spacer – ContinuedDETAIL C
SCALE 6 : 1SECTION F-F
SCALE 4 : 1

c) Springs and Dimples Dimensions

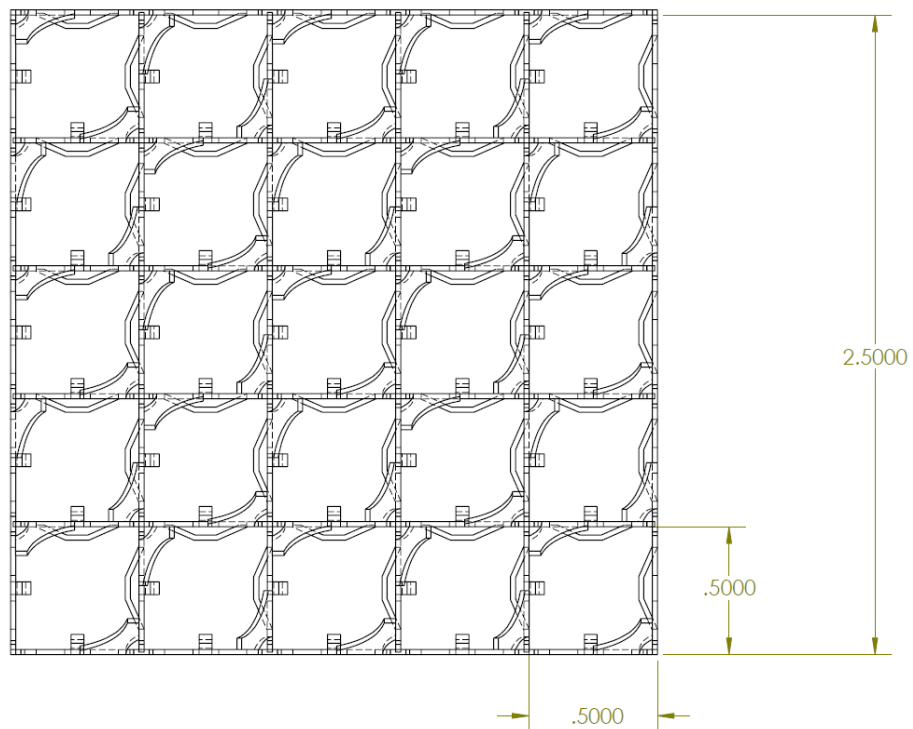
Figure 24: Dimensions of the Non-Mixing Vane Spacer – Continued



d) Side Views

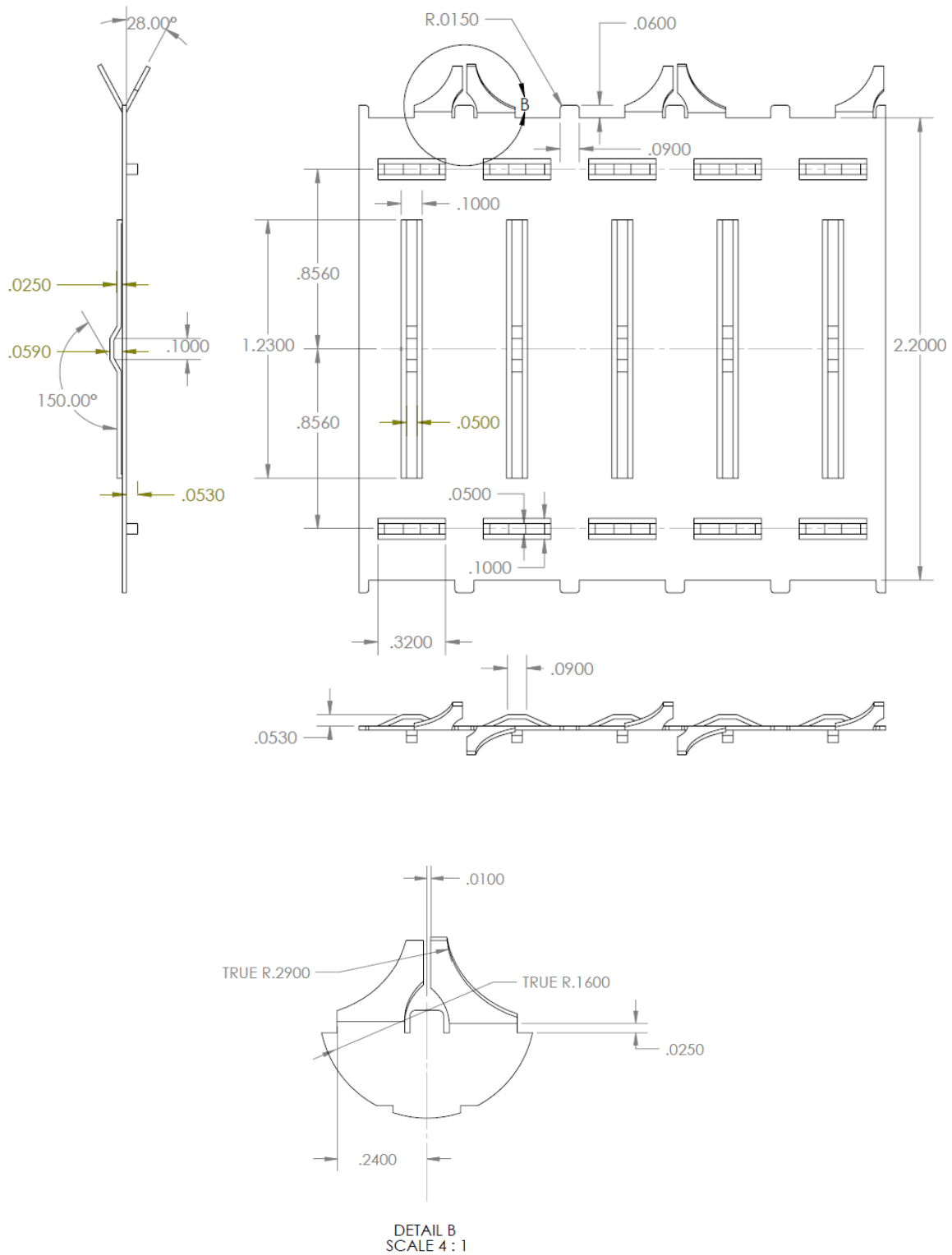
Figure 25: Dimensions of the Mixing Vane Spacer

a) Side View



b) Top View

Figure 25: Dimensions of the Mixing Vane Spacer – Continued



c) Mixing Vane Dimensions

3.3 DNB Measurement

Table 19 shows the assembly types used in the DNB measurements. The heater rods used in these bundles are of the same type as those used in the bundles in the void distribution measurement exercises.

Table 20 gives the geometry and power shape for one of the test assemblies, A0. Similar information for the other assembly types is provided.

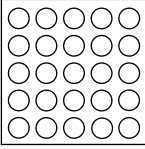
Table 17 provides information on the heating rods used in the rod bundles for this set of tests. Figure 28 displays the locations of the thermocouples for the test assemblies.

The DNB measurements were performed with two additional radial power distributions (type C and type D). Radial power distributions A and B are the same as those used in the void distribution measurements.

Table 19: Test Assemblies for DNB Measurements

Assembly	Reference fuel type	Rods array	Type of cell	Power distribution	
				Radial	Axial
A0	17×17 M	5×5	Typical cell	A	Uniform
A1			Typical cell	C	Uniform
A2			Typical cell	A	Uniform
A3		6×6	Typical cell	D	Uniform
A4		5×5	Typical cell	A	Cosine
A8			Thimble cell	B	Cosine
A11			Typical cell	A	Cosine
A12			Thimble cell	B	Cosine

Table 20: Geometry and Power Shape for Test Assembly A0

Item	Data
Assembly	 A0
Rods array	5×5
Number of heated rods	25
Number of thimble rods	0
Heated rod outer diameter (mm)	9.50
Thimble rod outer diameter (mm)	-
Heated rods pitch (mm)	12.60
Axial heated length (mm)	3 658
Flow channel inner width (mm)	64.9
Radial power shape	A
Axial power shape	Uniform
Number of MV spacers	5
Number of NMV spacers	2
Number of simple spacers	6
MV spacer location (mm)	610, 1 219, 1829, 2 438, 3 048
NMV spacer location (mm)	0, 3658
Simple spacer location (mm)	305, 914, 1524, 2134, 2 743, 3 353

○: Heated rod ⊕: Thimble rod

MV: Mixing vane, NMV: No mixing vane

Spacer location is distance from bottom of heated length to spacer bottom face.

Table 21: Geometry and Power Shape for Test Assembly A1, A2, and A3

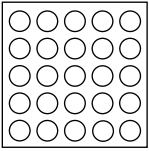
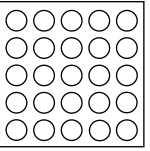
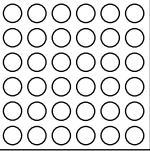
Item	Data		
Assembly	 A1	 A2	 A3
Rods array	5×5	5×5	6×6
Number of heated rods	25	25	36
Number of thimble rods	0	0	0
Heated rod outer diameter (mm)	9.50	9.50	9.50
Thimble rod outer diameter (mm)	-	-	-
Heated rods pitch (mm)	12.60	12.60	12.60
Axial heated length (mm)	3 658	3 658	3 658
Flow channel inner width (mm)	64.9	64.9	77.5
Radial power shape	C	A	D
Axial power shape	Uniform	Uniform	Uniform
Number of MV spacers	7	7	7
Number of NMV spacer	2	2	2
Number of simple spacers	8	8	8
MV spacer location (mm)	457, 914, 1 372, 1 829, 2 286, 2 743, 3 200		
NMV spacer location (mm)	0, 3 658		
Simple spacer location (mm)	229, 686, 1 143, 1 600, 2 057, 2 515, 2 972, 3 429		

Table 22: Geometry and Power Shape for Test Assembly A4, A8, A11, and A12

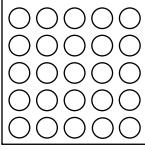
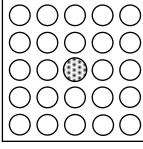
Item	Data	
Assembly	 A4, A11	 A8, A12
Rods array	5×5	5×5
Number of heated rods	25	24
Number of thimble rods	0	1
Heated rod outer diameter (mm)	9.50	9.50
Thimble rod outer diameter (mm)	-	12.24
Heated rods pitch (mm)	12.60	12.60
Axial heated length (mm)	3 658	3 658
Flow channel inner width (mm)	64.9	64.9
Radial power shape	A	B
Axial power shape	Cosine	Cosine
Number of MV spacers	7	7
Number of NMV spacer	2	2
Number of simple spacers	8	8
MV spacer location (mm)	471, 925, 1 378, 1 832, 2 285, 2 739, 3 247	
NMV spacer location (mm)	2.5, 3 755	
Simple spacer location (mm)	237, 698, 1 151, 1 605, 2 059, 2 512, 2 993, 3 501	

Figure 26: Radial Power Distribution Type C

1.00	1.00	0.25	0.25	0.25
1.00	1.00	1.00	0.25	0.25
1.00	1.00	0.25	0.25	0.25
1.00	1.00	1.00	0.25	0.25
1.00	1.00	0.25	0.25	0.25

Figure 27: Radial Power Distribution Type D

0.85	0.85	0.85	0.85	0.85	0.85
0.85	1.00	1.00	1.00	1.00	0.85
0.85	1.00	1.00	1.00	1.00	0.85
0.85	1.00	1.00	1.00	1.00	0.85
0.85	1.00	1.00	1.00	1.00	0.85
0.85	0.85	0.85	0.85	0.85	0.85

Figure 28: Location of Thermocouples for Test Assemblies

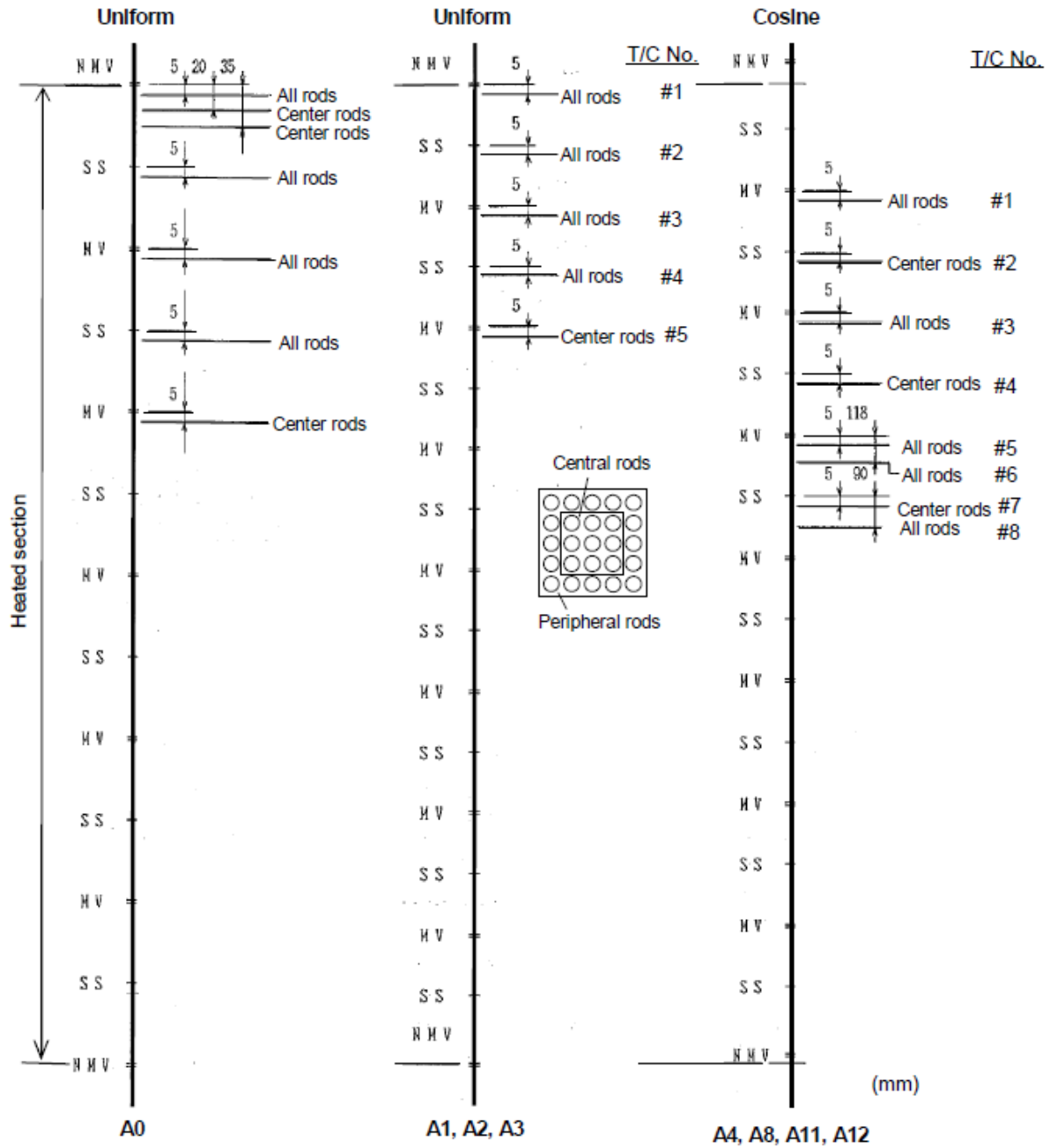
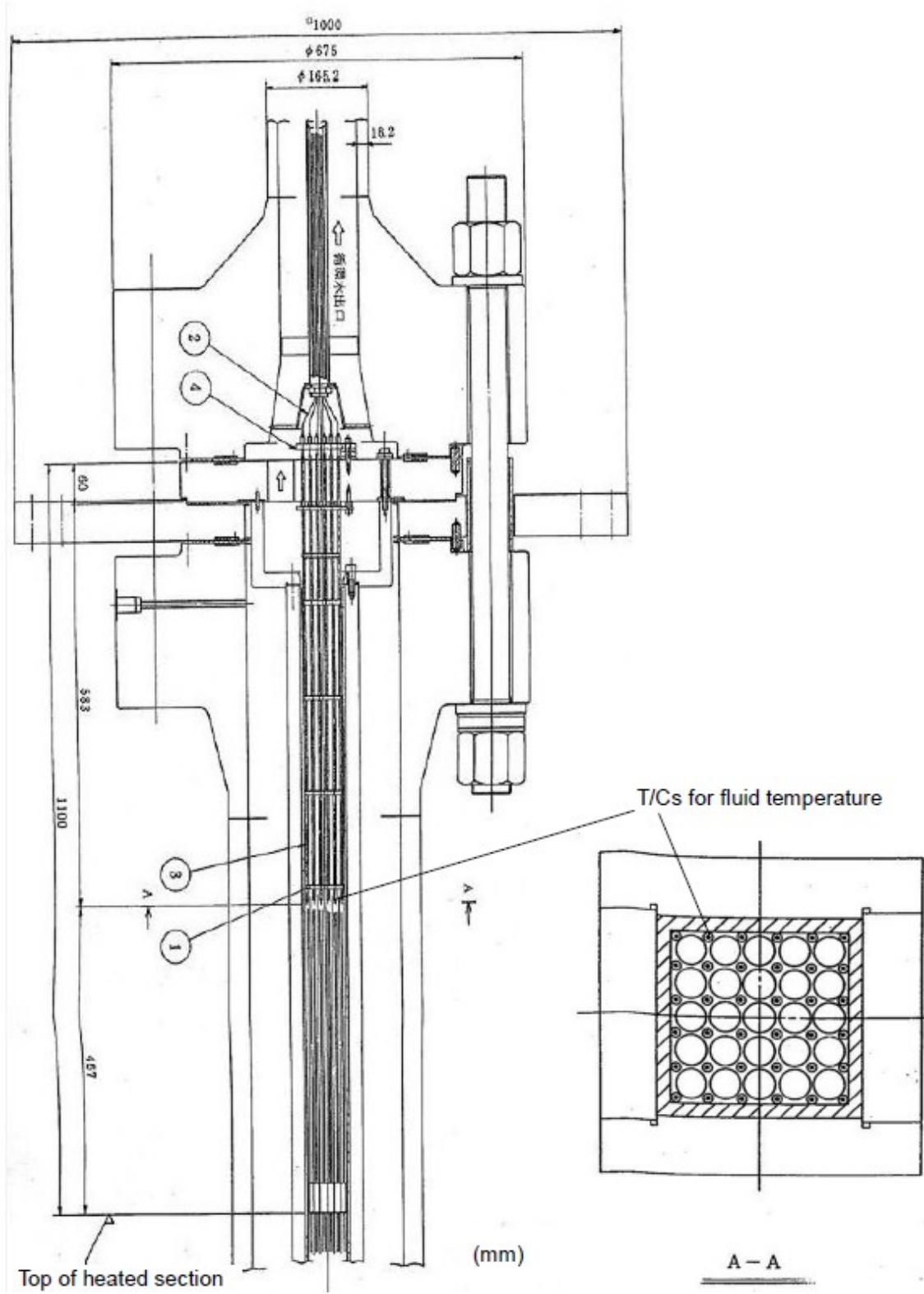


Figure 29: Fluid Temperature Measurements



3.4 Thermo-Mechanical Properties

The thermo-mechanical properties of Inconel 600 are based on the MATPRO model used in TRAC code. Since no information on the heat loss is available in the NUPEC PSBT database, an adiabatic condition is suggested for the benchmark.

3.4.1 Properties of Inconel 600

(1) Density

The density is:

$$\rho = 16.01846 \times (5.261008 \times 10^2 - 1.345453 \times 10^{-2} T_f - 1.194357 \times 10^{-7} T_f^2),$$

where ρ is the density (kg/m³) and T_f is the temperature (F).

(2) Specific Heat

The specific heat is:

$$c_p = 4186.8 \times (0.1014 + 4.378952 \times 10^{-5} T_f - 2.046138 \times 10^{-8} T_f^2 + 3.418111 \times 10^{-11} T_f^3 - 2.060318 \times 10^{-13} T_f^4 + 3.682836 \times 10^{-16} T_f^5 - 2.458648 \times 10^{-19} T_f^6 + 5.597571 \times 10^{-23} T_f^7)$$

where c_p is the specific heat (J/kg.K) and T_f is the temperature (F).

(3) Thermal Conductivity

The thermal conductivity is:

$$k = 1.729577 \times (8.011332 + 4.643719 \times 10^{-3} T_f + 1.872857 \times 10^{-6} T_f^2 - 3.914512 \times 10^{-9} T_f^3 + 3.475513 \times 10^{-12} T_f^4 - 9.936696 \times 10^{-16} T_f^5)$$

where k is the thermal conductivity (W/m.K) and T_f is the temperature (F).

3.4.2 Properties of Alumina

It is assumed that 99.5% Aluminum Oxide (Al₂O₃) is used.

(1) Density

A constant value of 3.89 g/cm³ is to be used.

(2) Specific Heat

A constant value of 880 J/kg-K is to be used.

(3) Thermal Conductivity

A constant value of 35 W/m-K is to be used.

3.4.3 Properties of Titanium

(1) **Density:** A constant value of 4.54 g/cm³ is to be used.

(2) **Specific Heat:** A constant value of 502.44 J/kg-K is to be used.

(3) **Thermal Conductivity:** A constant value of 16.44 W/m-K is to be used.

Chapter 4: Benchmark phases and exercises

4.1 Introduction

The OECD/NRC PSBT benchmark consists of two phases with each phase consisting of different exercises. The benchmark phases and exercises are described below.

Phase I – Void distribution benchmark

- Exercise I-1 – Steady-state single sub-channel benchmark
- Exercise I-2 – Steady-state bundle benchmark
- Exercise I-3 – Transient bundle benchmark
- Exercise I-4 – Pressure drop benchmark

Phase II – Departure from Nucleate Boiling benchmark

- Exercise II-1 – Steady-state fluid temperature benchmark
- Exercise II-2 – Steady-state DNB benchmark
- Exercise II-3 – Transient DNB benchmark

The sub-channel approach is categorised as the macroscopic grade approach that can resolve an element as small as a sub-channel size mesh. Time and space averaged formulations cause the loss of the heterogeneous and instantaneous void fraction information of the two-phase flow structure within the sub-channel. As a consequence, many macroscopic correlations are still indispensable for reproducing the experimental results. In recent years, there have been developed newer two-phase flow numerical approaches that can be categorised into meso-, micro- or molecular dynamics approaches. Taking into account the immaturity of numerical modelling for detailed void distribution, this benchmark specification is designed to accept as many potential numerical approaches as possible.

Table 23 provides a guide to the participants where to find the conditions for each benchmark case within each benchmark exercise and phase. Table 24 provides a guide where to find the data for the involved fuel assemblies.

Table 23: NUPEC PSBT Benchmark Database

Items of data	Test series
Void fraction measurements data - Steady-state void fraction in sub-channel by CT measurement - Steady-state void distribution image in sub-channel by CT measurement - Steady-state void fraction in rod bundle by chordal measurement - Steady-state void distribution image in rod bundle by chordal measurement - Transient void fraction in rod bundle by chordal measurement	1, 2, 3, 4 1, 2 5, 6, 7, 8 5, 6, 7, 8 5T, 6T, 7T
DNB measurements data - Steady-state DNB data in rod bundle - Steady-state DNB detected location in rod bundle - Steady-state fluid temperature distribution in rod bundle - Transient DNB data in rod bundle	0, 2, 3, 4, 8, 13 4, 8, 13 1 11T, 12T

Table 24: Benchmark Conditions

Phase	Exercises	Assembly ID	Test series number	Geometrical data	Test matrix / measurement conditions	Related section
Void distribution	<i>Steady-state sub-channel</i>	S1	1	Table 12	Table 26	4.2.1
		S2	2	Table 12	Table 27	4.2.1
		S3	3	Table 12	Table 28	4.2.1
		S4	4	Table 12	Table 29	4.2.1
	<i>Steady-state bundle</i>	B5	5	Table 15	Table 30	4.2.2
		B6	6	Table 15	Table 31	4.2.2
		B7	7	Table 15	Table 32	4.2.2
		B5	8	Table 15	Table 33	4.2.2
	<i>Transient bundle</i>	B5	5T	Table 15	Table 35	4.2.3
		B6	6T	Table 15	Table 35	4.2.3
B7		7T	Table 15	Table 35	4.2.3	
DNB measurement	<i>Steady-state fluid temperature</i>	A1	1	Table 21	Table 49	4.3.1
	<i>Steady-state DNB</i>	A0	0	Table 20	Table 50	4.3.2
		A2	2	Table 21	Table 51	4.3.2
		A3	3	Table 21	Table 52	4.3.2
		A4	4	Table 22	Table 53	4.3.2
		A8	8	Table 22	Table 54	4.3.2
		A4	13	Table 22	Table 55	4.3.2
	<i>Transient DNB</i>	A11	11T	Table 22	Table 56	4.3.3
		A12	12T	Table 22	Table 56	4.3.3

4.2 Phase I - Void Distribution Benchmark

Table 25 summarises the test series used for both the sub-channel and rod bundle void fraction measurements.

Table 25: Test Series for Void Fraction Measurement

Test series	Test section	Assembly	Test mode		Void measurement	
			Steady-state	Transient	CT	Chordal
1	Sub-channel	S1	Y		Y	Y
2		S2	Y		Y	Y
3		S3	Y		Y	Y
4		S4	Y		Y	Y
5	5×5 Rod bundle	B5	Y			Y
5T				Y		Y
6		B6	Y			Y
6T				Y		Y
7		B7	Y			Y
7T				Y		Y
8		B5	Y			Y

4.2.1 Exercise I-1 – Steady-State Single Sub-channel Benchmark

The available experimental data includes CT scan measurements of the void fraction (sub-channel averaged) of four representative sub-channel types: typical central, central with a guide tube, side, and corner sub-channels and images of the void distribution within two representative sub-channel types: typical central and central with a guide tube. The data can be used to assess and improve the current models for void generation (sub-channel/system and CFD codes) and void distribution within sub-channels (CFD codes).

The test matrixes for the steady-state single sub-channel void measurements - Test Series 1, 2, 3, and 4 - are given in Tables 26, 27, 28 and 29, respectively.

The highlighted cases are selected to be analysed as part of the benchmark. The cases in *italics* are selected to be modelled for the investigation of the axial variation of the void fraction.

Table 26: Test Conditions for Steady-State Void Measurement Test Series 1

Run No	Pressure (kg/cm ² a)	Mass flux (10 ⁶ kg/m ² hr)	Power (kW)	Inlet temperature (°C)
1.1221	169.1	10.95	49.9	329.7
<u>1.1222</u>	169.1	10.98	50.0	334.7
<u>1.1223</u>	169.1	11.00	49.9	339.7
1.2121	150.1	14.80	79.9	309.5
1.2122	149.9	14.89	80.1	319.7
<u>1.2211</u>	150.1	10.91	90.0	295.4
1.2212	150.1	10.88	90.0	299.4
<u>1.2221</u>	150.1	10.88	69.8	299.4
<u>1.2223</u>	150.1	10.91	69.8	319.6
1.2231	150.2	10.87	60.0	299.3
1.2233	150.2	10.89	59.9	309.6
1.2234	150.1	10.92	60.1	314.6
1.2235	150.1	10.89	59.9	319.6
1.2236	150.0	10.91	60.0	324.7
<u>1.2237</u>	150.3	10.93	60.0	329.6
1.2421	150.2	5.02	59.8	268.9
<u>1.2422</u>	150.1	5.00	60.0	284.1
<u>1.2423</u>	150.3	4.93	59.9	299.3
1.3221	125.0	11.10	59.9	294.4
1.3222	125.1	10.91	60.0	309.5
1.3223	124.9	11.10	60.1	319.7
1.4121	100.1	10.97	69.9	274.1
1.4122	99.8	10.90	69.8	304.5
<u>1.4311</u>	100.4	5.01	79.9	214.2
<u>1.4312</u>	100.2	5.03	79.8	248.9
1.4321	100.5	5.01	59.9	209.3
1.4323	100.5	5.03	59.9	229.2
1.4324	100.1	5.02	60.1	238.9
<u>1.4325</u>	100.3	5.03	59.8	253.8
<u>1.4326</u>	100.1	5.02	60.1	268.8
1.4327	100.1	4.96	59.9	289.0
1.4411	100.4	1.99	19.9	253.7
1.4412	100.3	1.99	20.0	284.0
<u>1.5221</u>	75.5	5.02	49.9	219.2
<u>1.5222</u>	75.0	5.02	50.0	243.9
1.5223	75.6	5.03	49.9	263.8
1.6211	50.4	5.02	79.7	164.1
1.6212	50.4	5.00	79.8	199.3
<u>1.6221</u>	50.5	5.01	50.0	189.2
<u>1.6222</u>	50.0	5.00	49.9	204.2
1.6223	50.5	5.03	49.9	239.0
1.6311	50.6	1.95	20.1	204.1
1.6312	50.6	1.96	20.1	238.9

Table 27: Test Conditions for Steady-State Void Measurement Test Series 2

Run No	Pressure (kg/cm ² a)	Mass flux (10 ⁶ kg/m ² hr)	Power (kW)	Inlet temperature (°C)
<u>2.1231</u>	168.9	10.98	37.5	335.0
<u>2.1232</u>	168.8	11.00	37.5	340.0
<u>2.1233</u>	168.8	11.01	37.5	345.0
2.2121	149.5	14.89	60.2	319.9
2.2122	149.5	14.88	60.1	325.1
2.2221	149.9	10.91	60.0	310.4
2.2222	149.9	10.92	60.1	314.9
2.2231	149.9	10.91	52.5	310.3
2.2233	149.9	10.95	52.5	330.6
2.2241	150.0	10.90	45.1	304.3
2.2243	149.9	10.91	45.2	314.5
2.2244	149.9	10.91	45.0	320.0
2.2245	149.9	10.91	45.0	325.5
2.2246	150.0	10.95	45.0	329.8
2.2247	150.0	10.98	45.1	334.8
2.2441	150.4	5.00	45.1	289.8
2.2442	150.4	4.98	45.1	304.8
2.2443	150.4	4.99	45.1	320.1
2.3231	125.2	10.90	45.0	304.6
<u>2.3232</u>	125.1	10.91	45.1	309.8
<u>2.3233</u>	125.0	10.91	45.1	319.9
2.4231	100.3	10.96	52.7	279.3
2.4232	100.2	10.89	52.7	299.6
<u>2.4421</u>	100.4	5.03	60.1	244.0
<u>2.4422</u>	100.5	5.02	60.1	279.2
2.4441	100.5	5.03	45.0	234.1
2.4443	100.5	5.03	45.2	253.9
2.4444	100.6	5.03	45.1	263.9
2.4445	100.5	5.02	45.0	274.0
2.4446	100.5	5.01	45.1	284.2
2.4447	100.5	4.98	45.2	299.4
<u>2.4551</u>	100.7	1.79	15.0	274.0
<u>2.4552</u>	100.7	1.78	15.1	294.3
2.5431	75.6	5.03	37.7	239.0
2.5432	75.7	5.03	37.5	263.9
2.5433	75.6	5.02	37.5	279.2
2.6411	50.5	5.01	60.1	194.2
2.6412	50.5	5.03	60.1	229.2
<u>2.6431</u>	50.6	5.01	37.5	209.2
<u>2.6432</u>	50.6	5.02	37.5	224.2
<u>2.6433</u>	50.5	5.03	37.6	253.9
2.6541	50.7	1.79	15.1	224.1
2.6542	50.7	1.79	15.2	253.7

Table 28: Test Conditions for Steady-State Void Measurement Test Series 3

Run No	Pressure (kg/cm ² a)	Mass flux (10 ⁶ kg/m ² hr)	Power (kW)	Inlet temperature (°C)
<u>3.2231</u>	149.9	10.90	40.4	309.4
<u>3.2232</u>	149.9	10.90	40.5	314.5
3.2251	150.0	10.89	30.0	304.3
3.2253	149.9	10.89	30.0	314.4
3.2254	149.9	10.90	30.1	319.5
3.2255	150.0	10.90	30.2	324.5
3.2256	150.0	10.93	30.1	329.6
3.2257	150.0	10.96	30.2	334.5
<u>3.2451</u>	150.3	4.96	30.2	283.8
<u>3.2452</u>	150.5	4.93	30.2	299.0
<u>3.2453</u>	150.3	4.94	30.2	314.3
3.4451	100.5	4.98	30.2	228.9
3.4453	100.5	4.98	30.3	248.8
3.4454	100.4	4.98	30.1	258.6
3.4455	100.6	4.98	30.3	268.8
3.4456	100.6	4.96	30.2	283.7
3.4457	100.6	4.93	30.2	299.0
<u>3.6431</u>	50.4	4.96	40.2	189.0
<u>3.6432</u>	50.4	4.97	40.1	223.9
<u>3.6461</u>	50.6	4.96	25.2	203.9

Table 29: Test Conditions for Steady-State Void Measurement Test Series 4

Run No	Pressure (kg/cm ² a)	Mass flux (10 ⁶ kg/m ² hr)	Power (kW)	Inlet temperature (°C)
4.2231	149.9	11.06	20.3	314.3
4.2232	149.9	11.06	20.3	319.3
<u>4.2251</u>	149.9	11.06	15.2	310.3
<u>4.2253</u>	150.0	11.06	15.1	318.4
4.2254	150.0	11.07	15.2	322.4
4.2255	150.0	11.08	15.2	326.5
<u>4.2256</u>	150.0	11.11	15.1	330.5
<u>4.2257</u>	149.9	11.12	15.1	334.5
4.2451	150.4	5.01	15.2	294.0
4.2452	150.4	5.01	15.2	309.2
4.2453	150.4	5.01	15.2	324.3
4.4451	100.6	5.05	15.2	238.8
4.4453	100.5	5.05	15.2	258.6
4.4454	100.5	5.04	15.1	268.7
<u>4.4455</u>	100.5	5.04	15.2	278.8
<u>4.4456</u>	100.5	5.02	15.2	289.0
4.4457	100.5	5.00	15.2	299.1
4.6431	50.6	5.02	20.2	204.1
4.6432	50.5	5.05	20.3	238.8
<u>4.6461</u>	50.6	5.03	12.5	214.0

4.2.2 Exercise I-2 – Steady-State Bundle Benchmark

The experimental data include X-ray densitometer measurements of void fraction (chordal averaged) at three axial elevations. The averaging is over the four central sub-channels. Images of the bundle void distribution are available as well. The data can be applied to thermal-hydraulic sub-channel and system codes and CFD codes.

The test matrixes for the steady-state bundle void measurements - Test Series 5, 6, 7, and 8 - are given in Tables 30, 31, 32 and 33, respectively.

The highlighted cases are selected to be analysed as part of the benchmark.

Table 30: Test Conditions for Steady-State Void Measurement Test Series 5

Run No	Pressure (kg/cm ² a)	Mass flux (10 ⁶ kg/m ² hr)	Power (kW)	Inlet temperature (°C)
5.1121	167.39	14.96	2 990	316.9
5.1122	167.25	15.02	2 995	322.0
<u>5.1221</u>	168.29	11.00	3 000	292.3
<u>5.1222</u>	168.27	10.98	2 998	297.3
5.1231	168.29	10.97	2 488	311.8
5.1232	168.29	10.98	2 486	316.6
5.1331	168.80	7.95	2 491	287.2
5.1332	168.71	7.93	2 491	292.2
5.1341	168.76	7.90	2 005	312.2
5.1342	168.83	7.91	2 005	317.2
5.1451	169.19	4.99	1 515	302.3
5.1452	169.19	4.98	1 516	312.5
<u>5.2111</u>	148.15	15.08	3 296	291.9
<u>5.2112</u>	148.04	14.98	3 294	296.8
5.2131	148.02	14.99	2 360	316.5
5.2132	147.67	15.01	2 361	321.8
5.2221	149.06	11.06	2 972	287.2
5.2222	149.18	11.04	2 965	292.5
5.2231	149.16	10.95	2 364	301.7
5.2232	148.83	11.01	2 360	311.8
5.2241	148.92	11.00	1 901	316.8
5.2242	148.78	11.01	1 898	321.6
5.2331	149.57	8.03	2 481	277.5
<u>5.2332</u>	149.82	7.94	2 523	287.8
5.2341	149.72	7.97	1 902	302.0
5.2342	149.51	7.91	1 901	312.2
5.2351	149.71	7.89	1 431	316.8
5.2352	149.63	7.94	1 433	321.9
<u>5.2442</u>	149.97	4.99	2 000	263.0
5.2451	150.10	4.94	979	311.4
5.2452	150.16	4.90	964	321.8
5.3111	123.65	15.10	3 480	276.7
5.3112	123.52	15.10	3 489	281.7
5.3221	124.55	11.06	2 997	271.8

Table 30: Test Conditions for Steady-State Void Measurement Test Series 5 – Continued

Run No	Pressure (kg/cm ² a)	Mass flux (10 ⁶ kg/m ² hr)	Power (kW)	Inlet temperature (°C)
5.3222	124.31	11.07	2 988	277.0
5.3321	124.88	8.00	3 000	243.0
5.3322	124.77	8.00	2 998	248.0
5.3331	124.89	8.00	2 491	267.1
5.3332	124.96	7.99	2 494	277.3
<u>5.3441</u>	125.22	5.00	2 014	247.9
<u>5.3442</u>	125.13	5.00	2 013	257.7
5.4211	98.71	11.12	3 478	242.6
5.4212	98.70	11.11	3 480	247.7
5.4321	99.28	8.09	2 984	237.9
5.4322	99.21	8.07	2 985	243.1
5.4431	99.89	4.91	2 507	199.2
5.4432	100.09	5.02	2 449	204.3
5.4441	100.02	4.97	2 003	223.2
5.4442	99.97	5.02	2 007	233.4
5.4561	100.33	2.03	1 018	204.4
<u>5.4562</u>	100.23	2.02	1 016	214.3
5.5201	74.44	11.07	4 018	208.2
5.5202	74.36	11.07	4 021	213.2
5.5311	74.95	8.07	3 506	193.8
5.5312	74.87	8.13	3 511	204.0
5.5321	75.00	8.05	3 017	203.6
5.5322	74.93	8.03	3 016	218.6
5.5431	75.21	5.07	2 520	174.2
5.5432	75.18	5.05	2 518	184.2
5.5441	75.13	5.01	2 020	203.6
5.5442	75.27	5.02	2 022	213.6
5.5551	75.41	2.00	1 028	183.0
5.5552	75.40	2.00	1 026	193.2
5.6311	48.99	7.86	3 496	163.8
5.6312	48.85	7.85	3 492	173.9
<u>5.6321</u>	49.20	7.87	3 000	173.5
<u>5.6322</u>	49.08	7.86	3 000	183.6
5.6431	49.82	4.93	2 507	149.4
5.6432	49.73	4.96	2 506	159.3
5.6441	49.92	4.96	2 016	168.6
5.6442	49.84	4.96	2 017	178.5
5.6551	50.17	2.00	1 028	149.1
<u>5.6552</u>	50.17	2.00	1 028	159.1

Table 31: Test Conditions for Steady-State Void Measurement Test Series 6

Run No	Pressure (kg/cm ² a)	Mass flux (10 ⁶ kg/m ² hr)	Power (kW)	Inlet temperature (°C)
6.1121	167.59	15.16	3 372	301.5
6.1122	167.56	15.17	3 376	306.7
6.1221	168.24	11.32	3 390	274.9
6.1222	168.28	11.32	3 391	280.2
6.1231	168.23	11.25	2 890	296.7
6.1232	168.26	11.25	2 889	301.9
6.1331	168.65	8.23	2 891	262.1
6.1332	168.68	8.22	2 891	267.2
6.1341	168.75	8.18	2 398	286.9
6.1342	168.67	8.18	2 398	291.9
6.1451	169.03	5.20	1 914	267.4
6.1452	169.06	5.20	1 915	272.5
6.2111	148.13	15.32	3 882	276.4
6.2112	148.60	15.30	3 879	281.5
6.2131	148.50	15.21	2 884	303.4
6.2132	148.40	15.23	2 886	311.8
6.2221	149.41	11.34	3 394	271.7
6.2222	149.21	11.07	3 597	277.3
6.2231	149.42	11.31	2 894	281.7
6.2232	149.27	11.30	2 894	291.9
6.2241	149.29	11.27	2 398	301.6
6.2242	149.24	11.25	2 396	306.8
6.2331	149.78	8.24	2 899	257.2
6.2332	149.64	7.97	3 013	267.2
6.2341	149.69	8.21	2 387	281.7
6.2342	149.75	8.21	2 398	289.0
6.2351	149.72	8.17	1 897	306.8
6.2352	149.71	8.17	1 897	313.8
6.2441	150.01	5.16	2 415	223.5
6.2442	150.02	5.12	2 412	228.4
6.2461	150.17	5.08	957	311.6
6.2462	150.20	5.09	957	321.7
6.3121	123.73	15.12	3 308	276.2
6.3122	123.62	15.12	3 305	286.4
6.3231	124.58	11.09	2 846	271.4
6.3232	124.37	11.09	2 842	281.8
6.3331	124.90	8.03	2 840	242.3
6.3332	124.84	8.02	2 839	252.1
6.3341	124.91	8.02	2 373	266.9
6.3342	124.91	8.01	2 375	282.1
6.3451	125.15	5.01	1 924	242.8
6.3452	125.20	5.00	1 920	262.5
6.4221	99.66	11.11	3 333	227.4
6.4222	99.53	11.11	3 317	241.3
6.4331	99.91	8.03	2 862	222.9
6.4332	99.94	8.04	2 854	242.6

Table 31: Test Conditions for Steady-State Void Measurement Test Series 6 - Continued

Run No	Pressure (kg/cm ² a)	Mass flux (10 ⁶ kg/m ² hr)	Power (kW)	Inlet temperature (°C)
6.4441	100.19	5.03	2 382	183.7
6.4442	100.11	5.03	2 833	204.3
6.4451	100.19	5.01	1 923	213.1
6.4452	100.22	5.01	1 922	232.9
<u>6.4561</u>	100.42	2.05	973	192.6
<u>6.4562</u>	100.41	2.05	972	213.0
6.5211	74.58	11.11	3 803	197.9
6.5212	74.53	11.09	3 802	213.0
6.5321	75.00	8.07	3 335	173.3
6.5322	74.95	8.06	3 336	193.5
6.5331	74.96	8.05	2 857	187.8
6.5332	75.04	8.03	2 862	202.8
6.5441	75.27	5.05	2 392	153.7
6.5442	75.25	5.05	2 392	173.8
6.5451	75.22	5.02	1 921	183.2
6.5452	75.25	5.01	1 920	203.8
6.5561	75.41	2.06	977	163.5
6.5562	75.41	2.06	974	178.2
6.6321	49.90	8.09	3 351	153.4
6.6322	49.80	8.09	3 344	168.5
6.6331	49.94	8.09	2 875	162.7
6.6332	49.93	8.08	2 876	178.3
6.6441	50.17	5.06	2 396	143.7
6.6442	50.19	5.05	2 394	158.7
6.6451	50.29	5.04	1 925	162.9
6.6452	50.28	5.06	1 930	178.2
<u>6.6561</u>	50.38	2.02	979	144.0
<u>6.6562</u>	50.40	2.00	979	158.5

Table 32: Test Conditions for Steady-State Void Measurement Test Series 7

Run No	Pressure (kg/cm ² a)	Mass flux (10 ⁶ kg/m ² hr)	Power (kW)	Inlet temperature (°C)
<u>7.1121</u>	167.48	15.07	3 385	301.8
<u>7.1122</u>	167.41	15.07	3 384	306.8
7.1221	168.32	11.05	3 391	277.4
7.1222	168.25	11.10	3 390	282.3
7.1231	168.27	11.04	2 892	297.0
7.1232	168.24	11.01	2 891	302.0
7.1331	168.73	7.97	2 994	268.0
7.1332	168.75	7.98	2 995	272.8
<u>7.1341</u>	168.74	7.92	2 391	289.4
<u>7.1342</u>	168.75	7.94	2 391	295.3
7.1451	169.17	4.99	1 963	273.0
7.1452	169.17	4.96	1 963	278.0
7.2111	148.63	15.06	3 992	281.8
7.2112	148.68	14.94	3 993	286.5
7.2131	148.74	14.77	2 993	306.2
7.2132	148.48	14.98	2 987	315.5
<u>7.2221</u>	149.29	11.01	3 503	272.1
7.2222	149.30	11.06	3 506	277.2
7.2231	149.28	11.00	3 004	286.8
7.2232	149.28	11.01	3 004	294.6
7.2241	149.24	10.96	2 407	306.1
7.2242	149.17	10.94	2 409	311.3
7.2331	149.73	7.99	2 958	257.6
7.2332	149.80	7.96	2 957	264.5
7.2341	149.72	7.97	2 447	282.0
7.2342	149.75	7.95	2 450	289.2
7.2351	149.73	7.91	1 958	306.4
7.2352	149.74	7.91	1 955	311.4
7.2441	149.99	4.98	2 516	223.9
7.2442	150.03	4.96	2 516	233.9
7.2461	150.10	4.96	1 019	311.2
7.2462	150.13	4.95	1 040	321.2
<u>7.3121</u>	123.68	15.20	3 502	276.1
7.3122	123.52	15.12	3 498	286.0
7.3231	124.36	11.41	3 011	270.9
7.3232	124.35	11.09	3 006	281.1
7.3331	124.77	8.00	3 012	242.7
7.3332	124.75	8.04	3 011	252.5
7.3341	124.77	8.01	2 480	266.0
7.3342	124.89	8.02	2 480	280.2
<u>7.3451</u>	125.07	5.03	2 023	242.8
<u>7.3452</u>	125.09	5.03	2 021	260.1
7.4221	99.58	11.12	3 508	227.7
7.4222	99.46	11.12	3 506	242.6
7.4331	100.03	8.02	3 017	223.0

Table 32: Test Conditions for Steady-State Void Measurement Test Series 7 – Continued

Run No	Pressure (kg/cm ² a)	Mass flux (10 ⁶ kg/m ² hr)	Power (kW)	Inlet temperature (°C)
7.4332	99.87	8.01	3 018	242.8
7.4441	100.13	5.05	2 520	183.9
7.4442	100.24	5.05	2 516	203.9
7.4551	100.19	4.99	2 030	213.2
7.4452	100.25	5.02	2 026	233.2
<u>7.4561</u>	100.28	2.16	1 023	196.8
<u>7.4562</u>	100.29	2.16	1 023	214.9
7.5211	74.47	11.15	4 032	198.0
7.5212	74.36	11.12	4 021	212.9
7.5321	74.81	8.07	3 536	173.5
7.5322	74.75	8.09	3 537	193.6
7.5331	74.80	8.02	3 036	188.5
7.5332	74.83	8.01	3 031	203.3
7.5441	75.10	5.14	2 534	154.0
7.5442	75.19	5.12	2 532	174.4
7.5451	75.13	5.08	2 035	183.4
7.5452	75.24	5.03	2 039	203.5
7.5561	75.34	2.14	1 029	162.7
7.5562	75.36	2.14	1 031	178.4
<u>7.6321</u>	49.84	8.10	3 541	153.5
<u>7.6322</u>	49.65	8.06	3 536	168.6
7.6331	49.88	8.07	3 037	163.1
7.6332	49.82	8.05	3 036	178.2
7.6441	50.09	5.16	2 540	144.0
7.6442	50.08	5.14	2 536	158.9
7.6451	50.17	5.04	2 046	163.3
7.6452	50.16	5.00	2 048	178.4
7.6561	50.68	2.18	1 040	143.4
7.6562	50.69	2.16	1 037	158.4

Table 33: Test Conditions for Steady-State Void Measurement Test Series 8

Run No	Pressure (kg/cm ² a)	Mass flux (10 ⁶ kg/m ² hr)	Power (kW)	Inlet temperature (°C)
8.1232	168.8	10.98	2511.8	316.8
8.1342	168.9	7.91	2011.7	316.9
8.1452	169.2	4.92	1520.2	312.0
8.2131	149.6	15.14	2354.7	316.3
8.2132	149.6	15.14	2356.4	321.3
8.2222	149.9	11.03	2996.2	292.0
8.2231	149.9	11.04	2356.9	301.5
8.2232	150.1	11.00	2359.3	311.9
8.2332	150.1	7.98	2505.4	287.1
8.2351	149.9	7.90	1426.8	316.6
8.2352	150.0	7.93	1424.9	321.6
8.2441	150.2	4.98	2012.1	257.5
8.2442	150.2	4.98	2012.0	262.5
8.2452	149.6	4.93	965.6	321.1
8.3221	124.9	11.10	3010.7	271.7
8.3222	125.0	11.10	3009.9	277.0
8.3332	125.1	8.00	2522.7	277.0
8.3442	125.3	4.98	2020.7	257.7
8.4211	100.0	11.11	3514.9	242.5
8.4212	100.0	11.11	3510.4	247.4
8.4431	100.2	5.00	2534.9	199.1
8.4432	100.2	4.99	2534.9	203.9
8.4562	99.6	2.10	1028.3	213.7
8.5311	75.3	8.05	3529.9	193.6
8.5312	75.4	8.07	3535.4	203.6
8.5442	75.0	4.99	2034.9	213.4
8.6321	50.5	8.05	3048.7	173.1
8.6322	50.7	8.09	3049.1	183.3
8.6441	50.3	5.05	2045.0	168.4
8.6442	50.5	5.05	2043.5	178.3
8.6551	50.3	2.08	1025.2	148.6

The same assembly type was used in Test Series 5 and Test Series 8. Therefore, test cases performed at similar conditions may be used to assess the repeatability of the measurements. The duplicated cases are listed in Table 34. The highlighted cases are benchmark exercise cases.

Table 34: Duplicated Cases in Test Series B5 and B8

B8 test cases	B5 (duplicated) test cases	B8 test cases	B5 (duplicated) test cases
8.1232	5.1232	8.3332	5.3332
8.1342	5.1342	8.3442	-
8.1452	5.1452	8.4211	5.4211
8.2131	5.2131	8.4212	5.4212
8.2132	5.2132	8.4431	5.4431
8.2222	5.2222	8.4432	5.4432
8.2231	5.2231	8.4562	5.4562
8.2232	5.2232	8.5311	5.5311
8.2332	5.2332	8.5312	5.5312
8.2351	5.2351	8.5442	5.5442
8.2352	5.2351	8.6321	5.6321
8.2441	5.2442	8.6322	5.6322
8.2442	5.2442	8.6441	5.6441
8.2452	5.2452	8.6442	5.6442
8.3221	5.3221	8.6551	5.6551
8.3222	5.3222		

4.2.3 Exercise I-3 – Transient Bundle Benchmark

The experimental data include X-ray densitometer measurements of void fraction (chordal averaged) at three axial elevations. The averaging is over the four central sub-channels. Data are collected for four transient scenarios: power increase; flow reduction; depressurisation; temperature increase. The data can be used to assess the sub-channel and system codes capabilities of predicting the void generation during transients.

Tables 36 through 47 contain the boundary conditions for each transient. Plots of each parameter are also included during the transient. These plots represent the ratio of the value of each parameter at a certain time to the value at the start of the transient.

All transient cases are to be analysed as part of the benchmark.

Table 35: Test Conditions for Transient Void Measurement Test Series 5T, 6T, 7T

Test series	Assembly	Initial conditions				Transients
		Pressure (kg/cm ² a)	Mass flux (10 ⁶ kg/m ² h)	Power (kW)	Inlet temperature (Celsius)	
5T	B5	154.2	11.95	2282.0	300.4	Power increase
		153.8	11.93	2244.0	301.2	Flow reduction
		153.0	11.92	2236.0	300.4	Depressurisation
		152.5	11.94	2230.0	301.7	Temperature increase
6T	B6	158.2	11.55	2621.0	288.1	Power increase
		158.4	12.03	2574.0	288.8	Flow reduction
		154.6	12.02	2556.0	288.2	Depressurisation
		157.2	11.92	2603.0	288.8	Temperature increase
7T	B7	158.2	12.02	2500.0	291.9	Power increase
		158.1	12.04	2405.0	292.0	Flow reduction
		155.0	11.99	2577.0	291.8	Depressurisation
		158.8	11.99	2496.0	290.2	Temperature increase

Table 36: Transient Void Fraction in Rod Bundle Test Series 5T (Power Increase)

Time (sec)	Pressure (kg/cm ² a)	Mass flux (10 ⁶ kg/m ² hr)	Power (kW)	Inlet temperature (°C)
30.0	154.2	11.95	2282.0	300.4
30.2	154.4	11.95	2261.0	300.4
30.4	154.3	11.94	2254.0	300.4
30.6	153.9	11.96	2256.0	300.4
30.8	154.1	11.96	2261.0	300.4
31.0	154.0	11.95	2182.0	300.5
31.2	154.1	11.95	2194.0	300.4
31.4	154.2	12.01	2228.0	300.6
31.6	154.3	12.00	2236.0	300.5
31.8	154.4	11.98	2249.0	300.5
32.0	154.4	11.95	2265.0	300.5
32.2	154.5	11.94	2295.0	300.5
32.4	154.3	11.93	2343.0	300.5
32.6	154.3	11.91	2389.0	300.4
32.8	154.3	11.92	2451.0	300.4
33.0	154.3	11.92	2511.0	300.4
33.2	154.4	11.90	2573.0	300.4
33.4	154.4	11.90	2639.0	300.5
33.6	154.5	11.87	2675.0	300.5
33.8	154.4	11.85	2717.0	300.7
34.0	154.5	11.84	2765.0	300.6
34.2	154.6	11.82	2834.0	300.6
34.4	154.5	11.82	2882.0	300.5
34.6	154.6	11.81	2948.0	300.4
34.8	154.4	11.79	2992.0	300.5
35.0	154.7	11.76	3074.0	300.4
35.2	154.8	11.73	3096.0	300.3
35.4	154.9	11.71	3079.0	300.3
35.6	155.0	11.79	3067.0	300.4
35.8	154.9	11.76	3062.0	300.5
36.0	155.2	11.75	3090.0	300.5
36.2	155.0	11.74	3100.0	300.7
36.4	155.0	11.72	3093.0	300.7
36.6	155.3	11.71	3074.0	300.6
36.8	155.1	11.73	3061.0	300.6
37.0	155.3	11.76	3092.0	300.5
37.2	155.0	11.78	3103.0	300.5
37.4	155.0	11.78	3104.0	300.4
37.6	155.0	11.78	3051.0	300.5
37.8	154.9	11.76	3052.0	300.5
38.0	155.1	11.76	3071.0	300.6
38.2	155.0	11.75	3073.0	300.6
38.4	155.1	11.75	3074.0	300.6
38.6	154.9	11.76	3089.0	300.7
38.8	154.9	11.76	3078.0	300.6
39.0	155.0	11.76	3062.0	300.6

Table 37: Transient Void Fraction in Rod Bundle Test Series 5T (Flow Reduction)

Time (sec)	Pressure (kg/cm²a)	Mass flux (10⁶ kg/m² hr)	Power (kW)	Inlet temperature (°C)
30.0	153.8	11.93	2244.0	301.2
30.2	153.9	11.93	2228.0	301.2
30.4	154.0	11.94	2234.0	301.2
30.6	153.9	11.95	2233.0	301.2
30.8	153.9	11.86	2259.0	301.1
31.0	154.0	11.13	2256.0	301.1
31.2	153.7	9.88	2259.0	301.2
31.4	153.8	8.68	2250.0	301.2
31.6	153.7	7.94	2241.0	301.2
31.8	153.6	7.63	2242.0	301.1
32.0	153.8	7.38	2233.0	301.2
32.2	153.9	7.06	2240.0	301.1
32.4	154.0	6.77	2219.0	301.2
32.6	154.0	6.59	2246.0	301.1
32.8	153.8	6.55	2240.0	301.2
33.0	153.8	6.69	2234.0	301.2
33.2	153.9	6.96	2239.0	301.2
33.4	153.9	7.22	2225.0	301.2
33.6	154.0	7.38	2233.0	301.1
33.8	154.1	7.49	2240.0	301.2
34.0	154.1	7.88	2228.0	301.2
34.2	154.2	8.53	2239.0	301.2
34.4	154.3	9.15	2228.0	301.2
34.6	154.1	9.55	2236.0	301.2
34.8	154.2	9.71	2234.0	301.3
35.0	154.2	9.77	2243.0	301.2

Figure 30: Variation of Properties during Transient for Data Series 5T (Power Increase)

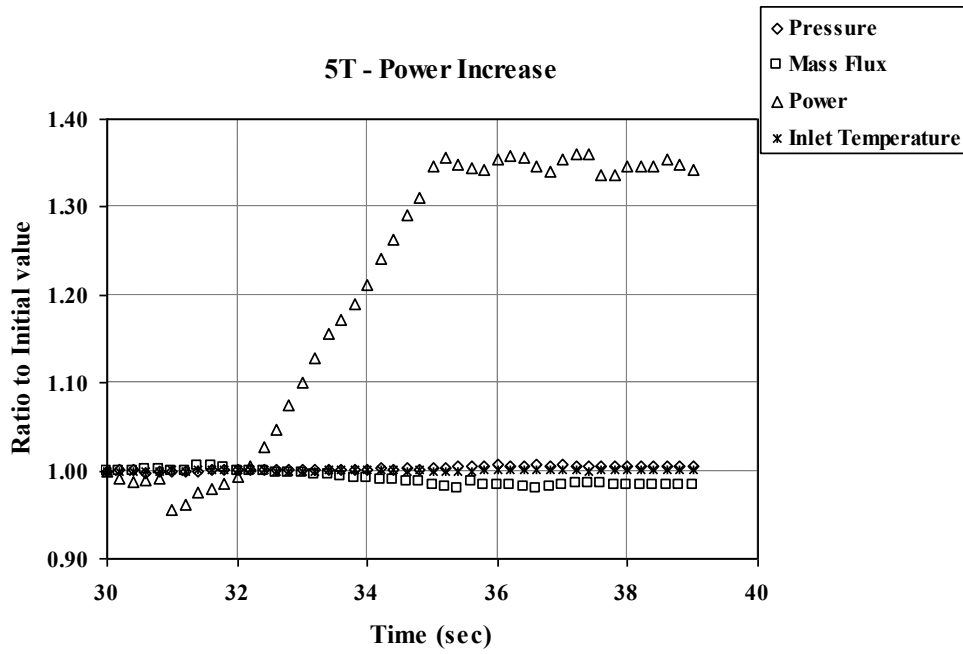


Figure 31: Variation of Properties during Transient for Data Series 5T (Flow Reduction)

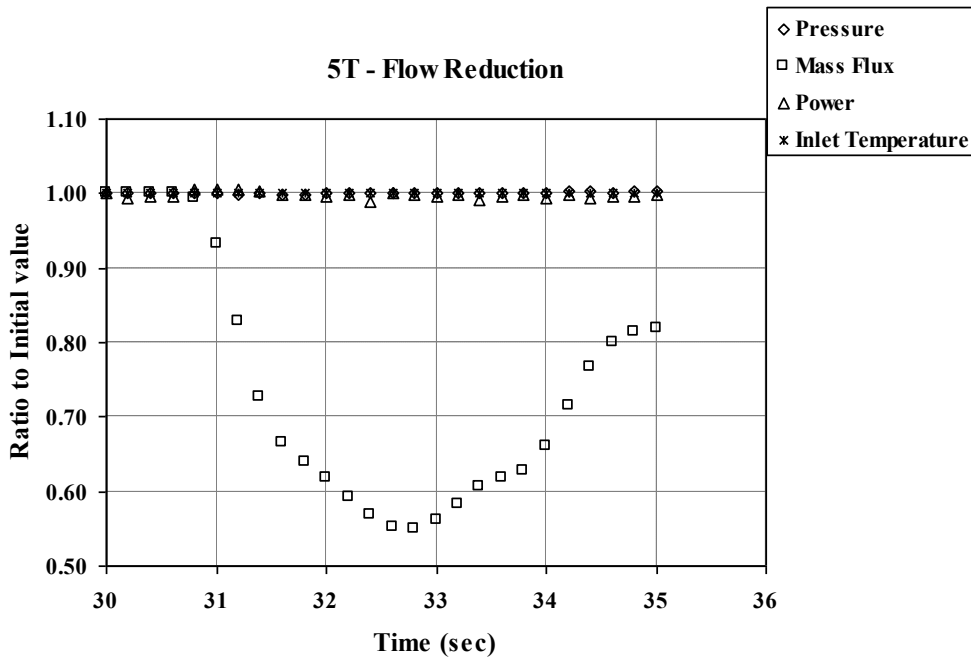


Table 38: Transient Void Fraction in Rod Bundle in Test Series 5T (Depressurisation)

Time (sec)	Pressure (kg/cm ² a)	Mass flux (10 ⁶ kg/m ² hr)	Power (kW)	Inlet temperature (°C)
20.0	153.0	11.92	2236.0	300.4
24.0	152.6	11.93	2251.0	300.4
28.0	152.3	11.93	2263.0	300.5
32.0	151.7	11.90	2247.0	300.5
36.0	151.1	11.93	2258.0	300.5
40.0	150.4	11.92	2253.0	300.5
44.0	149.5	11.91	2282.0	300.5
48.0	148.4	11.94	2255.0	300.5
52.0	147.5	11.93	2257.0	300.5
56.0	146.3	11.91	2257.0	300.5
60.0	145.2	11.90	2257.0	300.5
64.0	144.1	11.92	2260.0	300.5
68.0	142.9	11.94	2267.0	300.6
72.0	141.5	11.91	2264.0	300.5
76.0	140.6	11.91	2278.0	300.4
80.0	139.5	11.92	2267.0	300.0
84.0	138.2	11.93	2258.0	299.7
88.0	137.0	11.94	2263.0	299.3
92.0	135.8	11.96	2256.0	298.7
96.0	134.4	11.92	2170.0	298.2
100.0	132.8	11.94	2244.0	297.6
104.0	131.6	11.78	2246.0	297.1
108.0	130.4	11.58	2261.0	296.6
112.0	129.5	11.39	2248.0	296.2
116.0	128.7	11.21	2262.0	295.8
120.0	127.8	10.99	2269.0	295.4
124.0	126.8	10.82	2273.0	295.0
128.0	126.0	10.75	2260.0	294.6
132.0	125.2	10.78	2263.0	294.2
136.0	124.1	10.80	2273.0	293.8
138.0	123.8	10.75	2266.0	293.6
142.0	122.7	10.79	2273.0	293.1
146.0	121.6	10.76	2262.0	292.5
150.0	120.6	10.75	2264.0	291.8
154.0	119.5	10.80	2272.0	290.9
158.0	118.2	10.77	2269.0	290.0
162.0	116.9	10.73	2259.0	289.1
166.0	115.7	10.76	2269.0	288.2
170.0	114.7	10.80	2270.0	287.5
174.0	114.3	10.79	2270.0	286.7
178.0	114.2	10.80	2263.0	286.0

Table 39: Transient Void Fraction in Rod Bundle in Test Series 5T (Temperature Increase)

Time (sec)	Pressure (kg/cm ² a)	Mass flux (10 ⁶ kg/m ² hr)	Power (kW)	Inlet temperature (°C)
60.0	152.5	11.94	2230.0	301.7
62.0	152.5	11.96	2268.0	302.5
64.0	152.7	11.92	2270.0	304.1
66.0	152.3	11.94	2272.0	305.8
68.0	152.3	11.98	2264.0	307.9
70.0	152.5	11.93	2279.0	310.3
72.0	152.8	11.94	2263.0	312.7
74.0	152.7	11.95	2264.0	315.1
76.0	152.5	11.93	2264.0	317.6
78.0	152.7	11.94	2243.0	319.8
80.0	153.0	11.95	2245.0	322.1
82.0	153.5	12.00	2244.0	324.0
84.0	153.7	11.98	2272.0	325.7
86.0	153.7	12.00	2255.0	327.5
88.0	153.8	12.04	2260.0	328.9
90.0	154.8	12.05	2266.0	330.3
92.0	155.2	12.16	2250.0	331.3
94.0	155.3	12.23	2268.0	332.4
96.0	155.4	12.11	2266.0	333.4
98.0	156.0	12.10	2252.0	334.2
100.0	156.3	12.09	2237.0	334.9
102.0	156.4	12.09	2251.0	335.5
104.0	157.5	12.13	2250.0	335.6
106.0	157.6	12.12	2232.0	334.8
108.0	158.0	12.07	2240.0	333.6
110.0	158.4	12.12	2238.0	331.6
112.0	158.8	12.07	2240.0	329.8
114.0	159.0	12.06	2256.0	327.8
116.0	159.6	12.09	2274.0	326.1
118.0	159.7	12.05	2236.0	324.7
120.0	159.8	12.07	2247.0	323.4

Figure 32: Variation of Properties during Transient for Data Series 5T (Depressurisation)

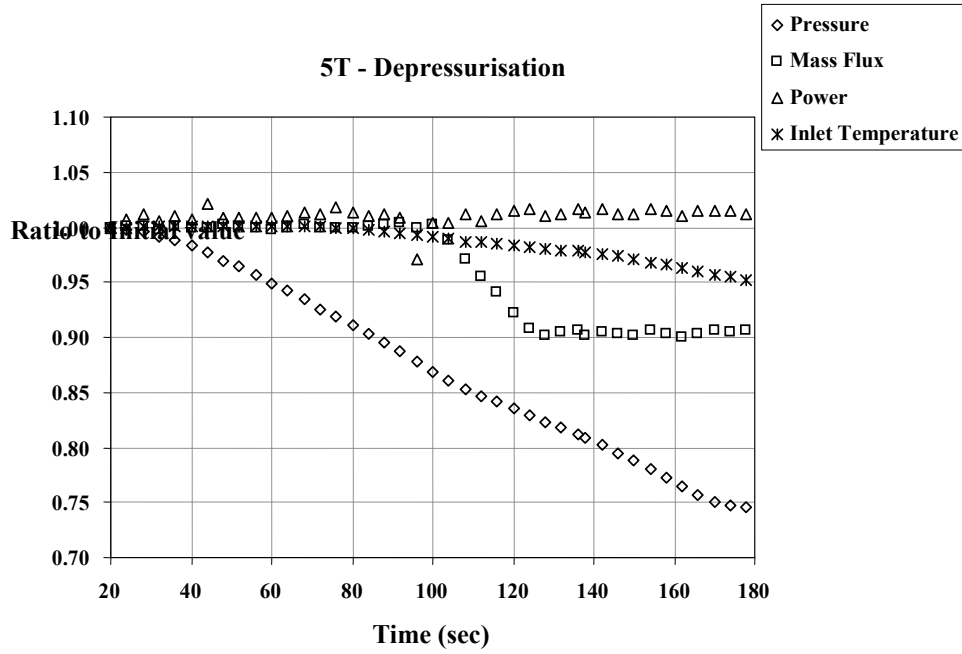


Figure 33: Variation of Properties during Transient for Data Series 5T (Temperature Increase)

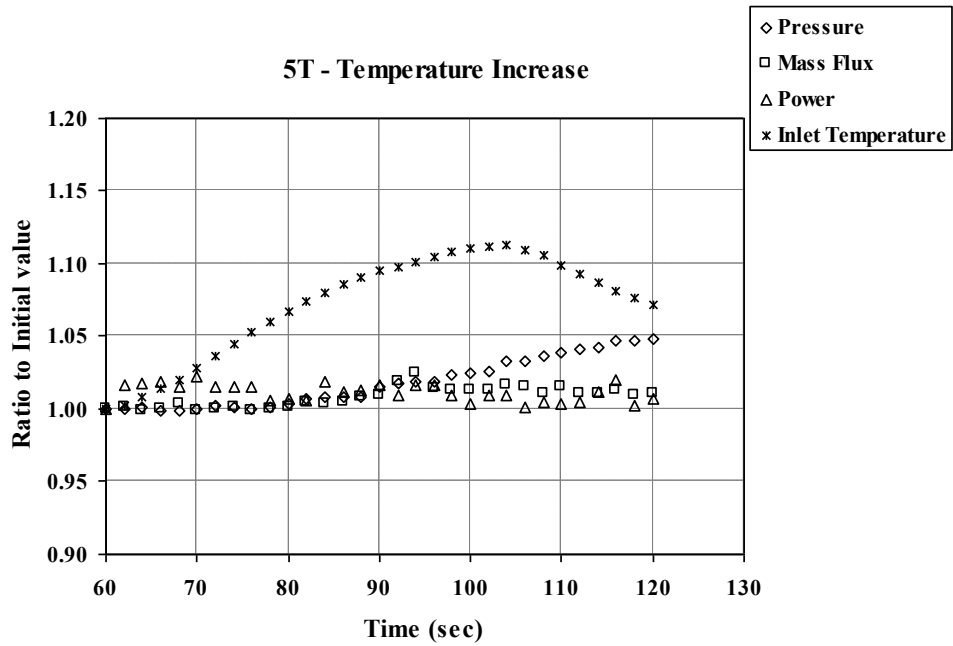


Table 40: Transient Void Fraction in Rod Bundle in Test Series 6T (Power Increase)

Time (sec)	Pressure (kg/cm ² a)	Mass flux (10 ⁶ kg/m ² hr)	Power (kW)	Inlet temperature (°C)
24.0	158.2	11.55	2621.0	288.1
24.2	158.2	11.54	2682.0	288.1
24.4	158.2	11.54	2750.0	288.1
24.6	158.2	11.53	2811.0	288.1
24.8	158.2	11.52	2886.0	288.2
25.0	158.2	11.50	2946.0	288.4
25.2	158.2	11.48	3020.0	288.4
25.4	158.3	11.43	3106.0	288.4
25.6	158.3	11.43	3181.0	288.5
25.8	158.4	11.41	3237.0	288.5
26.0	158.4	11.43	3283.0	288.5
26.2	158.5	11.41	3314.0	288.5
26.4	158.5	11.40	3321.0	288.6
26.6	158.6	11.40	3333.0	288.5
26.8	158.6	11.40	3339.0	288.6
27.0	158.6	11.40	3323.0	288.5
27.2	158.6	11.41	3317.0	288.5
27.4	158.7	11.40	3306.0	288.5
27.6	158.7	11.40	3306.0	288.5
27.8	158.7	11.41	3313.0	288.5
28.0	158.7	11.42	3305.0	288.6
28.2	158.7	11.41	3314.0	288.5
28.4	158.8	11.43	3311.0	288.5
28.6	158.8	11.43	3309.0	288.4
28.8	158.8	11.44	3302.0	288.5
29.0	158.8	11.45	3296.0	288.5
29.2	158.8	11.45	3302.0	288.5
29.4	158.8	11.45	3302.0	288.5
29.6	158.8	11.45	3293.0	288.5
29.8	158.9	11.44	3304.0	288.5
30.0	158.9	11.44	3305.0	288.5
30.2	158.9	11.44	3297.0	288.5
30.4	158.9	11.45	3240.0	288.6
30.6	158.9	11.47	3235.0	288.6
30.8	159.0	11.49	3248.0	288.6
31.0	159.0	11.49	3259.0	288.6
31.2	159.0	11.48	3294.0	288.6
31.4	159.0	11.47	3304.0	288.7
31.6	159.1	11.47	3276.0	288.6
31.8	159.1	11.47	3027.0	288.5
32.0	159.1	11.48	2432.0	288.2
32.2	159.0	11.53	1893.0	288.0
32.4	159.0	11.59	1537.0	287.8
32.6	158.9	11.63	1373.0	287.5
32.8	158.8	11.64	1356.0	287.5
33.0	158.7	11.64	1368.0	287.6

Table 41: Transient Void Fraction in Rod Bundle in Test Series 6T (Flow Reduction)

Time (sec)	Pressure (kg/cm²a)	Mass flux (10⁶ kg/m² hr)	Power (kW)	Inlet temperature (°C)
19.0	158.4	12.03	2574.0	288.8
19.2	158.5	12.02	2562.0	288.8
19.4	158.4	12.01	2561.0	288.8
19.6	158.3	12.01	2544.0	288.8
19.8	158.3	11.90	2548.0	288.8
20.0	158.1	11.22	2557.0	288.8
20.2	157.8	10.18	2560.0	289.0
20.4	157.7	9.14	2563.0	289.2
20.6	157.6	8.38	2571.0	289.3
20.8	157.6	7.97	2581.0	289.5
21.0	157.7	7.72	2583.0	289.5
21.2	157.8	7.50	2573.0	289.6
21.4	157.8	7.32	2575.0	289.6
21.6	157.8	7.17	2579.0	289.6
21.8	157.8	7.12	2583.0	289.7
22.0	157.8	7.16	2593.0	289.6
22.2	157.9	7.27	2551.0	289.6
22.4	157.9	7.37	2587.0	289.6
22.6	157.9	7.45	2572.0	289.6
22.8	158.0	7.53	2536.0	289.6
23.0	158.0	7.82	2484.0	289.5
23.2	158.0	8.29	2511.0	289.4
23.4	158.1	8.76	2541.0	289.3
23.6	158.2	9.12	2551.0	289.2
23.8	158.2	9.32	2571.0	289.2
24.0	158.3	9.49	2567.0	289.1
24.2	158.3	9.70	2574.0	289.0
24.4	158.4	9.89	2576.0	289.0
24.6	158.4	10.05	2572.0	289.1
24.8	158.4	10.15	2566.0	289.0
25.0	158.4	10.35	2559.0	289.1
25.2	158.4	10.61	2567.0	288.9
25.4	158.5	10.86	2564.0	288.9
25.6	158.5	11.05	2576.0	288.9
25.8	158.5	11.15	2572.0	288.9
26.0	158.5	11.22	2544.0	288.9
26.2	158.5	11.29	2537.0	288.9
26.4	158.5	11.34	2541.0	288.9
26.6	158.5	11.39	2550.0	289.0
26.8	158.5	11.39	2552.0	289.0
27.0	158.6	11.36	2557.0	289.1

Figure 34: Variation of Properties during Transient for Data Series 6T (Power Increase)

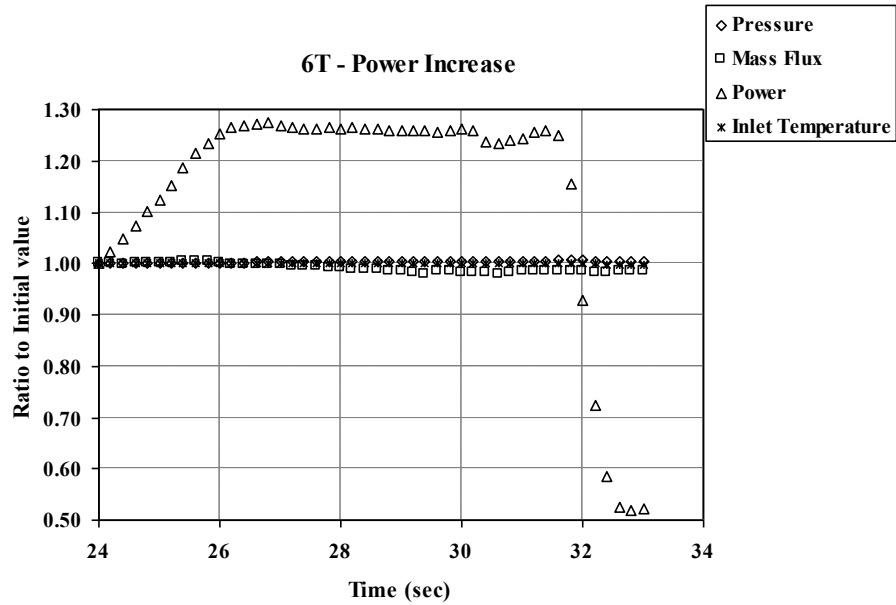


Figure 35: Variation of Properties during Transient for Data Series 6T (Flow Reduction)

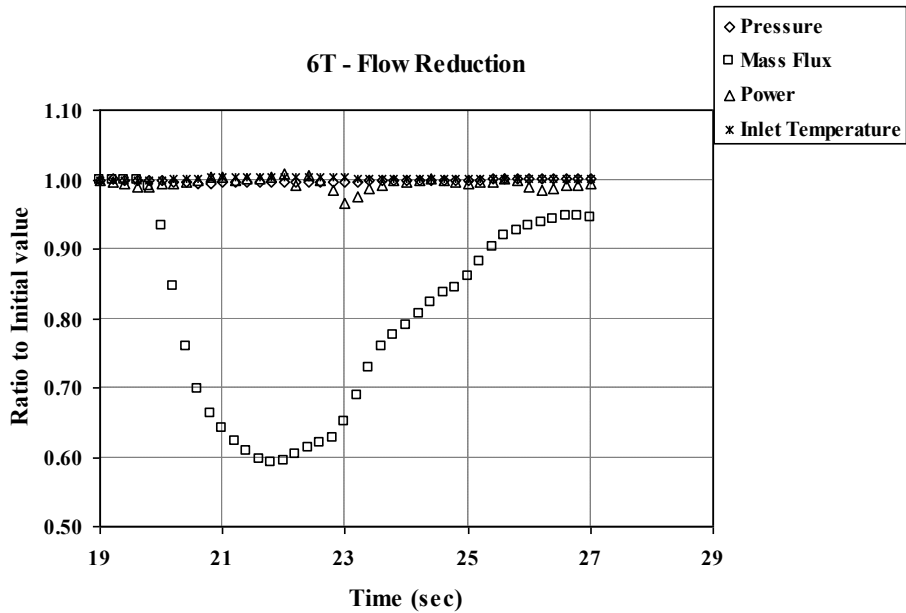


Table 42: Transient Void Fraction in Rod Bundle in Test Series 6T (Depressurisation)

Time (sec)	Pressure (kg/cm²a)	Mass flux (10⁶ kg/m² hr)	Power (kW)	Inlet temperature (°C)
0.0	154.6	12.02	2556.0	288.2
4.0	154.5	11.95	2597.0	288.0
8.0	154.3	11.90	2599.0	288.0
12.0	154.2	11.82	2599.0	287.8
16.0	153.9	11.75	2600.0	287.8
20.0	153.5	11.67	2600.0	287.8
24.0	153.0	11.62	2599.0	287.9
28.0	152.4	11.56	2602.0	287.7
32.0	151.7	11.49	2574.0	287.8
36.0	150.5	11.38	2612.0	287.7
40.0	149.2	11.36	2561.0	287.6
44.0	147.8	11.29	2595.0	287.6
48.0	146.5	11.20	2591.0	287.6
52.0	145.1	11.15	2591.0	287.7
56.0	143.8	11.07	2542.0	287.7
60.0	142.5	11.00	2590.0	287.8
64.0	141.2	10.93	2604.0	288.1
68.0	139.9	10.90	2565.0	288.2
72.0	138.6	10.83	2615.0	288.4
76.0	137.4	10.79	2626.0	288.5
80.0	136.3	10.78	2595.0	288.3
84.0	135.1	10.81	2582.0	287.8
88.0	134.0	10.82	2619.0	287.1
92.0	132.9	10.82	2599.0	286.3
96.0	131.8	10.80	2580.0	285.3
100.0	130.7	10.84	2594.0	284.4
104.0	129.7	10.86	2614.0	283.5
108.0	128.6	10.80	2597.0	282.8
112.0	127.5	10.84	2596.0	282.0
116.0	126.5	10.87	2611.0	281.2
120.0	125.4	10.84	2610.0	280.8
124.0	124.4	10.84	2600.0	280.3
128.0	123.3	10.84	2606.0	279.9
132.0	122.2	10.86	2618.0	279.4
136.0	121.2	10.85	2586.0	279.1
140.0	120.1	10.85	2602.0	278.7
144.0	119.0	10.85	2603.0	278.2
148.0	118.0	10.87	2615.0	277.9
152.0	116.9	10.82	2605.0	277.6
156.0	115.8	10.83	2588.0	277.3
160.0	114.8	10.84	2616.0	277.0
164.0	114.0	10.84	2608.0	276.7
168.0	113.9	10.84	2603.0	276.4
172.0	114.0	10.87	2616.0	276.3
176.0	114.2	10.87	2599.0	275.7
180.0	114.4	10.87	2576.0	275.3
184.0	114.6	10.87	2615.0	274.8
188.0	114.8	10.87	2598.0	274.3
192.0	115.0	10.90	2628.0	273.7
196.0	115.1	10.89	2586.0	272.9

Table 43: Transient Void Fraction in Rod Bundle in Test Series 6T (Temperature Increase)

Time (sec)	Pressure (kg/cm ² a)	Mass flux (10 ⁶ kg/m ² hr)	Power (kW)	Inlet temperature (°C)
56.0	157.2	11.92	2603.0	288.8
58.0	157.2	11.88	2582.0	288.9
60.0	157.1	11.87	2572.0	289.4
62.0	157.0	11.84	2559.0	290.3
64.0	157.0	11.82	2590.0	291.5
66.0	156.9	11.81	2582.0	293.0
68.0	156.8	11.78	2562.0	294.7
70.0	156.7	11.77	2574.0	296.4
72.0	156.7	11.76	2564.0	298.4
74.0	156.7	11.73	2556.0	300.2
76.0	156.6	11.75	2568.0	302.1
78.0	156.7	11.75	2578.0	303.8
80.0	156.7	11.76	2566.0	305.5
82.0	156.8	11.73	2566.0	307.1
84.0	156.9	11.72	2553.0	308.7
86.0	157.0	11.68	2557.0	310.1
88.0	157.1	11.66	2559.0	311.5
90.0	157.3	11.70	2561.0	312.9
92.0	157.4	11.69	2562.0	314.2
94.0	157.6	11.70	2551.0	315.4
96.0	157.8	11.70	2569.0	316.6
98.0	158.0	11.69	2561.0	317.6
100.0	158.2	11.72	2549.0	318.8
102.0	158.6	11.74	2567.0	319.7
104.0	158.9	11.70	2556.0	320.6
106.0	159.2	11.74	2568.0	321.4
108.0	159.6	11.72	2563.0	322.2
110.0	160.0	11.75	2544.0	322.9
112.0	160.4	11.75	2552.0	323.6
114.0	160.8	11.82	2464.0	324.2
116.0	161.3	11.82	2561.0	324.8
118.0	161.8	11.88	2558.0	325.4
120.0	162.2	11.90	2541.0	325.9
122.0	162.8	11.96	2563.0	326.3
124.0	163.3	11.99	2553.0	326.9
126.0	163.9	12.03	2576.0	327.3
128.0	164.5	12.08	2506.0	327.4
130.0	165.1	12.11	2543.0	327.3
132.0	165.7	12.14	2546.0	326.4
134.0	166.3	12.21	2531.0	325.4
136.0	166.8	12.19	2544.0	323.9
138.0	167.3	12.20	2556.0	322.2
140.0	167.7	12.24	2546.0	320.4
142.0	168.0	12.20	2568.0	318.6
144.0	168.3	12.26	2565.0	316.7
146.0	168.5	12.24	2537.0	315.1
148.0	168.6	12.23	2540.0	313.4
150.0	168.7	12.23	2551.0	312.0
152.0	168.7	12.24	2560.0	310.6
154.0	168.7	12.22	2567.0	309.3
156.0	168.6	12.22	2566.0	308.2
158.0	168.4	12.19	2542.0	307.1
160.0	168.3	12.17	2561.0	306.1

Figure 36: Variation of Properties during Transient for Data Series 6T (Depressurisation)

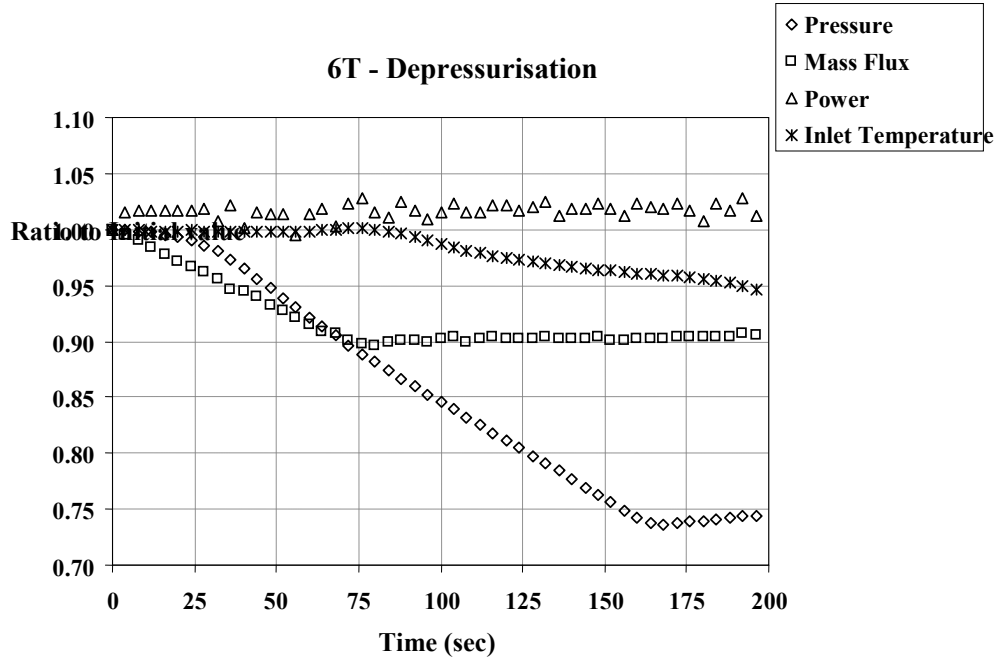


Figure 37: Variation of Properties during Transient for Data Series 6T (Temperature Increase)

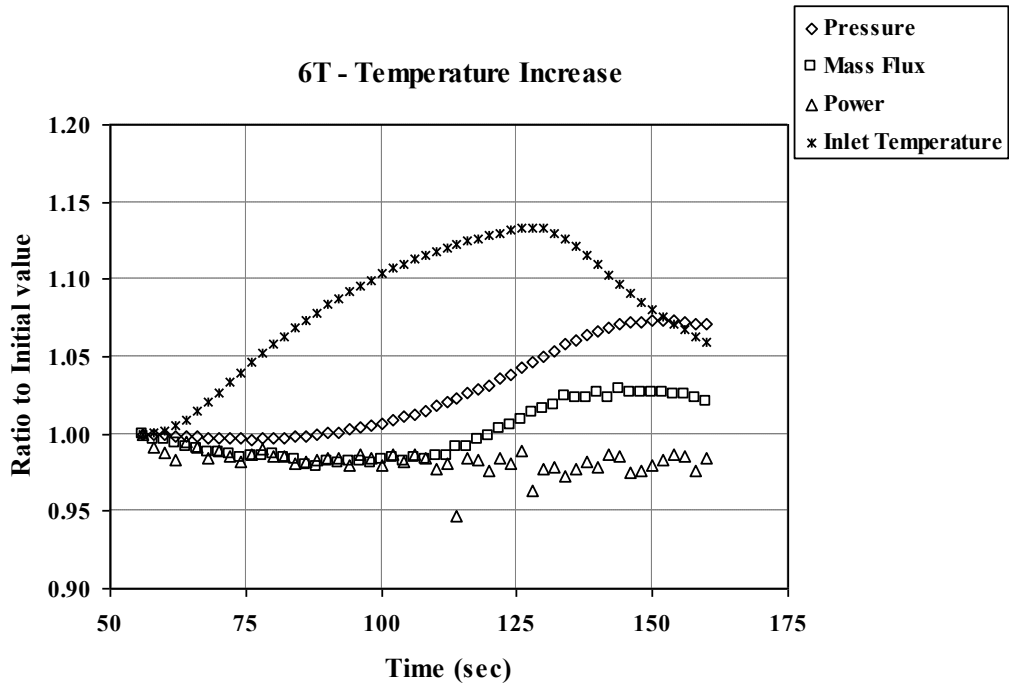


Table 44: Transient Void Fraction in Rod Bundle in Test Series 7T (Power Increase)

Time (sec)	Pressure (kg/cm ² a)	Mass flux (10 ⁶ kg/m ² hr)	Power (kW)	Inlet temperature (°C)
32.0	158.2	12.02	2500.0	291.9
32.2	158.2	12.02	2504.0	291.9
32.4	158.2	12.02	2503.0	291.9
32.6	158.2	12.02	2492.0	291.9
32.8	158.2	12.02	2490.0	291.9
33.0	158.2	12.03	2513.0	291.9
33.2	158.2	12.02	2561.0	291.9
33.4	158.2	12.01	2617.0	292.0
33.6	158.2	12.01	2680.0	292.1
33.8	158.2	11.99	2741.0	292.1
34.0	158.2	11.98	2803.0	292.1
34.2	158.2	11.96	2862.0	292.1
34.4	158.3	11.96	2913.0	292.2
34.6	158.3	11.95	2962.0	292.2
34.8	158.3	11.93	3027.0	292.3
35.0	158.4	11.91	3083.0	292.3
35.2	158.4	11.89	3141.0	292.3
35.4	158.5	11.88	3234.0	292.3
35.6	158.5	11.86	3294.0	292.4
35.8	158.6	11.85	3346.0	292.3
36.0	158.6	11.86	3408.0	292.3
36.2	158.7	11.84	3445.0	292.2
36.4	158.8	11.84	3444.0	292.3
36.6	158.8	11.83	3443.0	292.3
36.8	158.8	11.82	3451.0	292.3
37.0	158.9	11.81	3451.0	292.3
37.2	158.9	11.82	3448.0	292.3
37.4	158.9	11.83	3417.0	292.3
37.6	159.0	11.85	3421.0	292.4
37.8	159.0	11.84	3445.0	292.4
38.0	159.0	11.84	3450.0	292.4
38.2	159.1	11.83	3462.0	292.3
38.4	159.1	11.83	3448.0	292.3
38.6	159.1	11.82	3438.0	292.3
38.8	159.1	11.83	3455.0	292.2
39.0	159.2	11.83	3457.0	292.3
39.2	159.2	11.82	3468.0	292.4
39.4	159.2	11.83	3465.0	292.4
39.6	159.2	11.82	3433.0	292.4
39.8	159.3	11.82	3434.0	292.3
40.0	159.3	11.84	3435.0	292.3
40.2	159.3	11.85	3446.0	292.3
40.4	159.4	11.85	3450.0	292.4
40.6	159.4	11.85	3437.0	292.4
40.8	159.4	11.84	3441.0	292.4
41.0	159.5	11.84	3443.0	292.4
41.2	159.5	11.84	3444.0	292.4
41.4	159.5	11.84	3440.0	292.4
41.6	159.6	11.84	3435.0	292.4
41.8	159.6	11.84	3439.0	292.4
42.0	159.6	11.85	3467.0	292.4

Table 45: Transient Void Fraction in Rod Bundle in Test Series 7T (Flow Reduction)

Time (sec)	Pressure (kg/cm ² a)	Mass flux (10 ⁶ kg/m ² hr)	Power (kW)	Inlet temperature (°C)
157.0	158.1	12.04	2405.0	292.0
157.2	158.1	12.03	2426.0	292.0
157.4	158.1	12.04	2435.0	292.0
157.6	158.1	12.03	2433.0	292.0
157.8	158.1	11.77	2432.0	292.0
158.0	158.0	11.30	2418.0	292.0
158.2	157.9	10.79	2427.0	292.1
158.4	157.8	10.38	2430.0	292.2
158.6	157.7	10.13	2427.0	292.1
158.8	157.7	9.76	2430.0	292.2
159.0	157.5	9.21	2432.0	292.3
159.2	157.5	8.63	2431.0	292.4
159.4	157.5	8.20	2429.0	292.6
159.6	157.5	7.94	2432.0	292.6
159.8	157.6	7.69	2432.0	292.7
160.0	157.6	7.38	2441.0	295.7
160.2	157.6	7.04	2439.0	292.8
160.4	157.6	6.79	2426.0	292.7
160.6	157.7	6.66	2426.0	292.8
160.8	157.7	6.64	2428.0	292.8
161.0	157.8	6.69	2415.0	292.8
161.2	157.8	6.75	2414.0	292.8
161.4	157.9	6.79	2415.0	292.8
161.6	157.9	6.82	2420.0	292.8
161.8	158.0	6.89	2421.0	292.7
162.0	158.0	7.00	2425.0	292.8
162.2	158.1	7.11	2419.0	292.6
162.4	158.2	7.20	2431.0	292.7
162.6	158.2	7.25	2430.0	292.7
162.8	158.2	7.27	2425.0	292.8
163.0	158.3	7.27	2417.0	292.8
163.2	158.3	7.26	2420.0	292.9
163.4	158.4	7.26	2421.0	292.8
163.6	158.4	7.25	2428.0	292.7
163.8	158.4	7.26	2425.0	292.7
164.0	158.5	7.26	2417.0	292.7
164.2	158.5	7.27	2423.0	292.8
164.4	158.6	7.27	2416.0	292.7
164.6	158.6	7.27	2426.0	292.7
164.8	158.6	7.27	2420.0	292.8
165.0	158.7	7.27	2418.0	292.8
165.2	158.8	7.27	2418.0	292.8
165.4	158.8	7.26	2427.0	292.8
165.6	158.9	7.26	2433.0	292.8
165.8	158.9	7.27	2432.0	292.9
166.0	159.0	7.27	2431.0	293.0
166.2	159.1	7.26	2432.0	293.1
166.4	159.1	7.27	2435.0	293.1
166.6	159.2	7.28	2436.0	293.1
166.8	159.2	7.28	2428.0	293.2
167.0	159.3	7.27	2432.0	293.2

Figure 38: Variation of Properties during Transient for Data Series 7T (Power Increase)

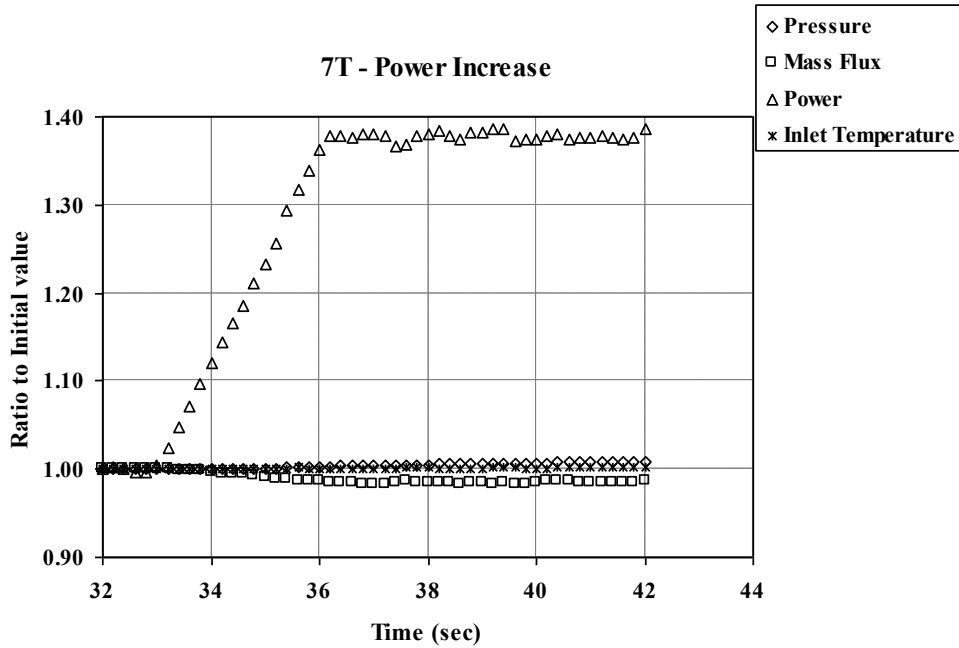


Figure 39: Variation of Properties during Transient for Data Series 7T (Flow Reduction)

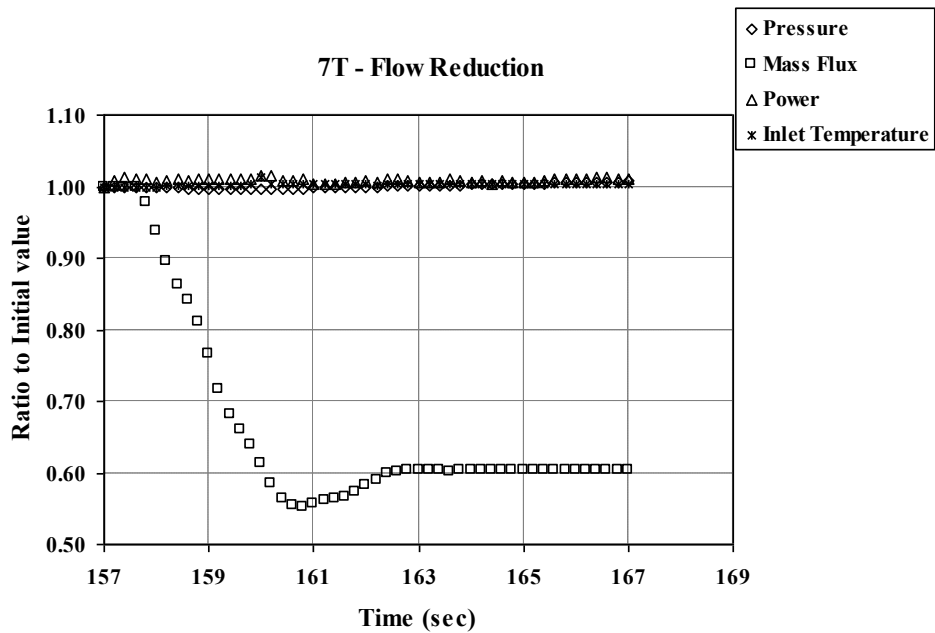


Table 46: Transient Void Fraction in Rod Bundle in Test Series 7T (Depressurisation)

Time (sec)	Pressure (kg/cm ² a)	Mass flux (10 ⁶ kg/m ² hr)	Power (kW)	Inlet temperature (°C)
6.0	155.0	11.99	2577.0	291.8
9.0	154.8	11.97	2592.0	291.8
12.0	154.4	11.98	2582.0	291.7
15.0	153.8	11.97	2578.0	291.6
18.0	153.2	11.99	2574.0	291.7
21.0	152.6	11.98	2577.0	291.7
24.0	151.9	11.95	2564.0	291.7
27.0	151.3	11.97	2581.0	291.7
30.0	150.7	11.96	2573.0	291.6
33.0	150.1	11.95	2558.0	291.6
36.0	149.3	11.93	2573.0	291.7
39.0	148.6	11.93	2573.0	291.7
42.0	147.9	11.93	2567.0	291.7
45.0	147.1	11.93	2566.0	291.8
48.0	146.2	11.93	2570.0	291.9
51.0	145.2	11.92	2575.0	292.2
54.0	144.2	11.92	2580.0	292.4
57.0	143.1	11.94	2585.0	292.6
60.0	142.1	11.96	2581.0	292.4
63.0	141.0	11.93	2541.0	292.1
66.0	140.0	11.92	2570.0	291.9
69.0	139.0	11.93	2582.0	291.5
72.0	138.0	11.91	2570.0	291.1
75.0	137.0	11.92	2562.0	290.6
78.0	136.0	11.90	2567.0	290.4
81.0	135.0	11.91	2566.0	290.1
84.0	134.1	11.91	2576.0	290.1
87.0	133.2	11.89	2584.0	290.3
90.0	132.3	11.91	2579.0	290.5
93.0	131.5	11.90	2570.0	290.5
96.0	130.5	11.92	2565.0	290.6
99.0	129.7	11.90	2580.0	290.5
102.0	129.0	11.91	2579.0	290.3
105.0	128.0	11.88	2574.0	290.1
108.0	127.2	11.91	2575.0	289.8
111.0	126.4	11.89	2587.0	289.5
114.0	125.6	11.91	2576.0	289.3
117.0	124.8	11.90	2581.0	289.1
120.0	124.0	11.90	2582.0	288.9
123.0	123.2	11.86	2566.0	288.8
126.0	122.5	11.89	2570.0	288.6
129.0	121.7	11.88	2548.0	288.5
132.0	120.9	11.87	2575.0	288.3
135.0	120.2	11.87	2573.0	288.2
138.0	119.5	11.85	2600.0	288.2
141.0	118.8	11.85	2578.0	288.1
144.0	118.1	11.83	2574.0	288.1
147.0	117.5	11.82	2578.0	288.2
150.0	116.9	11.82	2575.0	288.4
153.0	116.3	11.79	2585.0	288.3
156.0	115.7	11.78	2574.0	288.6
159.0	115.2	11.75	2570.0	288.7
162.0	114.7	11.74	2579.0	288.8

Table 47: Transient Void Fraction in Rod Bundle in Test Series 7T (Temperature Increase)

Time (sec)	Pressure (kg/cm ² a)	Mass flux (10 ⁶ kg/m ² hr)	Power (kW)	Inlet temperature (°C)
50.0	158.8	11.99	2496.0	290.2
52.0	158.8	11.97	2509.0	291.5
54.0	158.9	11.93	2509.0	292.5
56.0	158.9	11.92	2514.0	293.5
58.0	158.9	11.90	2494.0	294.3
60.0	159.0	11.91	2502.0	295.1
62.0	159.1	11.94	2501.0	296.2
64.0	159.1	11.90	2507.0	297.9
66.0	159.2	11.90	2500.0	300.2
68.0	159.3	11.91	2501.0	303.0
70.0	159.6	11.90	2505.0	305.7
72.0	159.5	11.93	2512.0	309.0
74.0	159.7	11.88	2504.0	312.2
76.0	160.1	11.91	2508.0	315.1
78.0	160.5	11.93	2512.0	318.1
80.0	161.1	11.95	2490.0	320.5
82.0	161.8	12.13	2484.0	322.6
84.0	162.5	12.12	2480.0	323.7
86.0	163.3	12.02	2497.0	324.6
88.0	164.1	12.08	2483.0	325.5
90.0	164.8	12.02	2503.0	326.3
92.0	165.7	12.05	2483.0	327.2
94.0	166.5	12.04	2494.0	328.0
96.0	167.3	12.04	2501.0	328.9
98.0	168.2	12.04	2486.0	329.5
100.0	169.0	12.04	2486.0	329.1
102.0	169.8	12.04	2501.0	327.8
104.0	170.5	12.02	2487.0	325.8
106.0	171.2	12.00	2500.0	323.6
108.0	171.7	12.00	2503.0	321.1
110.0	172.2	12.00	2503.0	319.1
112.0	172.5	11.98	2498.0	317.3
114.0	172.8	11.94	2509.0	315.6
116.0	173.1	11.99	2500.0	314.2
118.0	173.2	11.97	2478.0	313.1
120.0	173.3	11.93	2512.0	311.9
122.0	173.4	11.94	2516.0	311.1
124.0	173.5	11.98	2503.0	310.1
126.0	173.5	11.91	2502.0	309.2
128.0	173.5	11.92	2503.0	308.4
130.0	173.5	11.96	2503.0	307.7
132.0	173.4	11.93	2500.0	307.0
134.0	173.4	11.94	2505.0	306.4
136.0	173.3	11.93	2501.0	305.8
138.0	173.2	11.94	2525.0	305.1
140.0	173.2	11.92	2513.0	304.7
142.0	173.1	11.89	2503.0	304.1
144.0	173.0	11.92	2493.0	303.5
146.0	172.9	11.95	2491.0	303.1
148.0	172.8	11.95	2502.0	302.5

Figure 40: Variation of Properties during Transient for Data Series 7T (Depressurisation)

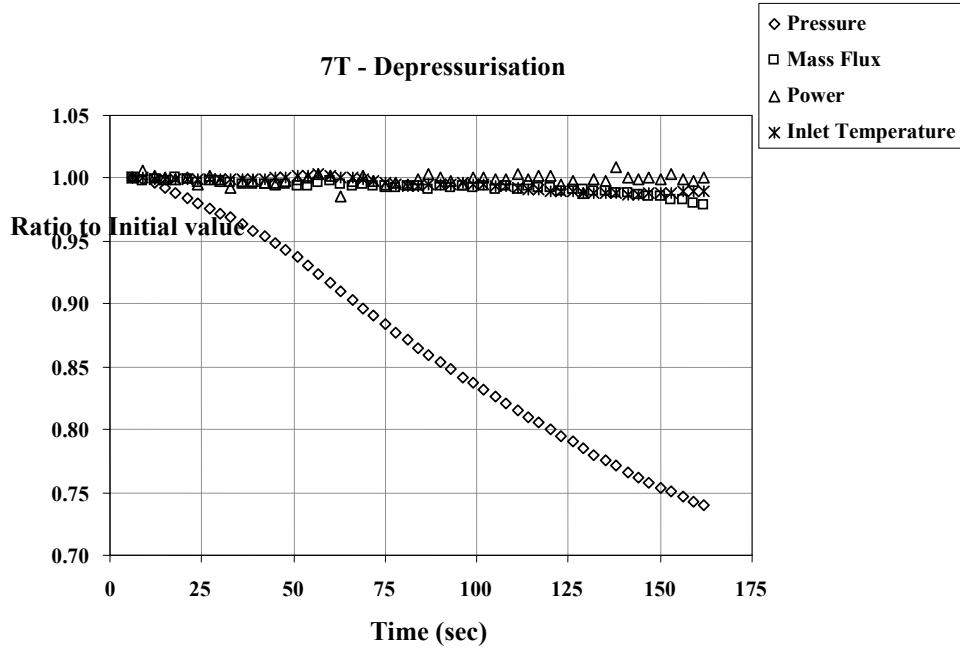
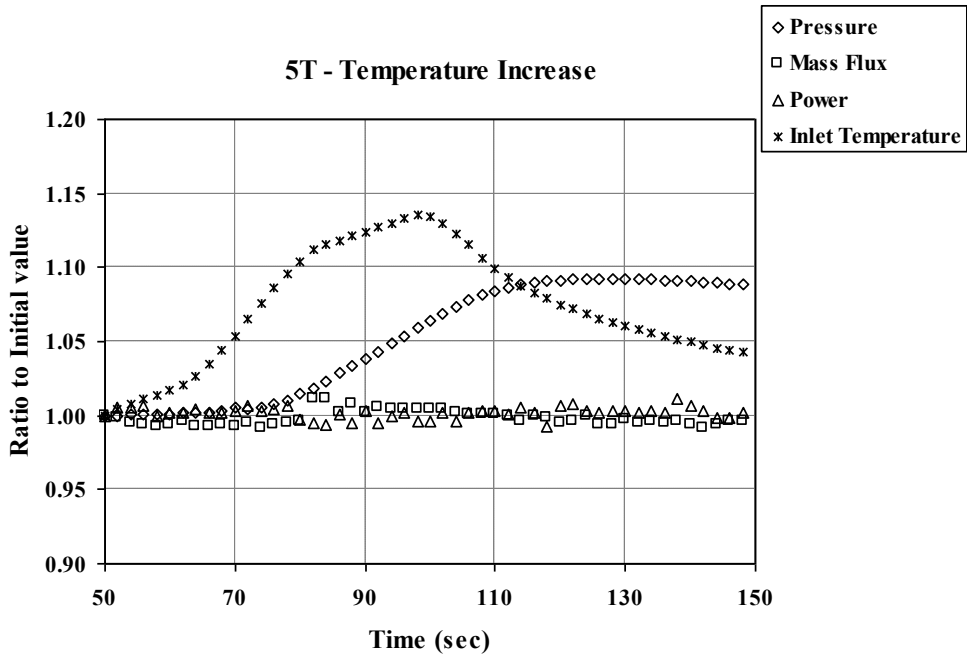


Figure 41: Variation of Properties during Transient for Data Series 7T (Temperature Increase)



4.2.4 Exercise I-4 – Pressure Drop Benchmark

As previously mentioned, no data is available for code-to-data pressure drop comparison. However, code-to-code comparisons will be performed on the pressure drop calculations for the typical central sub-channel. The boundary conditions include both single-phase and two-phase conditions. Exercise cases to be calculated correspond to Test Series 1 of the steady-state central sub-channel void measurements as given in Table 26. This benchmark will assess the wall friction and the two-phase multiplier models of the codes used.

Code-to-code comparisons will also be performed on the pressure drop calculations for the bundle. Exercise cases to be calculated correspond to Test Series 5 of the steady-state bundle void measurements as given in Table 30. This benchmark will assess the pressure loss and the two-phase multiplier models of the codes used.

4.3 Phase II: DNB Benchmark

Table 48 summarises the test series performed for the DNB measurements in Exercises 1, 2, and 3 of Phase II.

Table 48: Test Series for DNB Measurement

Test series	Test section	Assembly	Test mode		Measurement		
			Steady-state	Transient	DNB	Fluid temperature	
0	5×5	A0	Y		Y		
1		A1	Y			Y	
2		A2	Y		Y		
3	6×6	A3	Y		Y		
4	5×5	A4	Y		Y		
8		A8	Y		Y		
11T		A11		Y	Y		
12T		A12		Y	Y		
13		A4				Y	
			Y			Y	

4.3.1 Exercise II-1 – Steady-State Fluid Temperature Benchmark

In addition to the void distribution and DNB power measurements, data is available for the sub-channel exit fluid temperature. The data can be applied to both sub-channel/system and CFD codes.

The highlighted cases are selected to be analysed.

Table 49: Test Conditions for Steady-State Fluid Temperature Benchmark

Test number	Pressure (kg/cm ² a)	Mass flux (10 ⁶ kg/m ² hr)	Inlet temperature (°C)	Power (MW)
01-3233	100.0	4.62	166.1	0.98
01-3232	100.1	1.94	164.4	0.41
01-3239	100.1	1.24	165.3	0.25
01-3231	100.1	0.44	166.2	0.11
<u>01-5343</u>	150.3	5.03	165.3	1.25
<u>01-5342</u>	150.0	1.92	164.5	0.52
01-5242	149.9	1.92	185.1	0.41
01-5243	150.3	4.89	184.7	0.98
01-5143	150.2	4.66	202.9	0.70
01-5333	150.5	4.60	211.6	1.24
01-5233	150.4	4.91	230.9	0.97
01-5235	150.0	10.97	230.3	2.11
01-5325	150.3	10.99	255.7	2.68
01-5225	150.2	10.97	272.6	2.09
<u>01-5215</u>	150.3	10.95	282.9	2.09
<u>01-5125</u>	150.3	10.94	289.2	1.50
01-5123	150.8	4.91	288.5	0.70
01-5213	150.0	4.98	282.3	0.97
01-5223	150.1	4.99	272.2	0.97
01-5222	150.1	1.99	273.0	0.40
01-5212	150.1	1.97	282.2	0.40
01-5322	150.1	1.96	255.7	0.51
01-5133	150.0	4.98	247.1	0.70
01-5323	150.1	4.97	254.7	1.23
01-5135	150.0	11.03	247.0	1.50
<u>01-5237</u>	150.1	16.95	229.4	3.23
01-5335	150.1	11.01	211.7	2.71
01-5145	150.1	11.03	203.3	1.53
01-5245	150.1	11.06	184.4	2.12
01-5345	150.0	11.08	165.1	2.72
01-3225	100.3	11.07	224.5	2.12
01-3215	100.2	11.10	238.6	2.11
01-5231	150.0	0.69	230.9	0.11
01-6231	169.1	0.54	252.9	0.11
01-6239	169.0	1.18	254.5	0.26
01-5239	151.7	1.23	231.6	0.26
01-5332	150.0	2.00	211.5	0.53
01-5232	150.1	2.04	231.0	0.42
<u>01-6232</u>	169.1	2.10	251.5	0.42
<u>01-6233</u>	169.1	4.90	254.0	1.02
01-6235	169.2	11.00	253.0	2.20
01-6237	169.1	17.08	253.0	3.39
01-3235	101.1	11.05	164.8	2.24
01-3237	101.0	17.06	164.9	3.42
01-1231	50.8	0.73	98.6	0.11
01-1239	50.8	1.15	84.5	0.25

Table 49: Test Conditions for Steady-State Fluid Temperature Benchmark – Continued

Test number	Pressure (kg/cm ² a)	Mass flux (10 ⁶ kg/m ² hr)	Inlet temperature (°C)	Power (MW)
01-1232	50.9	2.00	87.2	0.41
01-1233	50.1	5.03	85.0	1.01
01-1235	50.0	11.05	86.0	2.24
<u>01-1237</u>	50.2	17.00	86.0	3.44
01-3245	100.1	10.99	103.6	2.22
01-5255	150.1	11.02	113.8	2.22
01-5355	150.0	11.03	94.3	2.85
01-5155	150.1	11.02	133.2	1.59
01-5153	150.1	5.05	132.9	0.72
01-5253	150.1	5.02	113.3	1.01
01-5353	150.0	5.03	93.4	1.31
01-5352	150.0	1.99	93.3	0.52
<u>01-5252</u>	150.0	1.95	113.9	0.41

4.3.2 Exercise II-2 – Steady-State DNB Benchmark

The experimental data include the power at which departure from nucleate boiling occurs and the corresponding location in the bundle (for selected test cases only). The data can be applied to thermal-hydraulic sub-channel and system codes and CFD codes.

The highlighted cases are selected to be analysed.

Table 50: Test Conditions for Steady-State DNB Test Series 0

Test number	Pressure (kg/cm ² a)	Mass flux (10 ⁶ kg/m ² hr)	Inlet temperature (°C)
00-3230	100.4	5.07	243.2
00-3240	100.7	8.13	242.7
00-3260	101.1	14.28	242.9
00-3270	101.0	17.20	240.9
00-4270	125.8	16.78	262.7
00-4260	126.3	14.27	262.7
00-4240	125.8	8.14	262.4
00-4230	125.2	5.07	263.0
00-5330	150.4	5.08	253.9
00-5340	150.3	8.09	253.1
<u>00-5350</u>	150.1	11.23	252.9
00-5360	150.7	14.28	252.8
00-5370	150.3	17.13	253.3
00-3550	102.6	11.28	147.1
00-4550	125.6	11.27	170.5
00-3460	103.7	14.36	179.8
00-3440	100.1	8.22	179.8
00-3430	100.1	5.12	180.1
00-4430	125.7	5.11	203.6
<u>00-4440</u>	125.6	8.09	202.4
<u>00-4460</u>	125.4	14.20	202.0
00-5560	150.7	14.23	191.8
00-5550	150.5	11.23	191.9
00-5540	152.8	8.19	192.7
00-5530	150.3	5.15	192.0
00-3770	100.8	17.18	193.4
00-3350	99.5	11.14	210.4
00-4770	126.7	17.13	216.0
<u>00-5450</u>	150.7	11.13	223.4
00-3551	103.1	11.31	147.2
00-4551	125.6	11.30	170.2
00-5551	150.1	11.26	192.1
00-6550	169.2	11.23	208.5
00-5451	151.8	11.14	224.0
00-5870	151.5	17.17	227.3
<u>00-6470</u>	169.8	17.16	238.6
00-6460	171.3	14.28	238.7

Table 50: Test Conditions for Steady-State DNB Test Series 0 – Continued

Test number	Pressure (kg/cm ² a)	Mass flux (10 ⁶ kg/m ² hr)	Inlet temperature (°C)
00-6440	171.0	8.13	238.6
00-6430	169.5	5.12	237.9
00-5331	150.4	5.13	253.4
00-5351	150.5	11.19	252.4
00-5371	150.5	17.21	252.7
00-5352	150.2	11.15	252.2
00-6350	169.3	11.12	278.6
00-6270	170.6	17.09	295.4
00-6260	169.3	14.16	294.4
00-6240	168.9	8.12	295.4
00-6230	169.2	5.12	296.2
00-5250	150.6	11.16	281.8
00-7680	159.7	12.23	287.1
00-5251	150.4	11.80	281.5
00-7681	159.8	12.22	288.2
00-4150	124.9	11.10	305.1
00-5130	150.0	5.08	321.6
00-5140	150.5	8.09	321.2
00-5150	150.7	11.09	321.3
00-5160	150.4	14.15	321.0
00-5170	150.8	17.80	321.4
00-6150	168.9	11.06	331.9
00-5151	150.5	11.09	320.9
00-6151	169.3	11.07	332.4
00-4151	125.5	11.10	304.8
00-3150	101.2	11.20	287.4
00-5252	150.6	11.14	281.0
00-3151	100.3	11.19	286.9
00-4350	125.3	11.20	232.5
00-3351	100.2	11.18	211.7
00-4351	125.3	10.95	232.8
00-3352	100.2	10.93	211.7
00-6551	169.1	10.92	208.8

Table 51: Test Conditions for Steady-State DNB Test Series 2

Test number	Pressure (kg/cm ² a)	Mass flux (10 ⁶ kg/m ² hr)	Inlet temperature (°C)
02-2430	75.9	5.03	154.4
<u>02-3430</u>	100.0	5.01	181.0
<u>02-3440</u>	100.5	7.98	178.9
02-2450	76.9	10.90	154.0
02-1450	51.7	10.81	123.2
02-1440	50.9	8.05	123.1
02-1430	50.8	4.97	125.6
02-1420	50.3	2.10	122.6
02-1490	53.5	1.24	128.4
02-4230	125.3	4.89	264.0
02-3230	100.3	4.97	243.4
02-3240	100.7	7.98	243.0
02-3260	100.5	14.13	241.9
02-3270	100.3	16.83	241.9
02-4350	125.7	10.97	233.6
<u>02-4370</u>	125.3	17.04	232.6
02-4270	125.4	16.98	262.9
02-5270	150.0	16.92	281.8
02-7680	158.6	12.03	289.9
02-5250	150.3	10.95	282.3
02-5340	150.0	7.98	253.1
02-5330	149.9	4.93	254.9
02-3420	100.3	2.02	186.4
<u>02-3490</u>	100.5	1.23	175.1
02-1220	50.4	2.09	190.3
02-1230	50.6	4.98	190.8
02-1240	50.9	8.00	189.5
02-1250	52.7	11.03	188.7
02-1260	52.5	14.03	189.0
<u>02-1360</u>	52.7	14.01	155.7
02-1270	53.5	16.89	188.8
02-2270	76.8	16.97	219.5
02-2250	77.4	11.01	219.2
02-1150	52.3	11.06	238.2
02-2150	77.7	11.03	265.4
02-3150	101.6	10.98	287.3
02-3241	100.5	7.98	243.0
02-2230	76.7	4.93	220.1
02-1290	49.4	1.14	200.9
<u>02-3290</u>	100.3	1.18	245.5
02-3220	99.8	1.96	244.7
02-4150	125.5	10.86	306.1
02-5251	150.7	10.93	282.4
02-7681	158.6	12.03	288.9
02-6330	169.8	5.02	268.0

Table 51: Test Conditions for Steady-State DNB Test Series 2 – Continued

Test number	Pressure (kg/cm ² a)	Mass flux (10 ⁶ kg/m ² hr)	Inlet temperature (°C)
02-6350	170.1	10.88	266.9
02-6370	169.7	16.90	267.4
02-5370	150.6	16.94	254.0
02-5360	150.7	14.04	252.9
02-5350	150.7	11.08	253.0
02-5290	150.0	1.20	274.8
02-5220	150.3	2.03	270.3
02-5130	150.1	4.92	322.4
02-5140	150.6	7.87	321.5
02-5490	151.5	1.27	225.9
<u>02-5420</u>	151.3	2.00	229.2
02-3242	100.9	7.97	242.9
02-5252	149.2	10.96	282.7
02-7682	157.2	11.98	288.5
02-5170	149.2	17.17	321.7
02-5160	150.2	13.94	322.7
02-5150	150.7	10.82	322.5
<u>02-6150</u>	169.5	10.89	333.8
02-6250	170.8	10.91	296.2
02-6450	169.4	10.89	238.8
02-6550	169.0	10.95	206.4
02-5450	149.7	10.92	222.2
02-5460	151.0	13.86	222.7
02-5550	150.1	10.96	189.6
02-5540	150.2	8.02	189.5
<u>02-5530</u>	150.3	5.03	190.3
<u>02-4430</u>	126.0	4.95	201.8
<u>02-3350</u>	101.1	10.76	212.4
02-3460	102.2	14.00	178.5
02-4550	124.9	11.03	168.3
02-3550	100.8	10.97	145.7

Table 52: Test Conditions for Steady-State DNB Test Series 3

Test number	Pressure (kg/cm ² a)	Mass flux (10 ⁶ kg/m ² hr)	Inlet temperature (°C)
03-3430	100.3	5.03	180.4
03-3440	100.3	8.05	179.6
03-4550	126.2	11.05	168.8
03-3350	100.6	11.02	210.8
03-3360	99.9	13.77	209.9
03-4350	125.5	10.71	233.3
03-4360	125.4	13.71	232.5
03-4370	126.0	16.76	233.4
<u>03-5460</u>	150.6	13.61	222.5
<u>03-5330</u>	150.3	4.95	254.0
03-5340	150.2	8.02	253.3
03-5250	150.3	11.00	282.5
03-7680	158.1	12.06	289.2
03-5350	150.5	11.02	253.2
03-5360	150.5	13.76	252.7
03-5370	150.7	16.93	252.8
03-5270	150.9	16.72	282.6
03-4270	125.5	16.71	262.8
<u>03-4260</u>	125.1	13.87	262.8
<u>03-4240</u>	125.1	7.99	263.3
03-4230	125.1	4.99	263.9
03-3230	100.1	5.00	243.5
03-3240	100.4	7.94	242.8
03-3260	100.5	13.74	241.5
03-3270	100.2	16.87	242.9
03-3550	100.9	10.83	161.4
03-5530	150.0	5.01	190.9
03-5540	150.3	7.98	190.4
03-4430	125.1	5.02	201.5
03-4440	125.2	7.99	201.4
03-3351	101.0	10.82	212.1
03-5550	150.2	10.92	190.3
03-5450	150.0	10.96	222.4
03-6460	169.6	13.77	238.5
<u>03-6450</u>	169.3	10.73	238.9
<u>03-6440</u>	169.8	7.98	238.5
03-6430	168.8	5.02	238.5
03-6330	169.2	4.96	268.6
03-6350	169.7	10.97	268.4
03-5351	150.5	11.03	252.1
03-5251	150.5	10.97	282.5
03-5352	150.6	11.06	252.9
<u>03-6370</u>	169.8	16.53	268.8
03-6270	169.5	16.62	297.0
03-6260	169.2	13.69	296.7

Table 52: Test Conditions for Steady-State DNB Test Series 3 – Continued

Test number	Pressure (kg/cm ² a)	Mass flux (10 ⁶ kg/m ² hr)	Inlet temperature (°C)
03-5252	150.3	10.76	282.8
03-6240	169.3	7.91	296.5
03-6230	169.3	4.94	296.9
03-5130	150.3	4.90	323.0
03-5140	150.3	7.79	322.8
03-5150	150.6	10.92	323
03-6150	168.9	10.95	334.5
03-5160	150.4	13.66	322.5
03-5170	150.4	16.71	322.7
03-4150	125.3	10.77	306.2
03-3150	100	10.78	287.8
03-3352	100.3	10.73	211.5

Table 53: Test Conditions for Steady-State DNB Test Series 4

Test number	Pressure (kg/cm ² a)	Mass flux (10 ⁶ kg/m ² hr)	Inlet temperature (°C)
04-3330	100.4	4.92	212.0
04-4330	125.1	4.93	233.1
04-3230	100.2	4.91	242.7
04-3240	100.5	7.93	242.0
04-3250	100.2	10.89	241.5
04-3760	100.5	14.09	262.4
04-3750	100.3	10.97	262.3
04-3730	99.9	4.95	263.8
04-4230	125.2	4.96	263.3
04-4250	125.3	10.92	261.8
04-4760	125.3	13.98	282.5
04-4750	125.3	10.95	282.6
04-4730	125.4	4.97	283.4
04-5230	150.1	4.91	281.8
<u>04-5240</u>	150.7	7.87	281.4
<u>04-5250</u>	150.4	10.87	281.5
<u>04-5760</u>	150.3	13.86	300.5
<u>04-5750</u>	150.5	10.84	300.7
<u>04-5730</u>	150.1	4.92	300.9
<u>04-5130</u>	150.1	4.89	321.5
<u>04-5140</u>	150.1	7.86	321.7
<u>04-5150</u>	150.0	10.87	321.3
<u>04-5160</u>	150.2	13.92	321.1
<u>04-5170</u>	150.4	16.78	321.0
04-6170	169.4	16.84	332.9
04-6150	169.3	10.85	332.9
04-6750	169.2	10.83	314.3
04-6250	169.3	10.88	295.0
04-6230	169.4	4.94	295.9
04-7680	158.5	11.94	288.2
04-4150	125.2	10.81	304.8
04-3150	100.3	10.83	286.2
04-3160	100.6	13.90	286.1
04-7681	158.3	12.00	287.2
<u>04-5251</u>	150.8	10.89	281.0
04-6330	169.1	4.94	267.5
<u>04-5330</u>	150.2	4.96	252.6
04-6430	169.4	4.94	237.5
<u>04-5430</u>	150.4	4.95	222.3
04-6530	169.4	4.92	205.9
04-4430	125.5	4.92	201.4
04-3241	100.6	7.93	241.3
04-2150	75.9	10.90	264.6
04-2750	75.3	10.97	236.9
04-2740	75.5	7.95	240.0
04-2730	75.4	4.95	240.8

Table 53: Test Conditions for Steady-State DNB Test Series 4 – Continued

Test number	Pressure (kg/cm ² a)	Mass flux (10 ⁶ kg/m ² hr)	Inlet temperature (°C)
04-2230	75.6	4.96	219.8
04-1730	50.7	4.94	213.3
04-1230	50.3	4.98	190.3
04-2330	75.5	5.00	188.6
04-1220	53.5	2.16	192.1
04-1320	50.8	2.18	148.2
04-2320	75.7	2.15	188.1
04-3320	100.4	2.09	217.2
04-2220	75.4	2.09	218.8
04-3220	100.2	2.23	244.3
04-4320	124.9	2.08	238.2
04-4220	125.1	2.19	264.3
<u>04-5320</u>	150.3	2.04	257.8
<u>04-5220</u>	150.3	2.15	283.1
04-6770	169.3	16.81	314.6
04-6270	169.5	16.83	294.6
<u>04-5260</u>	150.5	13.94	281.1
<u>04-5270</u>	150.5	16.90	281.6
04-4260	125.5	14.05	261.3
04-4270	126.0	17.01	261.5
04-3770	100.8	17.00	262.1
04-6350	169.0	10.99	267.2
04-6450	168.8	10.96	237.0
<u>04-5350</u>	151.7	10.93	251.9
<u>04-5360</u>	150.5	14.06	251.7
<u>04-5440</u>	150.5	7.93	221.8
04-4350	125.5	10.88	232.0
04-3260	100.8	13.96	240.9
04-3350	100.5	10.86	210.2
04-2250	75.4	10.88	217.6

Table 54: Test Conditions for Steady-State DNB Test Series 8

Test number	Pressure (kg/cm ² a)	Mass flux (10 ⁶ kg/m ² hr)	Inlet temperature (°C)
08-3330	100.5	5.05	211.8
08-4330	124.7	5.06	233.1
08-3230	100.2	5.07	242.5
08-3240	100.4	8.09	241.3
08-3250	100.6	11.22	241.3
08-3760	100.4	14.28	262.0
08-3750	100.5	11.09	262.1
08-3740	100.2	8.11	262.4
08-3730	100.2	5.05	263.4
08-4230	125.3	5.03	262.1
08-4240	125.2	8.08	261.9
08-4250	125.4	11.17	262.0
08-4760	125.1	14.21	282.4
08-4750	125.4	11.16	282.2
08-4740	125.2	8.11	282.4
08-4730	125.3	5.02	282.9
08-5230	150.6	4.98	281.6
08-5240	150.4	8.02	281.5
08-5250	149.9	11.05	280.9
08-7680	158.4	12.16	288.0
08-5760	150.1	14.15	300.7
08-5750	150.3	11.04	300.4
08-5740	150.4	8.00	300.5
08-5730	150.2	4.96	300.4
08-5130	150.1	4.95	321.6
08-5140	150.4	8.01	321.3
08-5150	150.2	11.03	321.0
08-5160	150.4	14.16	321.0
08-5170	150.4	17.10	320.9
08-6170	169.6	17.10	332.6
08-6150	168.5	11.04	332.5
08-6750	169.2	11.02	314.0
08-6250	168.9	11.01	295.5
08-6240	168.9	8.03	295.5
08-6230	169.1	4.99	295.6
08-7681	158.3	12.16	288.3
08-4150	125.2	11.04	304.6
08-4140	125.2	8.03	304.8
08-3140	100.6	8.06	286.4
08-3150	100.2	11.08	286.1
08-3160	100.2	14.25	285.9
08-5251	150.1	11.08	281.3
08-6340	169.2	8.06	267.3
08-6330	169.1	5.05	267.7
08-5340	150.4	8.08	252.6
08-5330	150.4	5.04	252.4

Table 54: Test Conditions for Steady-State DNB Test Series 8 – Continued

Test number	Pressure (kg/cm ² a)	Mass flux (10 ⁶ kg/m ² hr)	Inlet temperature (°C)
08-6430	169.1	5.01	237.6
<u>08-5430</u>	150.2	5.04	222.5
08-6530	169.2	5.00	206.4
08-4430	125.2	5.02	201.7
08-3241	100.5	8.09	241.6
08-2150	75.5	11.20	264.0
08-2750	75.3	11.20	239.3
08-2740	75.4	8.15	239.6
08-2730	75.2	5.04	240.8
08-2230	75.2	5.02	219.2
08-1730	50.2	5.02	212.8
08-1230	50.5	5.03	189.8
08-1220	50.2	2.10	189.3
08-1320	50.4	2.09	157.5
08-2320	75.1	2.09	187.8
08-2220	75.3	2.12	222.3
08-3320	100.5	2.12	208.0
08-3220	100.4	2.09	244.8
08-4320	124.8	2.11	230.4
08-4220	125.0	2.07	265.2
<u>08-5320</u>	150.3	2.12	248.7
<u>08-5220</u>	150.3	2.07	279.5
<u>08-5252</u>	150.2	11.13	281.5
08-7682	158.3	12.22	288.3
08-6770	169.5	17.20	314.4
08-6270	168.8	17.18	295.0
<u>08-5260</u>	150.4	14.25	281.3
<u>08-5270</u>	149.9	17.25	281.0
08-3242	100.3	8.06	241.4
08-4260	125.0	14.29	260.7
08-4270	125.8	17.33	262.0
08-6350	169.4	11.12	266.7
08-6450	169.1	11.14	237.0
08-7683	158.1	12.36	288.4
<u>08-5350</u>	150.5	11.35	251.9
<u>08-5360</u>	150.4	14.20	252.8
<u>08-5440</u>	150.0	8.09	222.6
08-4350	125.1	11.15	232.7
08-3770	100.5	17.34	262.2
08-3260	100.4	14.33	241.5
08-3350	100.3	11.14	210.9
08-2250	74.7	11.12	216.4
08-1150	50.2	11.20	237.5
08-1750	50.5	11.15	212.1
08-1250	50.3	11.15	188.4
08-2330	75.2	5.04	188.6
08-1330	50.2	5.08	158.2

Table 55: Test Conditions for Steady-State DNB Test Series 13

Test number	Pressure (kg/cm ² a)	Mass flux (10 ⁶ kg/m ² hr)	Inlet temperature (°C)
13-4240	125.2	7.79	265.7
13-4250	125.5	10.94	263.6
13-A250	138.1	10.91	273.6
13-A240	137.3	7.93	274.1
13-5340	150.2	8.04	254.3
13-5D40	150.4	8.05	269.1
13-5230	150.4	4.90	283.7
13-52A0	150.1	6.42	285.2
13-5240	150.3	7.91	283.1
13-52B0	150.3	9.45	284.6
13-5250	150.1	10.90	282.8
13-4251	125.0	11.00	262.4
13-4241	125.1	7.80	265.8
13-A241	137.6	8.04	272.1
13-A251	137.9	10.79	275.2
13-5341	150.1	8.04	254.4
13-5D41	150.3	8.05	269.1
13-5231	150.0	4.92	283.9
13-52A1	150.0	6.41	282.2
13-5241	150.1	7.90	283.3
13-52B1	150.3	9.48	284.7
13-5251	150.5	10.95	283.3
13-B240	159.5	7.98	288.6
13-B250	159.7	10.71	291.9
13-6250	169.5	10.84	297.2
13-6240	169.3	7.98	297.2
13-5C40	150.0	7.76	293.1
13-5B40	150.1	7.74	302.6
13-5A40	150.3	7.95	313.3
13-5140	150.2	7.89	323.1
13-51B0	150.2	9.37	322.3
13-5150	150.2	10.84	322.8
13-51C0	150.3	12.32	321.0
13-5160	150.3	13.90	322.7
13-5A50	150.1	10.69	312.8
13-5B50	150.0	10.69	302.0
13-5C50	150.1	10.66	297.5
13-6251	169.0	10.80	297.0
13-6241	169.0	7.99	295.5
13-B251	159.8	10.67	292.0
13-B241	159.7	7.97	290.5
13-5C41	150.0	7.76	293.4
13-5B41	150.4	7.94	302.7
13-5A41	149.7	7.97	313.2
13-5C51	150.3	10.61	293.0
13-52C0	150.6	12.31	282.7

Table 55: Test Conditions for Steady-State DNB Test Series 13 – Continued

Test number	Pressure (kg/cm ² a)	Mass flux (10 ⁶ kg/m ² hr)	Inlet temperature (°C)
<u>13-5D50</u>	150.1	10.66	269.0
13-5260	150.5	13.78	282.8
<u>13-5230</u>	150.1	10.95	254.0
<u>13-52C1</u>	150.5	12.38	282.3
<u>13-5261</u>	150.8	13.77	283.0
13-5D51	150.1	10.74	269.2
13-5141	150.4	7.86	320.2
13-51B1	150.6	9.35	318.1
13-5151	150.5	10.83	319.7
13-51C1	150.7	12.36	318.1
13-5161	151.4	13.89	319.6
13-5A51	150.0	10.69	310.2
13-5B51	150.2	10.67	299.3
13-5351	150.5	10.94	251.5

4.3.3 Exercise II-3 – Transient DNB Benchmark

The experimental data include the power at which departure from nuclear boiling occurs during four transient scenarios: power increase; flow reduction; depressurisation; temperature increase. A summary of the test conditions for transient DNB test series 11T and 12T is given in Table 56. The data can be applied to sub-channel and system codes.

Tables 57 through 64 contain the boundary conditions for each transient. Plots of each parameter are also included during the transient (Figures 42 through 49). These plots represent the ratio of the value of each parameter at a certain time to the value at the start of the transient.

All transient cases are to be analysed.

Table 56: Test Conditions for Transient DNB Test Series 11T and 12T

Test series	Assembly	Initial conditions				Transients
		Power (MW)	Mass flux ($10^6\text{kg/m}^2\text{h}$)	Pressure ($\text{kg/cm}^2\text{a}$)	Inlet temperature ($^{\circ}\text{C}$)	
11T	A4	2.50	11.18	156.2	291.0	Power increase
		2.50	11.19	156.1	293.1	Flow reduction
		2.52	11.28	156.3	291.7	Depressurisation
		2.48	11.04	154.6	291.6	Temperature increase
12T	A8	2.51	11.40	156.1	291.3	Power increase
		2.51	11.71	156.3	292.5	Flow reduction
		2.50	11.42	156.2	290.6	Depressurisation
		2.50	11.38	155.8	291.2	Temperature increase

Table 57: Transient DNB Data in Rod Bundle in Test Series 11T (Power Increase)

Time (sec)	Pressure (kg/cm²a)	Mass flux (10⁶ kg/m²hr)	Inlet temperature (°C)	Power (MW)
61	156.2	11.18	291.0	2.50
62	156.3	11.16	290.9	2.52
63	156.3	11.18	290.9	2.55
64	156.4	11.16	291.0	2.58
65	156.8	11.18	291.0	2.61
66	156.6	11.16	291.0	2.64
67	156.5	11.16	291.0	2.67
68	156.4	11.16	290.9	2.70
69	156.3	11.16	291.0	2.73
70	156.3	11.14	291.0	2.75
71	156.5	11.14	291.0	2.78
72	156.8	11.13	291.0	2.81
73	156.9	11.11	291.0	2.83
74	156.8	11.14	291.0	2.86
75	157.0	11.13	291.0	2.88
76	157.0	11.10	291.0	2.91
77	156.8	11.13	291.0	2.94
78	156.8	11.12	291.0	2.98
79	156.8	11.13	291.0	3.01
80	157.0	11.10	291.0	3.04
81	157.1	11.12	291.0	3.05
82	157.2	11.11	291.0	3.08
83	157.4	11.10	291.0	3.11
84	157.3	11.11	291.0	3.14
85	157.5	11.14	291.0	3.17
86	157.2	11.09	291.0	3.21
87	157.6	11.07	291.0	3.23
88	157.8	11.10	291.0	3.26
89	157.3	11.06	291.0	3.29
90	157.4	11.06	291.0	3.33
91	157.5	11.06	291.0	3.35
92	157.6	11.07	291.0	3.39
93	157.9	11.08	291.0	3.41
94	157.6	11.06	291.0	3.44
95	157.7	11.05	291.0	3.46
96	158.1	11.05	291.0	3.50
97	157.7	11.03	291.0	3.53
98	157.9	11.06	291.0	3.55
99	157.6	11.05	291.0	3.58
100	157.6	11.04	291.0	3.61
101	157.9	11.03	291.0	3.64
102	157.5	11.02	291.0	3.67
103	157.6	11.00	291.0	3.69
104	157.9	11.00	291.0	3.72
105	157.6	11.01	291.0	3.75
106	157.6	11.00	291.0	3.78
107	157.9	10.99	291.0	3.81
108	157.6	10.95	290.9	3.83

Table 58: Transient DNB Data in Rod Bundle in Test Series 11T (Flow Reduction)

Time (sec)	Pressure (kg/cm²a)	Mass flux (10⁶ kg/m² hr)	Inlet temperature (°C)	Power (MW)
20	156.1	11.19	293.1	2.50
21	156.3	11.19	293.1	2.50
22	156.4	11.19	293.1	2.50
23	156.3	11.16	293.1	2.50
24	156.3	10.88	293.2	2.50
25	156.2	10.58	293.2	2.50
26	156.1	10.34	293.2	2.51
27	156.3	10.20	293.2	2.50
28	156.1	10.13	293.2	2.50
29	156.5	10.05	293.1	2.50
30	156.1	9.89	293.1	2.50
31	156.1	9.66	293.2	2.50
32	156.5	9.46	293.1	2.50
33	156.3	9.26	293.2	2.50
34	156.4	9.13	293.2	2.49
35	156.3	8.99	293.2	2.49
36	156.3	8.82	293.2	2.49
37	156.5	8.57	293.2	2.50
38	156.6	8.31	293.2	2.50
39	156.4	8.10	293.2	2.50
40	156.6	7.98	293.2	2.50
41	156.8	7.90	293.2	2.50
42	156.9	7.76	293.3	2.50
43	157.1	7.49	293.3	2.50
44	157.2	7.21	293.3	2.49
45	156.9	6.98	293.3	2.49
46	156.9	6.89	293.3	2.50
47	157.3	6.77	293.3	2.49
48	157.3	6.53	293.3	2.49
49	157.2	6.36	293.2	2.50
50	157.4	6.31	293.3	2.50
51	157.7	6.25	293.2	2.50
52	157.6	6.05	293.2	2.50
53	157.7	5.75	293.2	2.50
54	158.1	5.51	293.2	2.50
55	157.8	5.34	293.2	2.50

Figure 42: Variation of Properties during Transient for Data Series 11T (Power Increase)

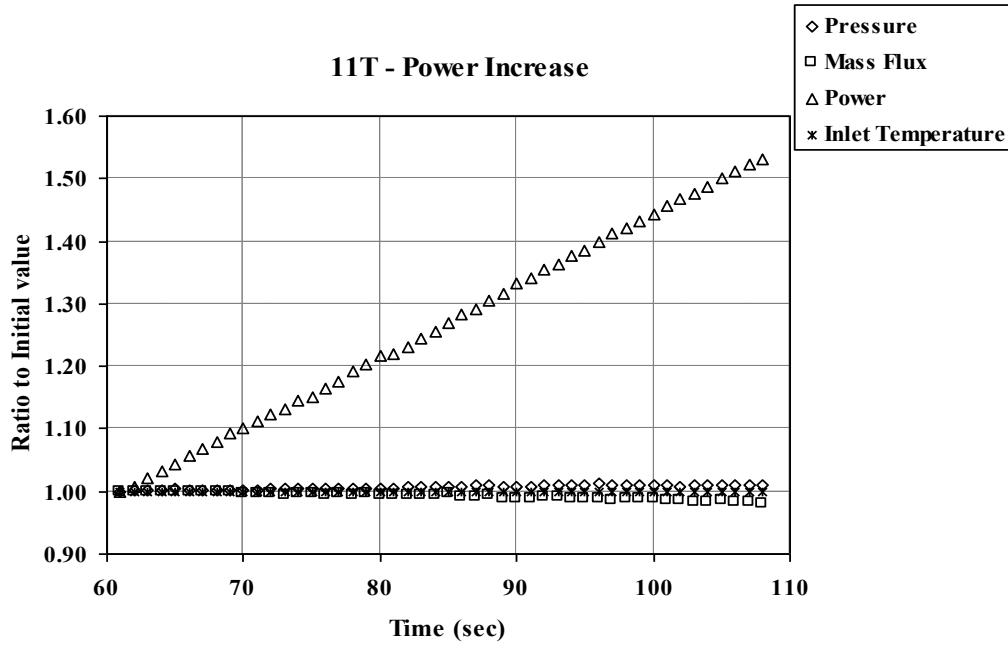


Figure 43: Variation of Properties during Transient for Data Series 11T (Flow Reduction)

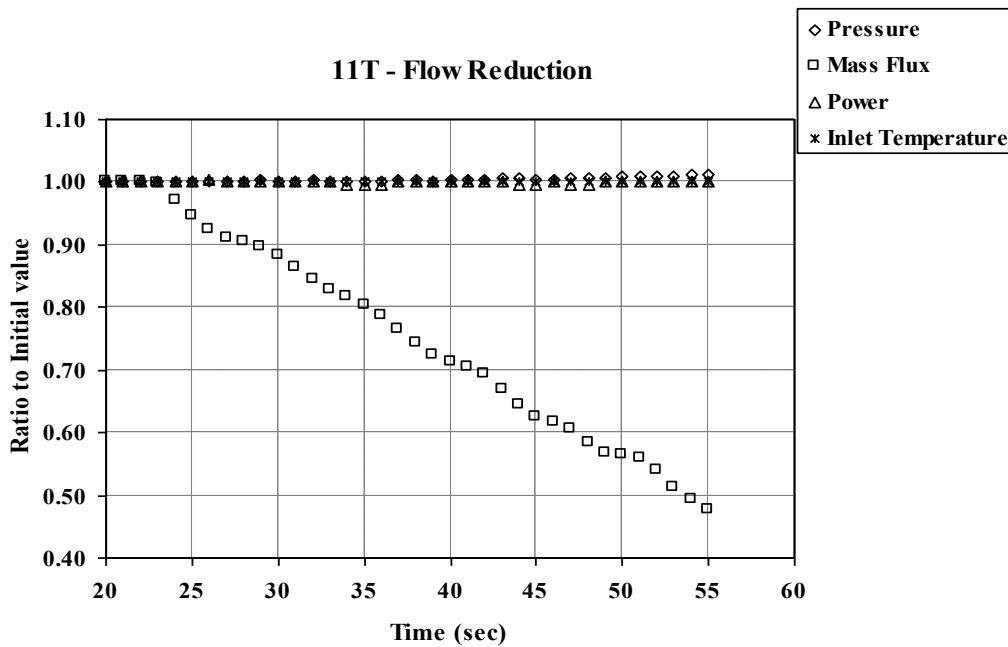


Table 59: Transient DNB Data in Rod Bundle in Test Series 11T (Depressurisation)

Time (sec)	Pressure (kg/cm ² a)	Mass flux (10 ⁶ kg/m ² hr)	Inlet temperature (°C)	Power (MW)
50	156.3	11.28	291.7	2.52
51	156.4	11.27	291.7	2.53
52	156.4	11.26	291.7	2.53
53	156.0	11.24	291.7	2.54
54	155.3	11.22	291.7	2.57
55	154.9	11.25	291.7	2.60
56	154.6	11.25	291.7	2.63
57	154.2	11.25	291.7	2.66
58	153.9	11.23	291.7	2.69
59	153.5	11.24	291.7	2.72
60	153.2	11.23	291.7	2.75
61	152.9	11.22	291.7	2.77
62	152.5	11.23	291.6	2.80
63	152.3	11.24	291.6	2.83
64	151.8	11.25	291.7	2.85
65	151.2	11.21	291.7	2.88
66	150.8	11.18	291.6	2.92
67	150.4	11.19	291.6	2.95
68	150.0	11.22	291.6	2.98
69	149.7	11.20	291.6	3.01
70	149.2	11.20	291.6	3.04
71	148.7	11.18	291.6	3.07
72	148.3	11.17	291.6	3.10
73	147.9	11.18	291.6	3.13
74	147.5	11.15	291.6	3.17
75	147.3	11.15	291.5	3.20
76	146.7	11.15	291.5	3.23
77	146.3	11.15	291.5	3.25
78	145.9	11.16	291.6	3.28
79	145.4	11.18	291.6	3.31
80	145.2	11.18	291.5	3.34
81	145.0	11.17	291.6	3.37
82	144.4	11.11	291.5	3.39
83	143.8	11.09	291.6	3.42
84	143.5	11.09	291.6	3.45
85	143.2	11.11	292.7	3.47
86	143.0	11.13	291.8	3.50
87	142.3	11.11	291.9	3.53
88	141.9	11.08	292.0	3.56
89	141.4	11.10	292.2	3.59
90	141.3	11.12	292.5	3.62
91	140.9	11.12	292.8	3.65
92	140.3	11.11	293.1	3.68
93	139.9	11.10	293.4	3.71
94	139.6	11.12	293.8	3.74
95	139.3	11.12	294.2	3.76
96	139.1	11.12	294.5	3.79

Table 60: Transient DNB Data in Rod Bundle in Test Series 11T (Temperature Increase)

Time (sec)	Pressure (kg/cm ² a)	Mass flux (10 ⁶ kg/m ² hr)	Inlet temperature (°C)	Power (MW)
96	154.6	11.04	291.6	2.48
97	154.4	11.04	291.6	2.48
98	154.3	11.03	291.6	2.49
99	154.5	11.02	291.7	2.50
100	154.2	11.01	291.8	2.51
101	154.2	11.02	291.8	2.53
102	154.6	11.03	292.0	2.55
103	154.3	11.02	292.3	2.56
104	154.3	10.98	292.6	2.57
105	154.2	11.00	293.1	2.59
106	154.4	11.01	293.5	2.60
107	154.1	11.02	294.0	2.62
108	154.3	11.00	294.7	2.64
109	154.2	10.99	295.3	2.65
110	154.2	11.02	296.0	2.66
111	154.2	11.05	296.7	2.68
112	154.2	11.06	297.5	2.70
113	154.4	11.03	298.2	2.72
114	154.9	11.04	299.1	2.74
115	154.9	11.03	299.8	2.75
116	154.6	11.03	300.6	2.77
117	154.5	11.06	301.3	2.79
118	154.6	11.04	302.0	2.80
119	154.7	11.05	302.8	2.82
120	155.0	11.05	303.5	2.84
121	154.9	11.06	304.1	2.85
122	155.0	11.07	304.9	2.87
123	155.1	11.08	305.4	2.88
124	155.3	11.08	306.0	2.89
125	155.5	11.05	306.6	2.91
126	155.6	11.06	307.2	2.93
127	155.6	11.09	307.8	2.94
128	155.8	11.09	308.3	2.96
129	156.0	11.09	308.9	2.97
130	156.3	11.09	309.4	2.99
131	156.4	11.07	309.9	3.00
132	156.8	11.06	310.3	3.02
133	156.4	11.06	310.7	3.04
134	157.0	11.08	311.2	3.05
135	156.6	11.10	311.5	3.07
136	156.6	11.10	311.9	3.09
137	156.6	11.11	312.2	3.10
138	156.7	11.11	312.6	3.11
139	157.1	11.15	312.9	3.12
140	157.1	11.17	313.3	3.14
141	156.8	11.19	313.6	3.16
142	157.0	11.22	313.9	3.18
143	156.9	11.22	314.2	3.19
144	157.1	11.21	314.4	3.21
145	156.9	11.18	314.7	3.22
146	157.1	11.17	314.9	3.24
147	157.0	11.19	315.1	3.25
148	157.0	11.24	315.4	3.27
149	157.3	11.25	315.5	3.28
150	157.1	11.25	315.8	3.30
151	157.3	11.17	315.8	3.30

Figure 44: Variation of Properties during Transient for Data Series 11T (Depressurisation)

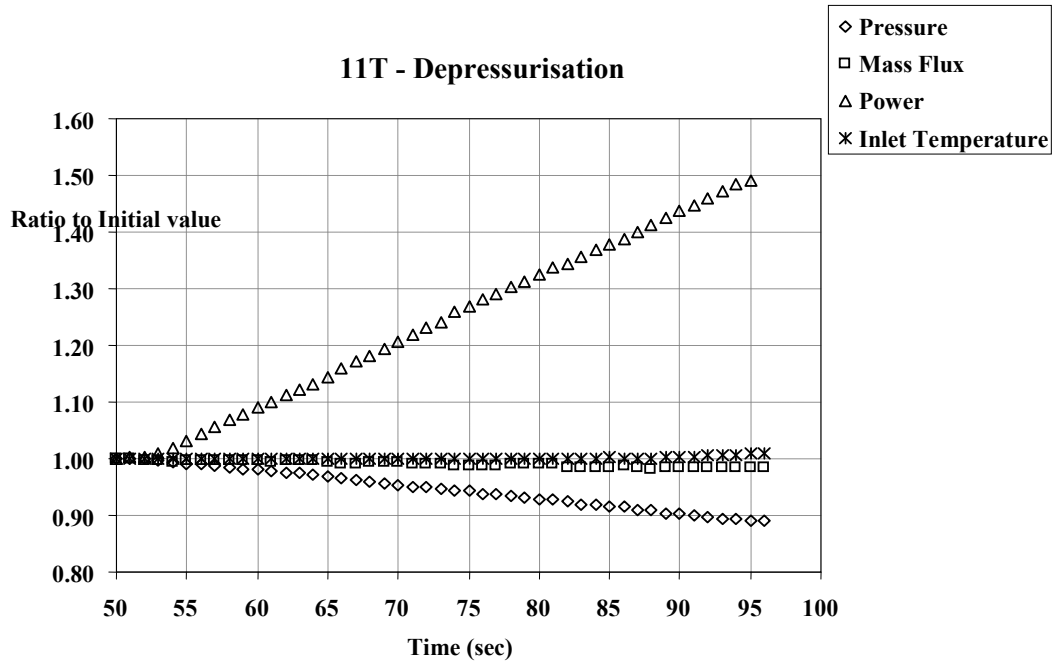


Figure 45: Variation of Properties during Transient for Data Series 11T (Temperature Increase)

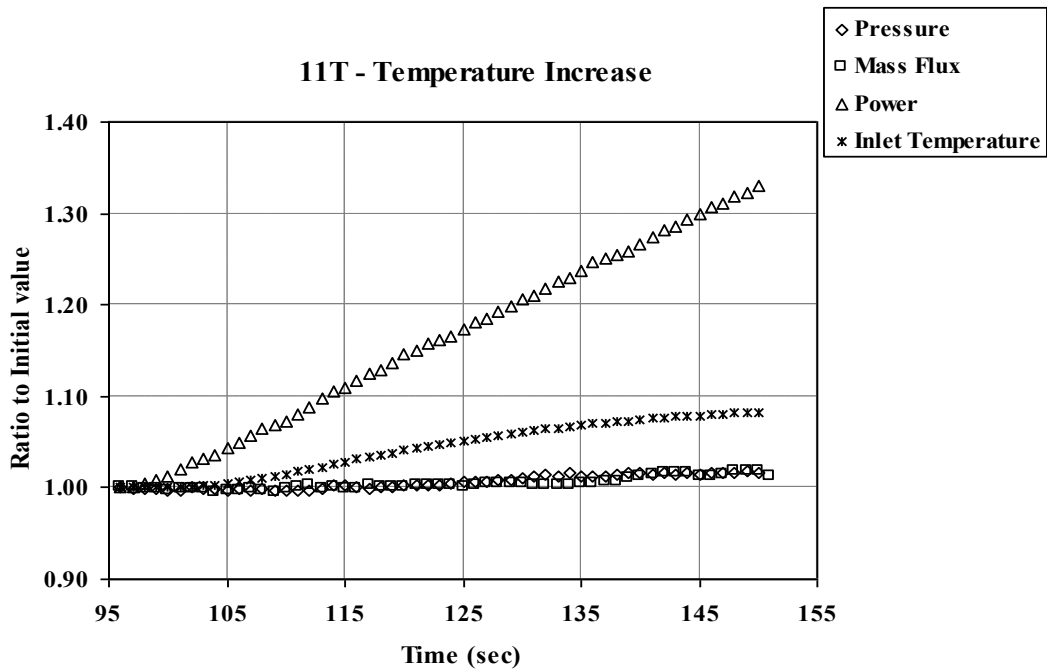


Table 61: Transient DNB Data in Rod Bundle in Test Series 12T (Power Increase)

Time (sec)	Pressure (kg/cm²a)	Mass flux (10⁶ kg/m² hr)	Inlet temperature (°C)	Power (MW)
46	156.1	11.40	291.3	2.51
47	156.1	11.42	291.3	2.52
48	156.1	11.40	291.3	2.56
49	156.1	11.39	291.2	2.59
50	156.2	11.39	291.3	2.62
51	156.2	11.41	291.3	2.65
52	156.2	11.39	291.2	2.68
53	156.6	11.38	291.2	2.71
54	156.3	11.38	291.1	2.75
55	156.3	11.37	291.2	2.78
56	156.4	11.38	291.2	2.81
57	156.4	11.38	291.1	2.85
58	156.5	11.39	291.1	2.87
59	156.5	11.38	291.1	2.90
60	156.6	11.35	291.1	2.93
61	156.8	11.35	291.1	2.96
62	156.7	11.37	291.0	3.00
63	156.8	11.37	291.0	3.04
64	156.9	11.39	291.0	3.07
65	157.2	11.37	291.0	3.10
66	157.3	11.37	291.0	3.13
67	157.1	11.37	290.9	3.17
68	157.2	11.35	291.0	3.20
69	157.3	11.39	290.9	3.24
70	157.3	11.35	290.9	3.27
71	157.6	11.36	290.9	3.31
72	157.6	11.35	290.9	3.34
73	157.6	11.34	290.8	3.37
74	157.7	11.34	290.8	3.40
75	157.8	11.34	290.8	3.43
76	158.0	11.32	290.9	3.47
77	158.0	11.34	290.8	3.50
78	158.1	11.31	290.8	3.52
79	158.3	11.29	290.8	3.57
80	158.4	11.31	290.8	3.59
81	158.6	11.30	290.8	3.62
82	158.5	11.31	290.8	3.65
83	158.8	11.28	290.8	3.68
84	158.7	11.29	290.8	3.71
85	158.8	11.28	290.8	3.75
86	158.9	11.26	290.8	3.78
87	159.1	11.26	290.9	3.81
88	159.2	11.25	290.8	3.84

Table 62: Transient DNB Data in Rod Bundle in Test Series 12T (Flow Reduction)

Time (sec)	Pressure (kg/cm²a)	Mass flux (10⁶ kg/m² hr)	Inlet temperature (°C)	Power (MW)
20	156.3	11.71	292.5	2.51
21	156.3	11.67	292.5	2.51
22	156.4	11.66	292.4	2.51
23	156.2	11.66	292.4	2.51
24	156.3	11.68	292.5	2.51
25	156.3	11.67	292.4	2.51
26	156.2	11.58	292.5	2.51
27	156.1	11.27	292.5	2.51
28	156.6	10.96	292.5	2.51
29	156.1	10.64	292.5	2.51
30	156.2	10.49	292.4	2.51
31	156.2	10.40	292.5	2.50
32	156.2	10.28	292.5	2.51
33	156.1	10.09	292.5	2.51
34	156.1	9.86	292.5	2.51
35	156.1	9.61	292.6	2.50
36	156.2	9.44	292.5	2.50
37	156.3	9.31	292.5	2.50
38	156.3	9.14	292.4	2.50
39	156.4	8.91	292.5	2.50
40	156.4	8.67	292.5	2.50
41	156.6	8.39	292.5	2.50
42	156.7	8.17	292.5	2.50
43	156.8	8.02	292.5	2.50
44	156.7	7.88	292.4	2.50
45	156.8	7.70	292.5	2.50
46	156.8	7.49	292.3	2.49
47	156.9	7.26	292.4	2.49
48	156.9	7.01	292.4	2.49
49	157.1	6.74	292.4	2.49
50	157.2	6.52	292.4	2.49
51	157.3	6.38	292.4	2.49
52	157.3	6.25	292.3	2.49
53	157.5	6.05	292.5	2.49
54	157.5	5.80	292.5	2.49
55	157.5	5.54	292.6	2.48
56	157.6	5.35	292.7	2.48
57	157.8	5.26	292.7	2.48
58	157.9	5.10	292.6	2.48

Figure 46: Variation of Properties during Transient for Data Series 12T (Power Increase)

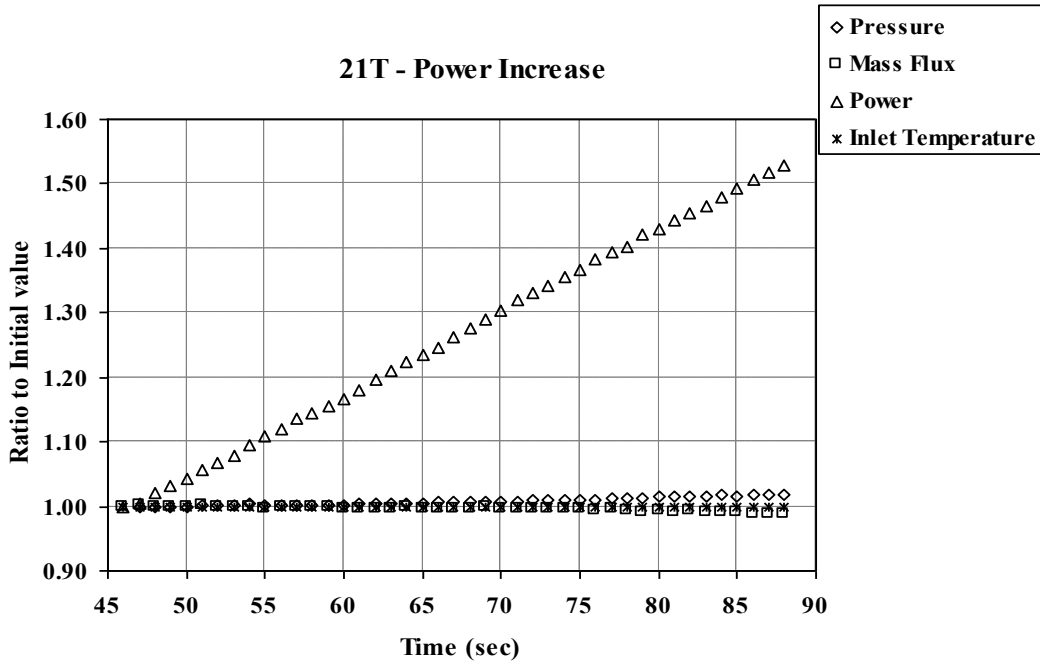


Figure 47: Variation of Properties during Transient for Data Series 12T (Flow Reduction)

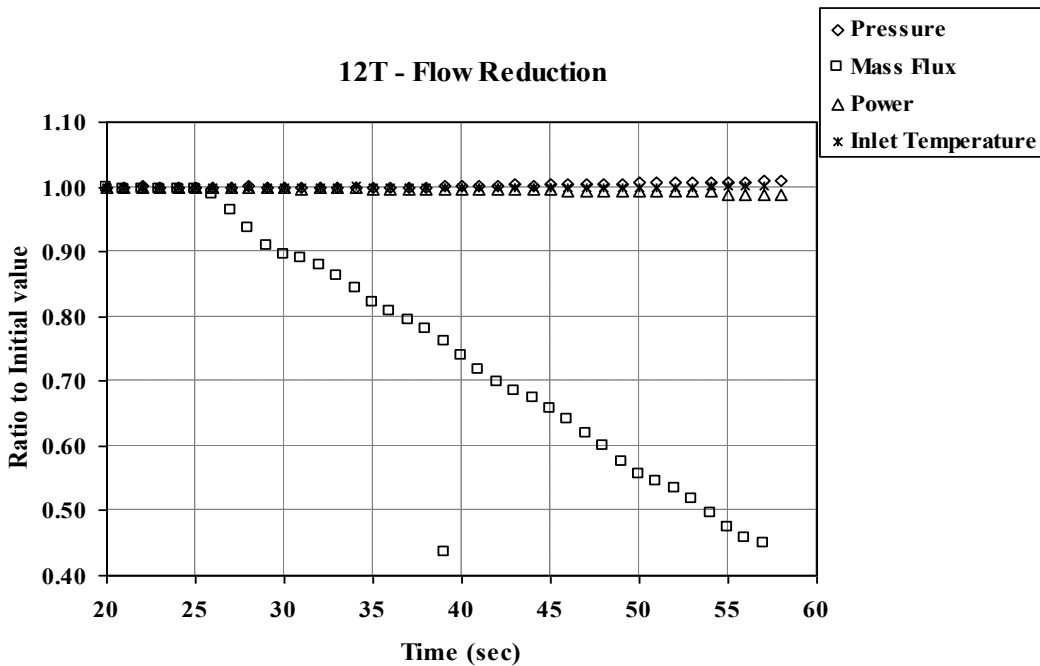


Table 63: Transient DNB Data in Rod Bundle in Test Series 12T (Depressurisation)

Time (sec)	Pressure (kg/cm²a)	Mass flux (10⁶ kg/m² hr)	Inlet temperature (°C)	Power (MW)
92	156.2	11.42	290.6	2.50
93	156.3	11.42	290.6	2.50
94	156.1	11.34	290.6	2.50
95	156.1	11.36	290.6	2.50
96	155.9	11.36	290.7	2.51
97	155.7	11.39	290.6	2.53
98	155.6	11.41	290.7	2.55
99	155.4	11.41	290.6	2.56
100	155.2	11.38	290.7	2.58
101	155.0	11.36	290.7	2.60
102	154.8	11.36	290.7	2.61
103	154.8	11.40	290.7	2.63
104	154.4	11.40	290.7	2.65
105	154.2	11.39	290.7	2.67
106	153.9	11.37	290.7	2.68
107	153.6	11.39	290.6	2.70
108	153.3	11.36	290.6	2.72
109	153.0	11.35	290.6	2.74
110	152.7	11.36	290.6	2.76
111	152.4	11.41	290.6	2.78
112	152.0	11.39	290.6	2.80
113	151.7	11.38	290.6	2.81
114	151.4	11.39	290.6	2.83
115	151.0	11.34	290.6	2.85
116	150.7	11.33	290.6	2.87
117	150.4	11.31	290.6	2.89
118	150.2	11.38	290.6	2.91
119	149.8	11.38	290.6	2.92
120	149.4	11.34	290.6	2.93
121	149.1	11.32	290.6	2.95
122	148.8	11.32	290.6	2.97
123	148.5	11.36	290.6	2.99
124	148.0	11.34	290.6	3.01
125	147.7	11.31	290.6	3.03
126	147.3	11.31	290.6	3.05
127	147.0	11.32	290.6	3.08
128	146.6	11.35	290.6	3.09
129	146.4	11.33	290.5	3.11
130	145.9	11.32	290.6	3.13
131	145.8	11.35	290.7	3.15
132	145.4	11.36	290.7	3.17
133	144.9	11.32	290.8	3.19
134	144.7	11.30	290.9	3.20
135	144.3	11.27	291.0	3.22
136	144.1	11.26	291.1	3.23
137	143.6	11.29	291.3	3.25
138	143.3	11.30	291.5	3.27
139	142.9	11.32	291.6	3.28
140	142.6	11.31	291.8	3.30
141	142.3	11.29	292.0	3.32
142	142.0	11.28	292.3	3.33
143	141.8	11.28	292.5	3.35
144	141.4	11.33	292.7	3.37
145	141.1	11.35	293.0	3.39
146	140.9	11.36	293.3	3.41

Table 64: Transient DNB Data in Rod Bundle in Test Series 12T (Temperature Increase)

Time (sec)	Pressure (kg/cm²a)	Mass flux (10⁶ kg/m² hr)	Inlet temperature (°C)	Power (MW)
83	155.8	11.38	291.2	2.5
84	155.8	11.39	291.2	2.5
85	155.6	11.36	291.2	2.5
86	155.6	11.32	291.2	2.51
87	155.5	11.34	291.2	2.51
88	155.5	11.37	291.2	2.51
89	155.4	11.37	291.2	2.53
90	155.5	11.34	291.2	2.54
91	155.4	11.32	291.2	2.56
92	155.5	11.29	291.2	2.58
93	155.3	11.25	291.2	2.6
94	155.2	11.23	291.2	2.61
95	155.2	11.23	291.2	2.63
96	155.2	11.27	291.2	2.65
97	155.2	11.28	291.2	2.66
98	155.1	11.28	291.2	2.67
99	155.4	11.21	291.2	2.69
100	155.1	11.20	291.3	2.71
101	155.2	11.22	291.3	2.73
102	155.2	11.24	291.3	2.75
103	155.2	11.22	291.4	2.77
104	155.0	11.23	291.5	2.79
105	155.0	11.20	291.7	2.81
106	155.2	11.19	292.0	2.83
107	155.0	11.19	292.3	2.84
108	155.0	11.23	292.7	2.86
109	155.0	11.18	293.3	2.88
110	155.0	11.16	293.8	2.9
111	155.1	11.12	294.4	2.91
112	155.1	11.14	295.0	2.92
113	155.3	11.18	295.7	2.94
114	155.3	11.22	296.4	2.95
115	155.4	11.22	297.1	2.97
116	155.3	11.14	297.8	2.99
117	155.4	11.19	298.6	3.01
118	155.4	11.21	299.4	3.02
119	155.4	11.25	300.2	3.04
120	155.5	11.22	301.0	3.06
121	155.7	11.24	301.9	3.08
122	155.7	11.21	302.7	3.1
123	155.8	11.22	303.5	3.12
124	155.9	11.24	304.4	3.14
125	156.1	11.24	305.3	3.15
126	156.1	11.26	306.2	3.17
127	156.4	11.25	307.2	3.18
128	156.4	11.26	308.0	3.2
129	156.7	11.23	308.8	3.22
130	156.9	11.26	309.7	3.24
131	157.0	11.26	310.5	3.25
132	157.2	11.25	311.4	3.28

Figure 48: Variation of Properties during Transient for Data Series 12T (Depressurisation)

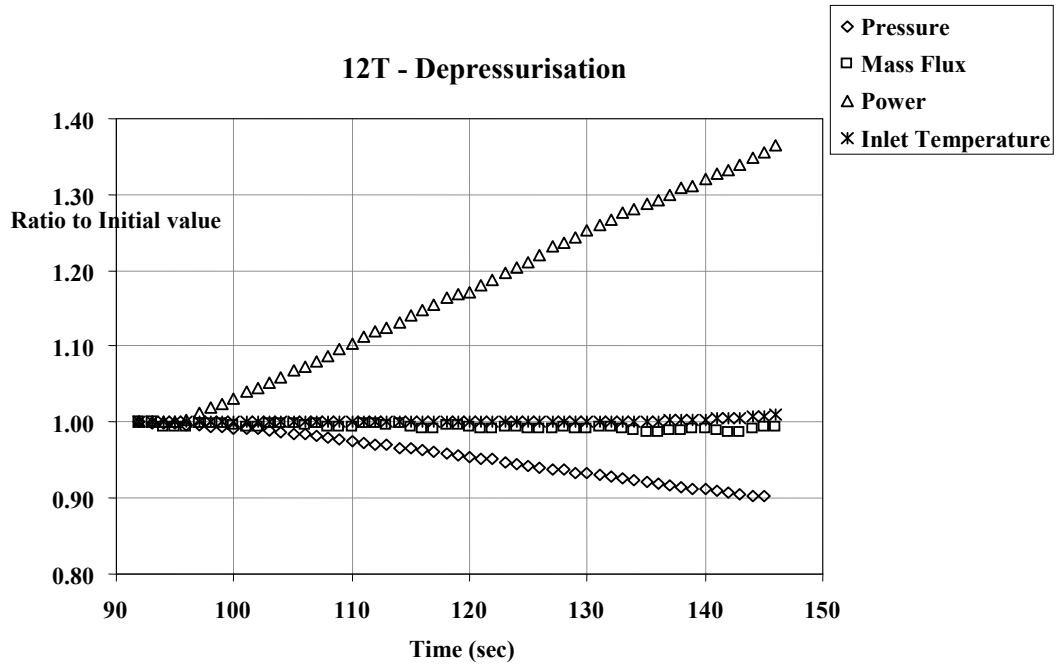
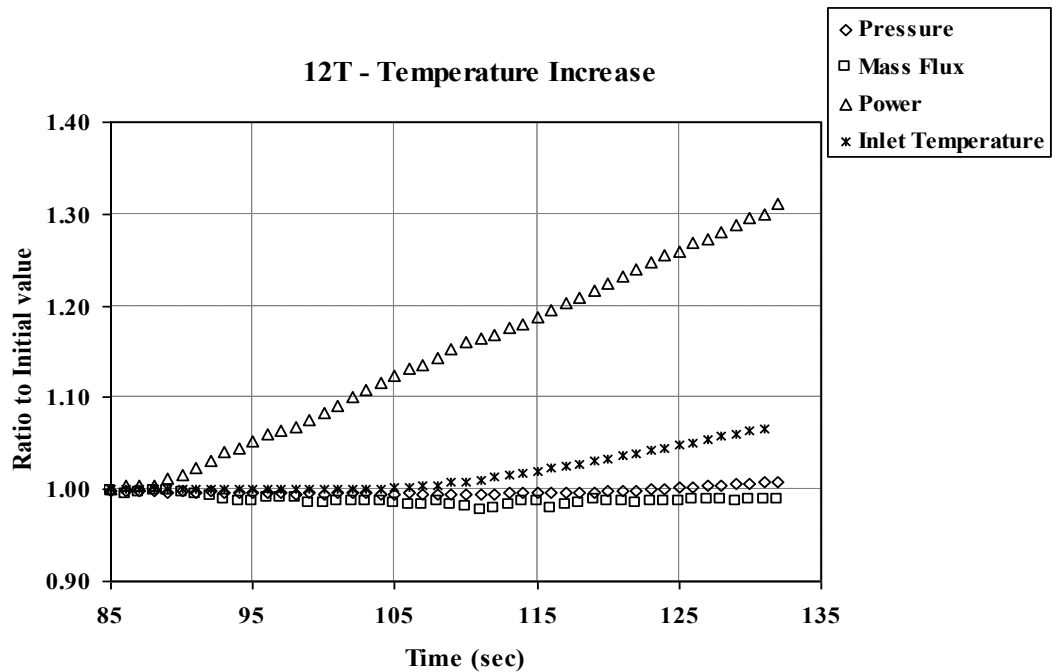


Figure 49: Variation of Properties during Transient for Data Series 12T (Temperature Increase)



Chapter 5: Output requested

5.1 Introduction

The participants should submit their results in an electronic format. All output should be in SI units.

Templates of requested output data for each exercise are provided by the benchmark team.

The PSU team has the obligation to:

- provide code-to-data comparisons for different submittals;
- provide code-to-code comparisons for different submittals;
- provide overall conclusions on current code capabilities to represent the key phenomena.

5.2 Void Distribution Benchmark

Exercise I-1: Steady-State Single Sub-channel Benchmark

For each of the test series 1, 2, 3 and 4, the calculated sub-channel averaged fluid densities and void fractions have to be submitted in the format shown in Table 65. The data have to be extracted at the axial elevation of 1.4 m from the beginning of the heated length (see Figure 3).

Participants using CFD codes should provide images of the in-channel void distribution for all four (4) test series, in addition to the tabulated output data.

Table 65: Output Format of Steady-State Single Sub-channel Benchmark

Exercise 1, Phase I
Test Series 1 – 4

Run number	Sub-channel averaged fluid density (kg/m ³)	Sub-channel averaged void fraction	Thermal equilibrium quality
X.XXX	X.XXX	X.XXX	X.XXX
X.XXX	X.XXX	X.XXX	X.XXX
X.XXX	X.XXX	X.XXX	X.XXX
...
X.XXX	X.XXX	X.XXX	X.XXX

Exercise I-2: Steady-State Bundle Benchmark

For each of the test series 5, 6, 7 and 8, the calculated region-averaged void fractions have to be submitted in the format shown in Table 66. The averaging has to be performed over the four central sub-channels of the bundle. The output data have to be extracted at three axial elevations: 2.216 m (lower), 2.669 m (middle), and 3.177 m (upper) from the beginning of the heated length (see Figure 4).

Table 66: Output Format of Steady-State Bundle Benchmark

Exercise 2, Phase I
Test Series 5 – 8

Run number	Region-averaged void fraction (-)			Bundle average void fraction
	Lower elevation (2.216m)	Middle elevation (2.669m)	Upper elevation (3.177m)	
X.XXX	X.XXX	X.XXX	X.XXX	X.XXX
X.XXX	X.XXX	X.XXX	X.XXX	X.XXX
X.XXX	X.XXX	X.XXX	X.XXX	X.XXX
...
X.XXX	X.XXX	X.XXX	X.XXX	X.XXX

Exercise I-3: Transient Bundle Benchmark

There are four different transient scenarios simulated for three different 5×5 bundle configurations. These bundle configurations, respectively B5, B6, and B7, are described in Table 15. The transient scenarios include power rise, flow reduction, depressurisation, and temperature increase. In total, twelve calculations are to be performed and for each calculation the results have to be submitted in the format shown in Table 67. Like with the Steady-State Bundle Benchmark, the averaging has to be performed over the four central sub-channels of the bundle. The output data have to be extracted at three axial elevations: 2.216 m (lower), 2.669 m (middle), and 3.177 m (upper) from the beginning of the heated length (see Figure 4).

Table 67: Output Format of Transient Bundle Benchmark

Exercise 3, Phase I
Test Series 5T (Power increase)

Time, [sec]	Region-averaged void fraction, (-)		
	Lower elevation 2.216 m	Middle elevation 2.669 m	Upper elevation 3.177 m
XX.X	X.XXX	X.XXX	X.XXX
XX.X	X.XXX	X.XXX	X.XXX
...
XX.X	X.XXX	X.XXX	X.XXX

Exercise I-4: Pressure Drop Benchmark

As discussed previously, although there is no available data, code-to-code benchmark on pressure drop of heated section for the typical central sub-channel is proposed. The reference value for the bundle under the rated condition (single-phase) is about 1.6 kg/cm² which is read from the initial value of the pressure drop over the heated section for the bundle B7 during power increase transient (test series 7T).

Participants are requested to submit the code predicted pressure drop over the heated length of the bundle test assembly B7, test series T7 before the transient is initialised.

In addition, participants are requested to submit the code predicted pressure drops over the heated length of the single sub-channel test assembly S1 and bundle test assembly B5 bundle for the exercise cases included in the Test Series 1 and Test Series 5. Results have to be submitted in the format shown in Tables 68 and 69.

Table 68: Output Format of Single Sub-channel Pressure Drop Benchmark

Exercise 4, Phase I
Test Series 1

Test number	Pressure drop, (kg/cm ²)
X.XXX	XXX.X
X.XXX	XXX.X
...	...
X.XXX	XXX.X

Table 69: Output Format of Bundle Pressure Drop Benchmark

Exercise 4, Phase I
Test Series 5

Test number	Pressure drop, [kg/cm ²]
X.XXX	XXX.X
X.XXX	XXX.X
...	...
X.XXX	XXX.X

5.3 DNB Benchmark

Exercise II-1: Steady-State Fluid Temperature Benchmark

The calculated results for a given exercise case should be submitted as a 6×6 matrix of space averaged fluid temperature in a sub-channel mesh size. An example of the output format of the Steady-State Fluid Temperature Benchmark is given in Table 70. The data have to be extracted at the axial elevation of 457 mm above the end of the heated length, where the actual measurements were conducted (see Figure 29).

Table 70: Output Format of Steady-State Fluid Temperature Benchmark

Exercise 1, Phase II
Test No.
Average Fluid Temperature, (°C)

y/x	1	2	3	4	5	6
1	xxx.x	xxx.x	xxx.x	xxx.x	xxx.x	xxx.x
2	xxx.x	xxx.x	xxx.x	xxx.x	xxx.x	xxx.x
3	xxx.x	xxx.x	xxx.x	xxx.x	xxx.x	xxx.x
4	xxx.x	xxx.x	xxx.x	xxx.x	xxx.x	xxx.x
5	xxx.x	xxx.x	xxx.x	xxx.x	xxx.x	xxx.x
6	xxx.x	xxx.x	xxx.x	xxx.x	xxx.x	xxx.x

Cross-sectional averaged: (°C)

Exercise II-2: Steady-State DNB Benchmark

For each of the test series 0, 2, 3, 4, 8 and 13, the predicted DNB powers; the axial elevation and radial position of the first predicted DNBs (test series 4, 8, and 13 only) have to be submitted in the format shown in Table 71.

Table 71: Output Format of Steady-State DNB Benchmark

Exercise 2, Phase II
Test Series 0, 2, and 3

Test number	Predicted DNB power, (MW)
xx-xxx	x.xx
xx-xxx	x.xx
...	...
xx-xxx	x.xx

Exercise 2, Phase II
Test Series 4, 8 and 13

Test number	Predicted DNB power, (MW)	Axial elevation of first predicted DNB, (m)	Radial position of first predicted DNB, central or peripheral rod
XX-XXX	X.XX	X.XXX	XXXXX
XX-XXX	X.XX	X.XXX	XXXXX
...
XX-XXX	X.XX	X.XXX	XXXXX

Exercise II-3: Transient DNB Benchmark

There are four different transient scenarios simulated for two different 5×5 bundle configurations. The two bundle configurations, respectively A11 and A12, are described in Table 22. The transient scenarios include power rise, flow reduction, depressurisation, and temperature increase. In total, eight calculations are to be performed and for each calculation the results have to be submitted in the format shown in Table 72.

Table 72: Output Format of Transient DNB Benchmark

Exercise 3, Phase II
Test Series 11T and 12T

Test number	Time of detected DNB, (sec)
11-0312	X.X
11-0112	X.X
11-0212	X.X
11-0321	X.X
12-0312	X.X
12-0112	X.X
12-0211	X.X
12-0321	X.X

Chapter 6: Conclusions

The objective of the PSBT benchmark specifications is to provide the participants with information on the benchmark database. Although it contains detailed information on the test cases and measurements for the complete NUPEC PWR database, specific exercises were selected for the OECD/NRC PSBT benchmark to reduce the amount of work; to make the analysis more precise and to avoid confusion when comparing the participant's results.

6.1 Phase I - Void Distribution Benchmark

Exercise I-1 – Steady-State Single Sub-channel Benchmark

The goal of this exercise is to benchmark the sub-channel, meso- and microscopic numerical approaches. The supplied measured data include space averaged void fraction in sub-channel mesh size. The test cases are selected at PWR rated conditions. Different types of single sub-channel test assemblies are used to investigate the effect of geometry on the phenomenon of concern.

Exercise I-2 – Steady-State Bundle Benchmark

This exercise is designed to benchmark meso-scopic numerical approaches. The test cases for this exercise are chosen at PWR rated conditions and deviations of quality from the rated conditions.

Exercise I-3 – Transient Bundle Benchmark

NUPEC PSBT database includes simulation of four representative transients of PWRs; power increase, flow reduction, depressurisation, and temperature increase. All four transients are selected as benchmark cases. Exercise 3 of Phase II is designed to benchmark sub-channel numerical approaches.

Exercise I-4 – Pressure Drop Benchmark

This exercise is designed to perform code-to-code comparisons concerning axial pressure drop. Although no empirical data is available, code results will be compared with relevant graphical data.

6.2 Phase II - DNB Benchmark

Exercise II-1 – Steady-State Fluid Temperature Benchmark

Exercise 1 of Phase II is designed to assess the thermal-hydraulic codes' capabilities of predicting the exit coolant temperature.

Exercise II-2 – Steady-State DNB Benchmark

The goal of Exercise 2 of Phase II is to assess the thermal-hydraulic codes' capabilities of correct prediction of DNB along rod bundles.

Exercise II-3 – Transient DNB Benchmark

Exercise 3 of Phase II is designed to enhance the ongoing development of truly mechanistic models for DNB prediction during the four postulated transients in PWRs.

References

- [1] “OECD/NEA (2009), Benchmark Based on NUPEC PWR Sub-channel and Bundle Tests (PSBT)”, JNES, April 2009.
- [2] “Proving Test on the Reliability for Nuclear Fuel Assemblies” (1989), Summary Report of Proving Tests on the Reliability for Nuclear Power Plant, Nuclear Power Engineering Test Center.
- [3] Hori, K. *et al.* (1993), “In Bundle Void Fraction Measurement of PWR Fuel Assembly”, ICON-2, Vol.1, pp.69-76, San Francisco, California, 21-24 March 1993.
- [4] Pamphlet of Takasago Engineering Laboratory, Nuclear Power Engineering Center (NUPEC).